STATISTICAL MECHANICAL STUDIES OF ELEMENTAL LIQUIDS AND BINARY MELTS

A THESIS SUBMITTED IN PARTIAL FULFILLMENT OF THE REQUIREMENTS FOR THE DEGREE OF DOCTOR OF PHILOSOPHY

C. LALNUNTLUANGA

MZU REGISTRATION NO. : 3752 of 2008-09

Ph.D. REGISTRATION NO. : MZU/Ph.D/675 of 16.05.2014

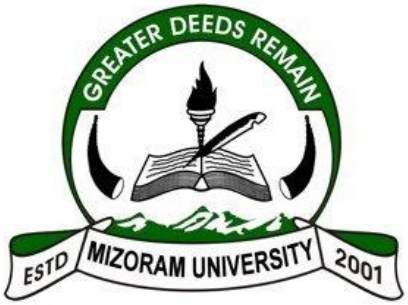

DEPARTMENT OF CHEMISTRY

SCHOOL OF PHYSICAL SCIENCES

DECEMBER, 2021

STATISTICAL MECHANICAL STUDIES OF ELEMENTAL LIQUIDS AND BINARY MELTS

BY

C. LALNUNTLUANGA

Department of Chemistry

Supervisor: Dr. ZODINPUIA PACHUAU

Co-Supervisor: Prof. RAJ KUMAR MISHRA

Submitted

In partial fulfillment of the requirement of the degree of Doctor of Philosophy in Chemistry of Mizoram University, Aizawl.

MIZORAM UNIVERSITY

(A central University under the Act of Parliament)

Department of Chemistry

School of Physical Sciences

CERTIFICATE

This is to certify that the thesis entitled "Statistical Mechanical Studies of Elemental Liquids and Binary Melts" submitted by **Mr. C. Lalnuntluanga** for the award of the degree of **Doctor of Philosophy** in the Mizoram University, Aizawl, Mizoram, embodies the original investigations carried out by him under my supervision. He has been duly registered and the thesis presented is worthy of being considered for the award of the Ph. D. degree. This has not been submitted for any degree in any other university.

Dated: 20th December, 2021

(Prof . Raj Kumar Mishra)
Co-Supervisor

(Dr. Zodinpuia Pachuau)
Supervisor

MIZORAM UNIVERSITY

TANHRIL

Month: December **Year: 2021**

DECLARATION

I C. Lalnuntluanga, hereby declare that the subject matter of this thesis is the record of work done by me, that the contents of this thesis did not form basis of the award of any previous degree to me or to do the best of my knowledge to anybody else, and that the thesis has not been submitted by me for any research degree in any other University/Institute.

This is being submitted to the Mizoram University for the degree of Doctor of Philosophy in Chemistry.

C. Lalnuntluanga
(MZU/Ph.D/675 of 16.05.2014)
(Candidate)

(Head)	Dr. Zodinpuia Pachuau	Prof. Raj Kumar Mishra
Department of Chemistry	(Supervisor)	(Co-supervisor)
	Department of Chemistry	Department of Chemistry
	Mizoram University	Institute of Science
		Banaras Hindu University

ACKNOWLEDGEMENTS

I would like to express my deep and sincere gratitude to my research supervisor Dr. Zodinpuia Pachuau (Associate Professor, Department of Chemistry, Mizoram University) and co-supervisor Dr. Raj Kumar Mishra (Professor, Department of Chemistry, Institute of Science, Banaras Hindu University) for giving me the opportunity to do research and providing invaluable guidance throughout this research. I am extremely grateful for what they have offered me.

I express my deep and sincere gratitude to Professor R. Venkatesh (Department of Chemistry, Institute of Science, Banaras Hindu University) with whom I had several very important discussions and for his valuable suggestions on Ph. D. research work.

I offer my sincere regards to the present and former Head, Professor Muthukumaran, R. and Professor Diwakar Tiwari, Department of Chemistry, School of Physical Sciences, Mizoram University for their many help and guidance during my Ph. D. research work.

I express my gratefulness to the present and former Deans, Professor Diwakar Tiwari and Professor Zaithanzauva Pachuau, School of Physical Sciences, Mizoram University for their support and encouragement in accomplishing the research work.

I am grateful to the faculty and staff members of the Department of Chemistry, Mizoram University for their cooperation on several occasions.

I am very much thankful to all my friends and fellow research scholars who in one way or another shared their support, either morally, financially and physically.

I also acknowledge the UGC, Government of India, New Delhi for their financial assistance through Nation Fellowship for Higher Education for ST students during the progress of the Ph.D. research work.

I am extremely grateful to my parents for their endless love, prayers, caring and sacrifices for educating and preparing me for my future career.

Above all, praise and thank to the God, the Almighty, for his showers of blessings, protection and guidance throughout my research work to complete the research successfully.

(C. LALNUNTLUANGA)

CONTENTS

LIST OF FIGURES

LIST OF TABLES

Chapter-1

INTRODUCTION

1.1. BACKGROUND

Statistical Mechanics is the fundamental branch of science which provides a framework for studying large collection of molecules and tells us how to average over positions and velocities to properly simulate the distribution of particles. The framework of Statistical Mechanics also provides efficient equations for computing thermodynamic properties from molecular properties. The subject has been applied with success to the study of matter in solids, liquids and gaseous states under different conditions of temperature and pressure etc.

The kinetic theory of gases is the study of the microscopic behavior of molecules and their interactions, which lead to macroscopic relationships like the ideal gas law, and hence this theory is one of the most pioneering studies of Statistical Mechanics and one can arrive at powerful quantitative conclusions. At very low pressure and at very high temperatures the gases tend to behave in accordance with the ideal systems. Under these conditions it is found that the mean free path is much larger than the diameter of molecules of gases, i.e. the gaseous molecules spend most of their time far from one another (Clark, 1989). In crystalline solids there is absence of translatory motion of the particles. The force of attractions between the particles of crystals is quite large and they rarely move from one lattice site to another.

A liquid, unlike a crystal may be regarded as if a finite fraction of lattice sites to be empty. Clearly crystals have a systematic arrangement of particles and the introduction of disorder over a small region cause disturbance in the long range and destroy the crystalline arrangement and its long-range order. The liquid may therefore be considered to have an ordered pattern over a short range instead of the entire mass i.e. short-range order and long-range disorder and a particle can migrate through it relatively rapidly. It must however be emphasized that short-range order in the liquid structure is continuously changing because of the thermal motion of the particles. In solids as the temperature of the crystal is increased the frequencies with which the particles vibrate about their mean positions increase and further if the

temperature is increased the kinetic energy of the particles increase so much that it overcomes the potential energy which keeps the particles in their positions. Particles, which have kinetic energy greater than their potential energy leave their lattice sites and create vacancies, thus forming defects. If number of such defects are increased by increasing the temperature the lattice collapse and becomes liquid.

However, in the liquid each particle is always interacting with many other neighboring particles, so that the simplification of kinetic theory of gases is not simply applicable to liquids nor liquids could be considered as having a systematic long – range arrangement of particles as in solids. But liquids do not have a simple interpolated status between gases and solids, although features adjacent to both the phases can be detected.

The structure of a liquid is investigated by means of X-rays scattering techniques and it was found that liquids survived some features of lattice structure of solids. The structure of liquids can be described by – g(r), known as Radial Distribution Function. Hence an understanding of liquid is possible if the distribution function is clearly perceived.

Examining the various degrees of freedom, it is necessary to consider the energy contribution in calculating the canonical partition function. The partition function is more generally written in terms of Hamiltonian. The Hamiltonian operator is separated into two parts, one involving only the center of mass i.e. $\hat{H}_{cm}$ and the other involving the intra molecular degrees of freedom i.e. $\hat{H}_{int}$, so that the total Hamiltonian $\hat{H}$ is written as

$$\hat{H} = \hat{H}_{cm} + \hat{H}_{int} \tag{1.1}$$

For a conservative system $\hat{H}$ is equal to E the total energy of the system. The transformation into wave mechanical form is as follows

$$-\sum \frac{\hbar^2}{2m_i} \nabla_i^2 \psi + U_N \psi = E\psi \tag{1.2}$$

or

$$\hat{H}\psi = E\psi \tag{1.3}$$

Substituting eqn. (1.1) in eqn. (1.3) and solving the resulting equation will give two separate wave equations for the centre of mass and internal co-ordinates. Solution of these two wave equations yields two independent sets of quantum states, one for translational degrees of freedom and one for internal degrees of freedom. The canonical partition function (Q_T) according to the assumption can be separated and is given as

$$Q_T = \sum_{i,j} \exp\left[-\frac{E_i^{cm} + E_j^{int}}{k_B T}\right]$$

$$= \sum_{i} \exp\left[-\frac{E_i^{cm}}{k_B T}\right] \quad \sum_{j} \exp\left[-\frac{E_j^{int}}{k_B T}\right]$$

$$= Q_{cm}(N, V, T) \qquad Q_{int}(N, T) \tag{1.4}$$

where k_B is the Boltzmann constant, T is the absolute temperature and rests of the symbols have their usual connotation. It is to be noted that the internal degrees of freedom depend only on the intra molecular structure (hence effect of vibrational, rotational etc. are to be considered) and is independent of volume or density, where as, translational degrees of freedom depend on center of mass (cm).

The translational Hamiltonian $\hat{H}_{cm}$ for the system of 'N' particles in which the potential energy depends only on positions $r_1, r_2, \ldots\ldots\ldots, r_{3N}$ molecular center of mass is given by

$$\hat{H}_{cm} = \sum_{i} \frac{P_{ix}^2 + P_{iy}^2 + P_{iz}^2}{2m} + U_N(r_1, r_2, \ldots\ldots\ldots, r_{3N}) \tag{1.5}$$

P_{ix}, P_{iy}, and P_{iz} are the three components of momentum vector P_i.

Assuming that the translational degrees of freedom are evaluated classically, Q_{cm} is given by

$$Q_{cm} = \frac{1}{N! h^{3N}} \int\ldots\int \exp\left[-\frac{H_{cm}}{k_B T}\right] dp^{3N} \ldots . dr^{3N} \tag{1.6}$$

Substituting eqn. (1.5) and integrating we get

$$Q_{cm} = \frac{Z_N}{\Lambda^{3N} N!} \tag{1.7}$$

where

$$\Lambda = \left(\frac{h^2}{2 \pi m k_B T} \right)^{1/2} \tag{1.8}$$

Λ is called thermal de Broglie wave length and

$$Z_N = \int .....\int \exp\ (-\frac{U_N}{k_B T})\ \bar{dr}_1 .....\bar{dr}_N \tag{1.9}$$

Here U_N is the potential energy of interaction, which depends on the relative positions of N atoms or molecules. Z_N is called the configurational integral, which is involved in various distribution functions.

1.2. THEORY OF DISTRIBUTION FUNCTIONS

Radial distribution function is used to describe the probability of finding a particle at a distance r if a particle is placed at the origin in the liquid.

Let us consider a liquid with 'N' particles at temperature 'T' and in a Volume 'V'. If the probability of a particle '1' is in the volume element $\bar{dr}_1$ at $\bar{r}_1$, particle '2' is in $\bar{dr}_2$ at $\bar{r}_2$ …….. and the particle 'N' is in $\bar{dr}_N$ at $\bar{r}_N$ is given by

$$P^{(N)}(\bar{r}_1, \bar{r}_2 ....., \bar{r}_N)\, \bar{dr}_1, \bar{dr}_2 ..... \bar{dr}_N = \frac{\exp(-U_N / k_B T)\, \bar{dr}_1\, \bar{dr}_2 ..... \bar{dr}_N}{Z_N} \tag{1.10}$$

This is called specific distribution function. The probability that a particle '1' is in the volume element $\bar{dr}_1$ at $\bar{r}_1$, particle '2' is in $\bar{dr}_2$ at $\bar{r}_2$, and the particle 'n' is in $\bar{dr}_n$ at $\bar{r}_n$ irrespective of the configuration of the remaining particles is given by

$$P^{(n)}(\bar{r}_1, \bar{r}_2 \ldots\ldots\ldots\ldots, \bar{r}_n)\, d\bar{r}_{n+1} \ldots\ldots\ldots\ldots d\bar{r}_N = \frac{\int \ldots \int \exp(-U_N/k_B T)\; d\bar{r}_{n+1} \ldots\ldots\ldots d\bar{r}_N}{Z_N} \tag{1.11}$$

The generic distribution function $\rho^{(n)}(\bar{r}_1, \bar{r}_2 \ldots\ldots\ldots, \bar{r}_n)$ is the probability that any particle is in the volume element $d\bar{r}_1$ at $\bar{r}_1$, any other particle is in $d\bar{r}_2$ at $\bar{r}_2$ …..……. and an n^{th} particle is in $d\bar{r}_n$ at $\bar{r}_n$ irrespective of the configuration of the rest of the particles is given by

$$\rho^{(n)}(\bar{r}_1, \bar{r}_2 \ldots\ldots\ldots \bar{r}_n) = \frac{N!}{(N-n)!}\; P^{(n)}(\bar{r}_1, \bar{r}_2 \ldots\ldots\ldots\ldots, \bar{r}_n) \tag{1.12}$$

The correlation function $g^{(n)}(\bar{r}_1, \bar{r}_2 \ldots\ldots, \bar{r}_n)$ is given by

$$\rho^{(n)}(\bar{r}_1, \bar{r}_2 \ldots\ldots\ldots \bar{r}_n) = \rho^n\; g^{(n)}(\bar{r}_1, \bar{r}_2 \ldots\ldots\ldots \bar{r}_n) \tag{1.13}$$

$$g^{(n)}(\bar{r}_1, \bar{r}_2 \ldots\ldots\ldots \bar{r}_n) = \frac{1}{\rho^n}\; \rho^{(n)}(\bar{r}_1, \bar{r}_2 \ldots\ldots\ldots \bar{r}_n)$$

$$= \frac{V^n\, N!}{N^n\, (N-n)!}\; \frac{\int \ldots \int \exp(-U_N/k_B T)\; d\bar{r}_{n+1} \ldots\ldots\ldots d\bar{r}_N}{Z_N} \tag{1.14}$$

Here ρ is the number density and is equal to N/V. It may be pointed out that the two particles correlation function $g^2(\bar{r}_1, \bar{r}_2)$ plays a very important role in understanding liquid state properties, which is given by

$$g^{(2)}(\bar{r}_1, \bar{r}_2) = \frac{1}{\rho^2}\; \rho^{(2)}(\bar{r}_1, \bar{r}_2) \tag{1.15}$$

Here $\rho^{(2)}(\bar{r}_1, \bar{r}_2)$ is designated as the pair distribution function. If particle at $\bar{r}_1$ exerts a spherically symmetrical force field then $g^{(2)}(\bar{r}_1, \bar{r}_2)$ and $\rho^{(2)}(\bar{r}_1, \bar{r}_2)$ depend on the relative distance between particles ‘1’ and ‘2’ i.e upon r_{12}, so we write as $g^{(2)}(r_{12})$ which for convenience is written as g(r). Further it is the Fourier transformation of experimentally measurable quantity called structure factor S(k). Important features of g(r) are:

(1) There is zero probability of the two particles occupying the same space, hence g(r) at r = 0 is zero.

(2) At a distance r_0, which is the minimum of the potential energy curve between two particles, there is maximum probability of finding a particle and hence g(r) is expected to be maximum as a first approximation.

(3) As $r \to \infty$, there is no long – range order, and so $g(r) \to 1$.

(4) g(r), the pair correlation function which when multiplies with number density gives local density $\rho(r)$ i.e. $\rho(r) = \rho\, g(r)$

(5) Since $4\pi r^2 \rho\, g(r)$ is the particle distribution function in a unit volume and this multiplied by dr gives the average number of particles between $\bar{r}$ and $\bar{r} + d\,\bar{r}$

(6) The Fourier inverse transformation of g(r) gives the function S(k), the structure factor in k – space, where $k = (4\pi/\lambda)\sin\theta$. [Here 2θ is the scattering angle and λ is the wavelength of the incident beam]. This function S(k) allows us to calculate various properties of metals and liquids.

1.3. INTEGRAL EQUATIONS

For simple liquids, which are characterized by spherically symmetric interactions, it is assumed that the forces act through the center of gravity and are pair wise decomposable i.e. total 'N' body configurational energy can be represented as a sum of pair interactions and hence it may be written as

$$U_N(\bar{r}_1, \bar{r}_2 \ldots\ldots \bar{r}_N) = \sum_{i<j}^{N} U(\bar{r}_{ij}) \tag{1.16}$$

and the radial distribution function is given by

$$g(r) = \frac{1}{\rho^2}\rho^{(2)}(\bar{r}_1, \bar{r}_2)$$

$$= \frac{N!}{\rho^2 Z_N (N-2)!} \int \ldots \int \exp(-U_N/k_B T)\, d\bar{r}_3 \ldots\ldots d\bar{r}_N \tag{1.17}$$

On differentiating the above equation and using eqn. (1.16) it can be found that

$$k_B T \frac{\partial g(r_{12})}{\partial \bar{r}_1} + \frac{\partial U(r_{12})}{\partial \bar{r}_1} g(r_{12}) + \rho \int \frac{\partial U(r_{13})}{\partial \bar{r}_1} g_{(3)}(r_{12}, r_{23}, r_{13}) \, d\bar{r}_3 = 0$$

(1.18 (1.18)

Eqn. (1.18) is an integro differential equation coupled with (N-1) equations and forms a hierarchy of equations. This can be solved using superposition approximation, which according to Kirkwood, states that the probability of observing some particular configuration of three molecules occupying positions 1, 2, and 3 equals the product of the probability of observing the three pairs of occupancies 12, 23 and 13 separately i.e.

$$g_{(3)}(r_{12}, r_{23}, r_{13}) = g(r_{12}) \, g(r_{23}) \; g(r_{13}) \tag{1.19}$$

So that eqn. (1.18) reduces to

$$k_B T \frac{\partial g(r_{12})}{\partial \bar{r}_1} + \frac{\partial U(r_{12})}{\partial \bar{r}_1} g(r_{12}) + \rho \int \frac{\partial U(r_{13})}{\partial \bar{r}_1} \; g(r_{12}) \; g(r_{23}) \; g(r_{13}) \; d\bar{r}_3 = 0 \tag{1.20}$$

The eqn. (1.20) is called Yvon-Born-Green (YBG) equation. Actually, the first structural theory of the fluid state is the work of Yvon (Yvon, 1935) and Kirkwood (Kirkwood, 1935) and then independently formulated by Bogoliubov (Bogoliubov, 1946), and, Born and Green (Born and Green, 1946). The superposition approximation is valid only at low densities and gives second and third virial coefficients correctly but not higher virial coefficients. The discrepancy at high densities is due to superposition approximation. The approximations together with improvements have been discussed by Henderson (Henderson, 1967), and, Rice and Gray (Rice and Gray, 1965). The general equation is given by

$$k_B T \frac{\partial g_{(h)}}{\partial \bar{r}_1} + \sum_{j=1}^{h} \frac{\partial U(r_{ij})}{\partial \bar{r}_1} g_{(h)} + \rho \int \frac{\partial U(r_{1,\,h+1})}{\partial \bar{r}_1} g_{(h+1)} \, d\bar{r}_{h+1} = 0 \tag{1.21}$$

The important four theories involving integral equations are the YBG theory, the hyper-netted chain (HNC) theory, the Percus Yevick (PY) theory and the perturbation theory (Reed and Gubbins, 1973). The YBG is the simplest of these and least accurate among the rest.

The HNC and PY equations make use of C(r), the direct correlation function (DCF) introduced first by Ornstein and Zernike (Ornstein and Zernike, 1914). The importance of it, in fluids is due to the following reasons.

(a) It can be calculated directly from experimental data and can be used to determine g(r) and S(k).

(b) The range of C(r) is shorter in comparison with h(r), the total correlation function defined by (Mikolaj and Pings, 1967; Mikolaj and Pings, 1967)

$$h(r) = g(r) - 1 \tag{1.22}$$

The PY and HNC approximations give expressions for C(r) in terms of g(r) and the potential function U(r). These are given by (Percus, 1962; Percus and Yevick, 1957)

$$\text{PY:} \quad C(r) = g(r)\,[1 - \exp\{\frac{U(r)}{k_B T}\}] \tag{1.23}$$

$$\text{HNC:} \quad C(r) = g(r) - 1 - \ln g(r) - \frac{U(r)}{k_B T} \tag{1.24}$$

Using these forms of C(r) in Ornstein-Zernike equation, which is given by

$$h(r_{12}) = C(r_{12}) + \rho \int C(r_{13})\, h(r_{23})\, d\bar{r}_3 \tag{1.25}$$

one gets the integral equations as

PY:

$$g(r_{12})\, \exp[\frac{U(r_{12})}{k_B T}] = 1 + \rho \int [g(r_{23}) - 1]\; g(r_{13})\,[1 - \exp\{\frac{U(r_{13})}{k_B T}\}]\; d\bar{r}_3 \tag{1.26}$$

HNC:

$$\ln g(r_{12}) + \frac{U(r_{12})}{k_B T} = \rho \int [g(r_{23}) - 1]\; [g(r_{13}) - \ln g(r_{13}) - 1 - \frac{U(r_{13})}{k_B T}]\; d\bar{r}_3 \tag{1.27}$$

It is possible to improve the PY and HNC approximations (Verlet, 1964) in a systematic manner, at the expense of increasing computational difficulty.

Understanding and detailed examining the above theories depicts various conclusions. The conclusions are:

(1) The theories work well at low and moderate densities but fail to give quantitative agreement at high densities.

(2) The failure at high densities is noticeable in calculating pressure, which depends in a sensitive way on details of g(r).

The PY and HNC theories are distinctly better than YBG (except in predicting the phase transition). Under most conditions, PY equation is superior to HNC. However HNC seems to be superior at low temperatures and moderate densities and also its application to electrolyte solutions. The PY theories have an unexpected advantage (Thiele, 1963; Wertheim, 1963; Wertheim, 1964; Baxter, 1967) as the equation can be solved exactly for a fluid of hard spheres.

When an approximate theory of g(r) is used to calculate the pressure, two different answers are obtained from pressure equations and compressibility equation. The discrepancy is an indication of the inaccuracy of the theory. Otherwise g(r) would give the same calculated pressure from both the equations. (pair wise additivity is assumed but even when pair wise additivity does not hold, the compressibility equation is still valid but not pressure equation of state).

According to self consistent approach (SCA) (Rowlinson, 1965), the equation for C(r) is written involving an unknown function ϕ, which depends on temperature and density (and composition in mixtures) but not on the separation r. The function φ is so chosen that pressure and compressibility equations yield the same pressure at every state.

C(r) for pure fluid is given by

$$C_{SC}(r, \rho, T) = C_{PY}(r, \rho, T) + d(r, \rho, T) \qquad (1.28)$$

where C_{PY} is given by PY approximation and d is a function to be determined.

$$d(r, \rho, T) = \varphi(\rho, T)\,[g(r)\ \exp\{U(r) / k_B T\} - 1 - \ln g(r) - U(r) / k_B T] \qquad (1.29)$$

When function φ = 0 eqn. (1.28) reduces to PY approximation, where as when function φ = 1, it gives HNC approximation. Self-Consistent results are better than HNC or PY results in general.

The following are other types of integral equations. The energy equation of state for N molecules is given by

$$E = \frac{3}{2} N k_B T + \frac{1}{2} \rho N \int_0^\infty U(r)\, g(r)\, 4\pi r^2\, dr \qquad (1.30)$$

The pressure equation of state is given by

$$\frac{p}{\rho k_B T} = 1 - \frac{\rho}{6 k_B T} \int_0^\infty r \frac{dU}{dr} g(r)\, 4\pi r^2 dr \qquad (1.31)$$

While the compressibility equation of state is given by

$$\rho \chi_T k_B T = 1 + \int_0^\infty [g(r) - 1]\, 4\pi r^2\, dr \qquad (1.32)$$

where, χ_T, is the compressibility and is given by $-\frac{1}{v}[\frac{dv}{dp}]_T$. Further it is possible to relate transport properties to g(r), which are described in chapter 4.

1.4. PERTURBATION THEORIES

The simplest model potential is the hard sphere potential function. The hard sphere potential has no attractive part and simulates the steep part (repulsive) of realistic potential. If σ is defined as the diameter of the molecules, then the potential function is given by

$$U(r) = \begin{cases} \infty & ; \quad r < \sigma \\ 0 & ; \quad r > \sigma \end{cases} \qquad (1.33)$$

i.e. the potential is zero when the distance between molecules is greater than the diameter of the molecules and infinity for distances less than the diameter.

Much evidence points to the fact that the structure of a liquid is primarily determined by short range repulsive forces and that the relatively long range attractive part of the potential provides a net force that gives a uniform attractive

background (Handerson, 1971) . So the repulsive part of the potential function determines the structure of a liquid and the attractive part holds the molecules together at some specified density. In the case of hard sphere potential the absence of attractive forces means that there is only a single fluid phase (Lebowitz and Percus, 1966). It is important to note that the PY equation is solved exactly for a fluid of hard spheres by Wertheim and Thiele (Thiele, 1963; Wertheim, 1963; Wertheim, 1964). The PY equation for this potential requires

$$C(r) = 0 \qquad ; r > \sigma \tag{1.34}$$

In the hard-core region C(r) is found to be [17,18]

$$-C(r) = \alpha + \beta\,(r/\sigma) + \gamma\,(r/\sigma)^3 \qquad ; r < \sigma \tag{1.35}$$

where

$$\alpha = \frac{(1+2\eta)^2}{(1-\eta)^4}$$

$$\beta = -\frac{6\eta\,(1+\eta/2)^2}{(1-\eta)^4}$$

$$\gamma = \frac{\eta\alpha}{2}$$

where η is called packing fraction and is given by

$$\eta = \frac{\pi\rho\sigma^3}{6} \tag{1.36}$$

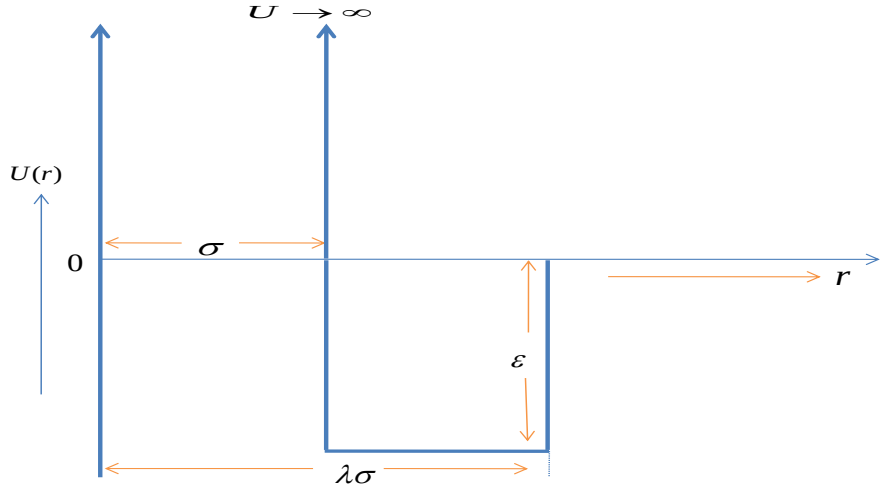

Figure 1.1: Square-Well potential function

The square well potential is an extension of hard sphere potential as it retains hard sphere repulsive properties but allows the particles to attract one another and this potential function is defined by

$$U(r) = \begin{cases} \infty & ; \quad r < \sigma \\ -\varepsilon & ; \quad \sigma < r < \lambda\sigma \\ 0 & ; \quad r > \lambda\sigma \end{cases} \tag{1.37}$$

where σ is the diameter of the particles, r is the separation between the particles, λ and ε are the breadth and depth of the potential well. We emphasize that square well potential gives analytical expressions in which numerical computations dominate relatively and hence even other potentials, if attempted to solve structure and associated properties we feel that analytical expressions are more appropriate and hence the applicability of square well potential to be more superior than the rest especially for liquid metals and alloys.

An important model system is the mean spherical model approximation (MSMA) and was first proposed by Lebowitz and Percus (Lebowitz and Percus, 1966) and is expressed as

$$\left.\begin{aligned} g(r) &= 0 \quad ; \quad r < \sigma \\ C(r) &= -U(r)/k_B T \quad ; \quad r > \sigma \end{aligned}\right\} \tag{1.38}$$

Hard sphere potential function given by eqn. (1.33) lacks the realistic aspects, as the attraction between the particles are not considered at all though this potential function explains fairly many properties of liquids.

The general theory of perturbation treatment was first described by Zwanzig (Zwanzig, 1954). This treatment gives a power series in $U_N^{(1)} / k_BT$, where $U_N^{(1)}$ is the perturbing potential. So theories have since been developed to relate the hard sphere properties of liquids with realistic potentials based on perturbation theories (Zwanzig, 1954; Barker and Henderson, 1967; Barker and Henderson, 1971; Barker and Henderson, 1972; Smith *et al*., 1970; Barker and Henderson, 1967; Barker and Henderson, 1968; Barker and Henderson, 1971; Chandler and Weeks, 1970; Weeks *et al*., 1971; Adersen *et al*., 1972; Mansoori and Canfield, 1969, 1969, 1969, 1970; Mansoori and Canfield, 1970; Stell, 1971; Snider, 1966, 1967; Hiroike, 1972)

The reference system is usually taken to be hard sphere system (but this is not a necessary condition). We can write the real potential U_N as a sum of two terms namely the reference potential $U_N^{(0)}$ and the perturbing potential $U_N^{(1)}$. Thus we have

$$U_N = U_N^{(0)} + U_N^{(1)} \tag{1.39}$$

Substituting U_N from eqn. (1.39) in eqn. (1.9), Z_N, the configurational integral is obtained. The configurational integral of the hard spheres is given by $Z_N^{(0)}$, which is expressed as

$$Z_N^{(0)} = \int \ldots\ldots \int \exp\left[-\frac{U_N^{(0)}}{k_B T}\right] d\bar{r}_1 \ldots\ldots d\bar{r}_N \tag{1.40}$$

So

$$Z_N = Z_N^{(0)} \frac{Z_N}{Z_N^{(0)}}$$

$$= Z_N^{(0)} < \exp\{-U_N^{(1)} / k_B T\} >_0 \tag{1.41}$$

$< >_0$ = indicates a canonical average in the unperturbed system.

In perturbation theory the Helmholtz function is described from a reference system plus a perturbation terms which are obtained from the radial distribution function of the reference system. The Helmholtz free energy 'A' is given as

$$A = -k_B T \ln Q \tag{1.42}$$

Here

$$Q = \frac{Z_N}{N!\Lambda^{3N}} \tag{1.43}$$

Substituting eqn. (1.41) into eqn. (1.43) and then putting the value of Q into eqn. (1.42) we get

$$-\frac{A}{k_B T} = \ln\left(\frac{Z_N^{(0)}}{N!\Lambda^{3N}}\right) + \ln < \exp\{-U_N^{(1)} / k_B T\} >_0 \tag{1.44}$$

Using the perturbation approach, the Helmholtz function of a system can be expressed as an expansion in inverse temperature in addition to the Helmholtz function of a reference system whose structure and thermodynamic properties are computed.

$$-\frac{A}{k_B T} = -\frac{A_0}{k_B T} - \frac{A^{(1)}}{k_B T} \tag{1.45}$$

where A_0 is the free energy of the reference system and $A^{(1)}$ is the perturbation free energy:

$$A^{(1)} = -k_B T \ln [< \exp\{-U_N^{(1)} / k_B T\} >_0] \tag{1.46}$$

we can rearrange eqn. (1.46) as

$$\exp\left(-\frac{A^{(1)}}{k_B T}\right) = < \exp\{-U_N^{(1)} / k_B T\} >_0 \tag{1.47}$$

and now we expand $A^{(1)}$ in powers of 1/T we get

$$A^{(1)} = < U_N^{(1)} >_0 + \text{Higher order terms of inverse temperature} \tag{1.48}$$

we further assume that $U_N^{(1)}$ is pair-wise additive and is of the form

$$< U_N^{(1)} >_0 = < \sum_{i<j} U^{(1)}(r_{ij}) >_0 = \frac{\rho N}{2} \int_0^\infty U^{(1)}(r) g_0(r)\ d\bar{r} \qquad (1.49)$$

However higher order terms in the expansion of eqn. (1.47) contain at least three and four body correlation functions, which even for hard spheres are not well known. An alternative to truncating the series after the first term is to write the exact relationship

$$A = A_0 + \frac{N\rho}{2} \int_\sigma^\infty U^{(1)}(r) g_0(r)\, d\bar{r} \qquad (1.50)$$

Barker and Henderson (Barker and Henderson, 1967; Barker and Henderson, 1971; Barker and Henderson, 1972; Smith *et al*., 1970; Barker and Henderson, 1967; Barker and Henderson, 1968; Barker and Henderson, 1971) were the first to consider the higher order terms in (1/T) in expansion of eqn. (1.44) and obtained the Helmholtz function up to the second order perturbation terms as

$$\begin{aligned} A = A_0 &+ \frac{N\rho}{2} \int_\sigma^\infty U^{(1)}(r) g_0(r)\ d\bar{r} \\ &- \frac{N\rho}{4 k_B T} \int_\sigma^\infty [\, U^{(1)}(r)\,]^2 \left(\frac{\partial \rho}{\partial P}\right)_0 g_0(r)\ d\bar{r} + 0\,(1/k_B T)^3 \end{aligned} \qquad (1.51)$$

We can use local compressibility term in eqn. (1.51), related to the pressure derivative of the density at a distance r from a given molecule at origin; i.e., on replacing $(\partial\rho/\partial p)_0 g_0(r)$ by $[\frac{\partial}{\partial P}(\rho\, g_0(r)]$. This is the so-called local compressibility approximation given by

$$\begin{aligned} A = A_0 &+ \frac{N\rho}{2} \int_\sigma^\infty U^{(1)}(r) g_0(r)\ d\bar{r} \\ &- \frac{N\rho}{4 k_B T} \int_\sigma^\infty [\, U^{(1)}(r)\,]^2 \left(\frac{\partial [\rho\, g_0(r)]}{\partial P}\right)_0 d\bar{r} + 0\,(1/k_B T)^3 \end{aligned} \qquad (1.52)$$

where N is the number of molecules, k_B is Boltzmann's constant, P, V and T are pressure, volume and absolute temperature respectively, $\rho = \frac{N}{V}$ and $g_0(r)$ is the pair correlation function for hard spheres.

In applying this equation to a square well fluid, Barker and Henderson took the hard sphere repulsive part as their unperturbed potential and the square well attractive part as perturbing potential. The expression for Helmholtz free energy of a square well fluid worked out to the second order in the Barker Henderson perturbation theory ((Barker and Henderson, 1967) is given by

$$\frac{A - A_0}{Nk_BT} = -2\pi\rho\left(\frac{\varepsilon}{k_BT}\right)\int_{\sigma}^{\lambda\sigma} r^2 g_O(r)\,dr - \frac{(1-\eta)^4}{1+4\eta+4\eta^2}\pi\rho \times \left(\frac{\varepsilon}{k_BT}\right)^2 \frac{\partial}{\partial\rho}\left[\rho\int_{\sigma}^{\lambda\sigma} r^2 g_0(r)\,dr\right] \tag{1.53}$$

The Barker-Henderson theory was the first successful perturbation theory and showed that perturbation theory is probably most appealing approach to the liquid state. The Chandler-weeks-Andersen model (CWA) (Chandler and Weeks, 1970; Weeks *et al.*, 1971; Adersen *et al.*, 1972) is an important and widely cited perturbation theory. In common with the Barker and Hendrson approach, Chandler et. al. also divided the intermolecular (pair) potential into a reference system pair potential and a perturbation potential part. Thus the intermolecular potential, according to CWA theory is given by

$$U(r) = U_0(r) + U_P(r) \tag{1.54}$$

The differences between Barker – Henderson and CWA approaches are in the definition of the reference potential and the density dependence of the size of representative hard spheres. Chandler *et. al.* assumed that the reference potential includes all the repulsive forces in the Lennard-Jones (LJ) potential and the perturbation potential includes all the attractions and proposed the choice

$$\left.\begin{aligned} U_0(r) &= U(r) - U(r_{min}) \quad ; \quad r < r_{min} \\ &= 0 \quad ; \quad r > r_{min} \\ U_P(r) &= U(r_{min}) \quad ; \quad r < r_{min} \\ &= U(r) \quad ; \quad r > r_{min} \end{aligned}\right\} \tag{1.55}$$

where $r_{min} = 2^{1/6}\,\sigma$ is the distance to the minimum in the LJ 6-12 potential. This theory establishes that the two effects (repulsive and attractive) are best understood on Fourier transform of h(r), the total correlation function i.e.

$$h(k) = \int [g(r) - 1]\, e^{-i\bar{k}.\bar{r}} d\bar{r} \tag{1.56}$$

Chandler and weeks proposed a hypothesis on the behaviour of the function h(k) and empirically verified on the system of LJ 6-12 molecules. This hypothesis is based on the results of Verlet's studies and is summarized as follows:

(1) At intermediate and large wave vectors, the quantitative behaviour of the function h(k) is dominated by the repulsive forces and the attractive forces are manifested in the small wave vector region ($k\sigma < \pi$).

(2) For high densities the behaviour of h(k), even at small wave vectors, is determined at least quantitatively by the repulsive forces.

According to the first order perturbation theory, the Helmholtz function was shown by CWA as

$$A = A_0 + \frac{N\rho}{2} \int U_P(r)\, g_0(r)\, \overline{dr} \tag{1.57}$$

Both these approaches are very appealing and are numerically quite satisfactory.

1.5. STRUCTURE FACTOR IN LIQUIDS

Electromagnetic radiations X-rays, neutrons and electrons, diffracted from fluid samples, yield information on the structures of the fluid through the relationship of the intensity of diffracted beam, I, with the angle θ by which it has been diffracted. The properties of atoms as scattering centers differ for neutron and for electron ray diffraction, occurring from nuclei and from electrons, respectively. Furthermore the

inelastic or incoherent scattering process is approximately independent of the scattering angle.

The knowledge of the atomic structure of condensed matter results from X-ray diffraction studies is of extreme importance. The structural information about the liquid state can be obtained by X-ray diffraction techniques and has been known since Debye (Debye, 1915) and Ehrenfest (Ehrenfest, 1915). These scientists have shown that the periodicity of a crystal structure is not required for the production of diffraction effects. Debye and Menke (Debye and Menke, 1930) made the first quantitative application to liquid Hg.

The individual atoms work as scattering centers and the scattering results are presented as angle dependent scattering intensities, I(θ), where instead of the angle the variable k is used

$$k = \frac{4\pi}{\lambda}\sin(\theta/2) \tag{1.58}$$

The intensity in electron units scattered by a non-crystalline array of atoms at an angle θ is given by 'Debye's equation'

$$I_{eu}^{coh}(k) = \sum_n \sum_m f_n f_m \frac{\sin kr_{nm}}{kr_{nm}} \tag{1.59}$$

where f_n, f_m are the atomic scattering factors for the n^{th} and m^{th} atoms respectively, r_{nm} is the magnitude of the vector separating these two atoms. For monatomic liquids $f_n = f_m = f$. The summation in Debye's eqn. (1.59) should be performed at first for the atom at the origin and next extending to all atoms of the liquid specimen over all distances. Summation for the atom at the origin lead to unity, since in the limit as $r_{nm} \rightarrow 0$, $(\sin kr_{nm} / kr_{nm}) \rightarrow 1$. If N is the total number of atoms,

$$I_{eu}^{coh}(k) = Nf^2[1 + \sum_{n'} \frac{\sin kr_{nm}}{kr_{nm}}] \tag{1.60}$$

where the $\sum_{n'}$ excludes the atom at the origin. If it is assumed that there is continuous distribution of atoms, then the above summation may be replaced by an integral. If ρ(r) is the density of atoms at distance r from the atom at the origin, then

the number of atoms in the spherical shell of radius r and thickness dr is $4\pi r^2\rho(r)dr$, then eqn. (1.60) can be written as

$$I_{eu}^{coh}(k) = Nf^2[1 + \int_O^\infty 4\pi r^2 \rho(r) \frac{\sin kr_{nm}}{kr_{nm}} dr] \tag{1.61}$$

If we take ρ as the constant average density of atoms, then eqn. (1.61) can be written as

$$I_{eu}^{coh}(k) = Nf^2[1 + \int_0^\infty 4\pi r^2[\rho(r) - \rho] \frac{\sin kr_{nm}}{kr_{nm}} dr] + \int_0^\infty 4\pi r^2 \rho \frac{\sin kr_{nm}}{kr_{nm}} dr \tag{1.62}$$

The second integral is negligible since it corresponds to forward scattering (Hansen and Mc Donald, 1976).

Hence eqn. (1.62) can be written as

$$I_{eu}^{coh}(k) = Nf^2[1 + \int_0^\infty 4\pi r^2[\rho(r) - \rho] \frac{\sin kr_{nm}}{kr_{nm}} dr] \tag{1.63}$$

The structure factor of a liquid S(k), which is the autocorrelation function of the Fourier components of density of particles is defined as

$$S(k) = \frac{I_{eu}^{coh}(k)}{Nf^2} \tag{1.64}$$

so that

$$\begin{aligned} S(k) &= 1 + \int_0^\infty 4\pi r^2[\rho(r) - \rho] \frac{\sin kr_{nm}}{kr_{nm}} dr \\ &= 1 + \int_0^\infty 4\pi r^2[g(r) - 1]\rho \frac{\sin kr_{nm}}{kr_{nm}} dr \end{aligned} \tag{1.65}$$

Due to lacking of long range order in liquids, the best way to characterize the structure of a liquid is through correlation functions. The pair correlation function or radial distribution function is one of the important parameter to explain the structural features of a liquid. This is also formed as density-density correlation which is defined as the probability of finding an atom at a distance 'r' at time 't' from an atom at origin at time t=0. The average number of nearest neighbor to first coordination

cells which is called coordination numbers are reported in recent years due to its importance in explaining the local structure of liquid metals and alloys. These local structural functions are correlated with important macroscopic properties of liquid metals and alloys like diffusion

The Fourier inversion of S(k) gives, the radial distribution function, g(r), and it is given by

$$g(r) = 1 + \frac{1}{2\pi^2\rho}\int_0^\infty k^2[S(k)-1]\frac{\sin kr_{nm}}{kr_{nm}}dk \qquad (1.66)$$

Thus from the measured values of S(k) it is possible to compute g(r). It can be shown that the structure factor in the long wave limit (i.e. when k = 0) is give by

$$S(0) = \rho k_B T \beta_T \qquad (1.67)$$

The structure factor calculations using model potential requires a set of potential parameters, which can be further used to calculate various transport properties of liquids. Transport properties of liquids, together with structural and thermodynamic information, provide the basis for the theories of liquid state.

1.6. TRANSPORT, SURFACE AND SCALING PROPERTIES IN LIQUID BINARY ALLOYS

Statistical mechanics provides equations relating the thermodynamic and transport properties of liquids. Since the development of perturbation theories (Barker and Henderson, 1967; Barker and Henderson, 1971; Barker and Henderson, 1972; Smith *et al.*, 1970) there have been rapid advances in methods for calculating liquid state properties from statistical mechanics.

Self-diffusion coefficients, which are related to the simple translational movements of species within a liquid, uncomplicated by concentration gradients, are important measurable properties of liquids. Many theories give reasonable agreement with experiment, have been put forward to describe diffusion in simple liquids (Rice and Gray, 1963) and thus have contributed much to our understanding of liquid structure.

One of the most widely used approaches is to attempt to relate the movement of particles in fluid to the theory of Brownian motion. The best known of this theory is due to Kirkwood (Kirkwood, 1946) and is similar to the distribution function approach to the equilibrium theory. In an extension of the Brownian motion concepts (War, 2014) to the description of classical non-equilibrium processes in dense fluids, the friction coefficients, ξ, in the well known Einstein formulation of the diffusion coefficient, D, for monatomic liquids

$$D = \frac{k_B T}{\xi} \tag{1.68}$$

plays a role of central importance. Much effort has been devoted to the calculation of the friction coefficient (Rice and Gray, 1963). Of all the analyses, we prefer to use thelinear trajectory (LT) approximation (Helfand, 1961).

Helfand (Helfand, 1961) has analysed friction coefficient ξ in liquid on the assumption that interparticle pair potential, U(r) can be divided conveniently into two parts.

$$U(r) = U^H(r) + U^S(r) \tag{1.69}$$

Accordingly, the force may be divided into two parts, F_H a hard-core contribution, and F_S, a soft force, and one can write the friction constant in the form

$$\xi = \xi^H + [\xi^S + \xi^{SH}] \tag{1.70}$$

The first term in the above expression, ξ^H, has been explained by several investigators (Toole and Dahler, 1960), the second, ξ^S, by Hefand (Helfand, 1961) and the third term, ξ^{SH}, by Davis and Polyvos (Davis and Polyvos, 1967). Rao and Murthy (Gopala Rao and Murthy, 1975) used square well potential linear trajectory calculations. Polivos and Davis (Polyvos and Davis, 1967; Rice *et al*., 1968) extended the LT approximation of Helfand for binary mixture.

The square-well potential model has been successfully used for the computation of relation between structure and dynamic properties of various liquid

metals and binary melts (Gopala Rao and Venkatesh, 1989; Venkatesh et al., 2003; Venkatesh and Mishra, 2005; Dubinin et al., 2009; Yu et al., 2001).

It has been reported that the concentration-dependent viscosity is related to intermetallic compounds present in various metallic systems (Mudry *et al.*, 2013) The diffusion coefficient of Brownian particles and the shear viscosity of fluids can be related through the Stokes-Einstein relation (Meyer *et al.*, 2019; Trybula, 2016; Souto *et al.*, 2013)

$$\eta = \frac{k_B T}{2\pi r^{max} D} \tag{1.71}$$

Several authors have studied the correlation between surface tension and self-diffusion coefficients (Lu *et al.*, 2005; Blairs, 2016). The values of surface tension are not well known even for many simple metals as reported by Lu *et al.*. The concentration-dependent surface tension of liquid can be determined by incorporating modified Stokes-Einstein relation in the equation for binary system (Venkatesh *et al.*, 2003). The computed results of surface tension were compared with available experimental values which gives us confidence in our square-well model calculations.

Dzugutov (Dzugutov, 1996) and Rosenfeld scaling law relating the transport coefficients and the excess entropy of a liquid have been examined by several workers using embedded atom method (EAM) through *ab initio* molecular dynamic simulations (Jakse and Pasturel, 2015; Jakse and Pasturel, 2016; Hoyt *et al.*, 2000; Samanta *et al.*, 2004; Li *et al.*, 2005). The square-well model potential as well is used for investigating the relationship between the dimensionless diffusion coefficient, D* and viscosity coefficient η* as a function of excess entropy S^{ex}/k_B for the investigated binary melts.

1.7. THERMODYNAMIC PROPERTIES OF LIQUID BINARY ALLOYS

Study on the thermodynamic properties of binary alloys is important from the point of view of process metallurgy and also for an understanding of the thermochemical behavior of materials. Experimental procedure for some systems can be very complicated and may also require utmost care since these systems can be

very reactive and they may also be very expensive. Therefore, theoretical or empirical methods for their studies are of great interest (Arzpeyma *et al*., 2013).

Several authors explain the composition dependent thermodynamic mixing parameters of liquid binary alloys using various experimental methods, thus drawing the attention of theoreticians to extract further microscopic information of binary alloys (Lalnuntluanga *et al*., 2021; Akinlade *et al*., 2000; Akinlade and Singh, 2002). The computation of thermodynamic properties of an alloy is a difficult task and the model calculations are not universally applicable. Hence, the investigation of transport and thermodynamic properties through microscopic structural functions in liquid alloys is always interesting and opens a new door to the applicability of alloys.

1.8. TEMPERATURE EFFECT ON STRUCTURAL AND TRANSPORT COEFFICIENT OF LIQUID COPPER

The knowledge of the structure and transfer properties of liquid metals and alloys helps physists, chemists and technologists in their applications for various useful purposes. The structure factor S(k) of liquid Cu was investigated in the temperature range from 1370 K to 1873 K, using square-well (SW) potential perturbation over hard sphere reference system. Computed S(k) and SW potential were applied to determine the self diffusion of liquid Cu within the available experimental temperature range by using well known Einstein's equation $D=k_BT/\xi$. Then the computed results were compared with available experimental results obtained by Quasielastic Neutron Scattering (QNS). Also, the viscosity coefficient, co-ordination number and the coefficient of thermal expansion were computed from the equation of states for square-well fluids within the temperature range for investigation of structure factor.

1.9. OUTLINES OF PRESENT WORK

After a general introduction, a detailed understanding of the structural features of binary alloys is described in the second chapter. Using the Lebowitz solution of hard sphere mixtures as a reference system, and perturbed the hard sphere

direct correlation function with square well attractive tail the partial and total structure factors, radial distribution functions and associated derived properties of Cu-In and Fe-Al alloys at different compositions have been calculated and compared with the available experimental values. There is an excellent agreement between theoretical and experimental results. We also obtained partial and total coordination numbers from partial and total pair correlation functions respectively. Finally we emphasize that square-well potential is an appealing model in understanding the structural aspects of binary alloys.

In the third chapter, thermodynamically important Bhatia-Thornton correlation functions and in specific the concentration-concentration correlation functions at various compositions of the Cu-In and Fe-Al alloys in the entire momentum space with special emphasis on the values at long wave limit of the same alloys are calculated. The chemical short-range order parameter has been computed as a function of composition for the same systems through structural studies in the long wave limit, which gives valuable information regarding the nature of the liquid alloys at various compositions.

The fourth chapter describes the calculation of diffusion coefficients of binary alloys through their structural studies. A detailed investigation on transport properties of binary alloys is considered. The diffusion coefficient of the alloys is calculated through the use of Helfand's linear trajectory principle. Equations have been derived for the temperature variation of diffusion coefficients, which were applied successfully to the investigated binary alloys. The viscosity coefficients of pure components in liquid binary alloys are determined by assuming Stokes-Einstein (SE) form of equations. The concentration-dependent surface tension of liquid binary alloys is derived by extending the equation for binary system. Further, Dzugutov and Rosenfeld universal scaling law has been tested for the investigation of correlation between atomic dynamics and thermodynamics with square-well model potential.

In fifth chapter, we deduce information on thermodynamic mixing parameters of binary alloys such as, Gibbs free energy of mixing, enthalpy of mixing and entropy of mixing through investigated square-well model structural functions and transport

coefficients of liquid binary alloys. The Romanov-Kozlov-Petrov (RKP) model, which correlates the viscosity with enthalpy of mixing, has been used for estimating the enthalpy of mixing. The entropy of mixing has been calculated using a SW model of pair correlation function under two body approximations. The Gibbs free energy of mixing was the computed from the difference between the computed enthalpy of mixing and entropy of mixing.

In sixth chapter, we investigated a detailed effect of temperature on structure and transport properties of liquid Cu using a square-well model potential under random phase approximation. Computed structure factor and square-well potential were applied to determine the self diffusion of liquid Cu within the available experimental temperature range by using well known Einstein's equation. Then the computed results were compared with available experimental results obtained by Quasielastic Neutron Scattering (QNS). Also, the viscosity coefficient, co-ordination number and the coefficient of thermal expansion were computed from the equation of states for square-well fluids within the temperature range for investigation of structure factor.

Chapter-2

PARTIAL AND TOTAL STRUCTURAL CHARACTERISTICS OF LIQUID BINARY ALLOYS

2.1. INTRODUCTION

It is now a fact in condensed matter research that the transport and thermodynamic properties of matter can be derived through their microscopic structural functions. It is a well known fact that the structure of materials along with their physicochemical properties helps to understand their utility for useful purposes.

Various factors like intermolecular forces and the arrangement of constituent atoms in a liquid state make their studies much more complicated than solids or gases. Works on the atomic scale correlations and derive associated properties of Al-Fe metallic melts have been performed through theoretical calculations, atomistic simulation techniques, and experimental approaches (Roik *et al.*, 2014; Bel'tyukov *et al.,* 2015; Dubinin *et al.*, 2014; Trybula, 2016; Trybula *et al.,* 2014). Knowledge of structure and physicochemical properties of liquids provides a better understanding of their nucleation process, glass formation, metallurgy and technological applications (Yuan *et al.*, 2013; Jakse and Pasturel, 2008; Yan, 2018; Dubinin, 2019).

The techniques of X-ray and neutron diffraction help to understand the distribution of atoms in a liquid by the Fourier transforming of how they scatter incident radiation. This idea of using X-ray diffraction for liquid structural studies were first carried out by Gringrich (Gringrich, 1952), Gingrichet, *et al.* (Gingrich and Henderson, 1952) and others (Orton *et al.*, 1960; Enderby and North, 1968).

To determine structure functions and derived physicochemical properties, we use square-well (SW) potential parameters of pure components under Mean Spherical Model Approximation (MSMA). Partial and total correlation functions and coordination numbers are important sources for understanding the change in interatomic bonding due to alloying of metals and hence the change in thermodynamic properties of the alloys.

The total structure factor, $S(k)$ which determines the main characteristic properties of a binary fluid, depends on three partial structure factors (PSFs). For 'l' and 'm' types of species in a binary melts, we derived the Ashcroft-Langreth (AL) type PSFs (Ashcroft and Langreth, 1967) $S_{ll}(k)$, $S_{mm}(k)$ and $S_{lm}(k)$ in momentum space of the SW interatomic potentials by obtaining the direct correlations between l-l, m-m, and l-m in repulsive and attractive regions of SW potential in momentum space (Cromer, 1965). Fourier transform of the three PSFs gives its corresponding three partial radial distribution functions, $g_{ll}(r)$, $g_{mm}(r)$ and $g_{lm}(r)$ in binary melts.

The liquid Cu-In alloy is a compound forming system and can be used for various industrial purposes like lead-free soldering materials and provides a new dimension for investigating the properties of ternary alloy like In-Bi-Cu and Cu-In-Sb etc.(Mudry *et al.*, 2013; Akinlade and Singh, 2002). Fe-Al alloys possess low density and significantly better corrosion resistance as compared to stainless steel and thus highly applicable for industrial purposes (Morris and Gunther, 1996; Il'inskii *et al.*, 2002), as well as considered as a starting material for many important alloys.

In this chapter, a detailed discussion on the microscopic structural functions of Cu-In and Fe-Al liquid binary alloys is presented. In recent times, several theoretical and atomistic simulation techniques have been reported to establish the relationship between thermodynamic, transport, and atomic-level structural functions in metallic melts; for liquid Cu-In alloys (Mudry *et al.*, 2013; Akinlade and Singh, 2002; Dubinin *et al.*, 2014; Wang *et al.*, 2015; Meyer *et al.*, 2019; Trybula, 2016; Trybula, 2014); for liquid Fe-Al alloys (Il'inskii *et al.*, 2002; Roik *et al.*, 2014; Bel'tyukov *et al.*,2015; Akinlade *et al.*, 2000).

Recently, Mudry *et al.* (Mudry *et al.*, 2013) reported X-ray diffraction studies on liquid Cu-In alloys at five different compositions. The total structure factors S(k) and radial distribution functions g(r) in liquid Cu-In alloys have been computed as a function of In concentration from 0.25 to 0.35 atomic fraction of In. The computed values are in good agreement with the experimental results obtained by X-ray scattering method (Mudry *et al.*, 2013). Roik *et al.* (Roik *et al.*, 2014) reported X-ray

diffraction studies on liquid Fe-Al alloys at six different compositions. We find a fair agreement between values obtained through theoretical formulation and computation of total structure factor with X-ray diffraction data of liquid Fe-Al alloys (Roik *et al.*, 2014) at all investigated compositions and in the entire momentum space (*k*-space).

Although, various efforts on theoretical/computational or experimental data of atomic structures and transport coefficients measurements of liquid Cu-In and Fe-Al alloys have been performed, their microscopic structural functions and their relation with thermo-physical and thermodynamic properties of the liquids are still not well understood.

The radial distribution function (RDF) which is the Fourier transform of structure factors (SFs), gives the probability of finding a particle from the origin, and thus employed in the structural description at the atomic scale of liquid metals and alloys. In this chapter, we present three PSFs, total structure factors (TSFs) and their corresponding partial and radial distribution functions along with partial and total co-ordination number for both Cu-In and Fe-Al alloys as function of temperature and composition.

2.2. THEORY

For a system containing more than one kind of atoms, the intensity of the X-ray scattering can be written as

$$\frac{I_{coh}}{N} = \left\langle f^2 \right\rangle + \left\langle f \right\rangle^2 \int_0^\infty 4\pi r^2 \left[\rho(r)-\rho\right] j_o\left(r\right) dr \tag{2.1}$$

where $j_o\left(r\right)$ is the Bessel function of the zeroth order. Further

$$\left\langle f \right\rangle = \sum_{l=1}^{n} c_l f_l \tag{2.2}$$

$$\left\langle f^2 \right\rangle = \sum_{l=1}^{n} c_l f_l^2 \tag{2.3}$$

and

$$\rho(r)=\frac{\sum_{l=1}^{n}\sum_{m=1}^{n} c_l f_l f_m \rho_{lm}(r)}{\left[\sum_{l=1}^{n} c_l f_l\right]^2} \tag{2.4}$$

where c_l is the atomic percent of l^{th} atom in the alloy, f_1 and f_m are the scattering factors of l^{th} and m^{th} -type atoms respectively, $\rho_{lm}(r)$ is the number of m-type atoms per unit volume at the distance r from an l-type atom and n is the number of atoms.

$$\rho(r)=\left[c_1 f_1^2 \rho_{11}(r)+c_2 f_2^2 \rho_{22}(r)+2c_1 c_2 f_1 f_2 \rho_{12}(r)\right]\left[c_1 f_1+c_1 f\right]^{-2} \tag{2.5}$$

Considering $c_1\rho_{12}(r)=c_2\rho_{21}(r)$ the total structure factor binary system can be written as

$$S(k)=\frac{c_1^2 f_1^2}{\langle f\rangle^2} I_{11}(k)+\frac{c_2^2 f_2^2}{\langle f\rangle^2} I_{22}(k)+\frac{2c_1 c_2 f_1 f_2}{\langle f\rangle^2} I_{12}(k) \tag{2.6}$$

where

$$I_{11}(k)=1+\int_0^{\infty} 4\pi r^2\left[\frac{\rho_{11}(r)}{c_1}-\rho\right] j_o(kr)\,dr \tag{2.7}$$

$$I_{22}(k)=1+\int_0^{\infty} 4\pi r^2\left[\frac{\rho_{22}(r)}{c_2}-\rho\right] j_o(kr)\,dr \tag{2.8}$$

$$I_{12}(k)=1+\int_0^{\infty} 4\pi r^2\left[\frac{\rho_{12}(r)}{c_2}-\rho\right] j_o(kr)\,dr \tag{2.9}$$

As mentioned earlier we use hard sphere reference system as it dominates in deciding the structural aspects of liquids but we note that this reference system lacks realistic properties and hence the hard sphere solution of Percus-Yevicks's equation obtained by Lebowitz is perturbed with square-well attractive tail under Mean Spherical Model Approximation (MSMA) to obtain the direct correlation function (DCF) between 'l' and 'm' species in a binary mixture and can be given as

$$C_{lm}(r)=\begin{cases} C_{lm}^{0}(r) & ; \quad 0 < r < \sigma_{lm} \\ -\varepsilon_{lm}/k_B T & ; \quad \sigma_{lm} < r < \lambda_{lm}\,\sigma_{lm} \\ 0 & ; \quad r > \lambda_{lm}\,\sigma_{lm} \end{cases} \tag{2.10}$$

where $C_{lm}^{0}(r)$ stands for Hard Sphere solution of Percus-Yevick's equation, σ_{lm}, λ_{lm} and ε_{lm} are the hard sphere diameter, potential energy breadth and depth respectively of the square-well potential. Lorentz-Berthelot (LB) rule (Gopala Rao and Das, 1987) is applied to obtain mixed parameter for this work as follows

$$\left.\begin{aligned} \sigma_{12} &= (\sigma_1+\sigma_2)/2 \\ \varepsilon_{12} &= (\varepsilon_{11}\varepsilon_{22})^{1/2} \\ \lambda_{22} &= \frac{\lambda_{11}\sigma_1+\lambda_{22}\sigma_2}{2\sigma_{12}} \end{aligned}\right\} \tag{2.11}$$

The radial distribution function $g_{lm}(r)$ is related to the correlation function, $h_{lm}(r)$ as given equation

$$h_{lm}(r)=g_{lm}(r)-1 \tag{2.12}$$

Further, $h_{lm}(r)$ is related to DCF through the generalized OZ equation (Mc. Quarrie, 1976) for a system containing more than one species can be written as

$$h_{lm}(r)=C_{lm}(r)+\sum_{n=1,2}\rho_n \int C_{ln}(\bar{r}-\bar{r}')h_{mn}(\bar{r}')\bar{dr} \tag{2.13}$$

where ρ_n is the bulk density of n^{th} species. Fourier transforming the OZ equation and using convolution theorem $h_{lm}(k)$ can be obtained as

$$h_{lm}(k)=C_{lm}(k)+\sum_{n=1,2}\rho_n \int C_{ln}(k)h_{mn}(k) \tag{2.14}$$

For a binary system with

l=1, m=1

$$h_{11}(k)=C_{11}(k)+\rho_1 C_{11}(k)h_{11}(k)+\rho_2 C_{12}(k)h_{12}(k) \tag{2.15}$$

l=1, m=2

$$h_{12}(k)=C_{12}(k)+\rho_1 C_{11}(k)h_{21}(k)+\rho_2 C_{12}(k)h_{22}(k) \tag{2.16}$$

l=2, m=1

$$h_{21}(k)=C_{21}(k)+\rho_1 C_{21}(k)h_{11}+\rho_2 C_{22}(k)h_{12}(k) \quad (2.17)$$

l=2, m=2

$$h_{22}(k)=C_{22}(k)+\rho_1 C_{21}(k)h_{21}(k)+\rho_2 C_{22}(k)h_{22}(k) \quad (2.18)$$

These equations on solving for $h_{lm}(k)$ give rise to

$$h_{11}(k)=[C_{11}(k)\{1-\rho_2 C_{22}(k)\}+\rho_2 C_{12}^2(k)][B(k)]^{-1} \quad (2.19)$$

$$h_{22}(k)=[C_{22}(k)\{1-\rho_1 C_{11}(k)\}+\rho_1 C_{12}^2(k)+[B(k)]^{-1} \quad (2.20)$$

$$h_{12}(k)=h_{21}(k)=C_{12}(k)[B(k)]^{-1} \quad (2.21)$$

where $B(k)$ is given

$$B(k)=[1-\rho_1 C_{11}(k)-\rho_2 C_{22}(k)+\rho_1\rho_2 C_{11}(k)C_{22}(k)-\rho_1\rho_2 C_{12}^2(k)] \quad (2.22)$$

Further, we have the result connecting the partial structure factor $S_{lm}(k)$ and $h_{lm}(k)$ as

$$S_{lm}(k)=\delta_{lm}(k)+(\rho_l\rho_m)^{1/2}(k)[h_{lm}(k)] \quad (2.23)$$

where δ_{lm} is the kronecker delta and is defined as

$$\delta_{lm}=\begin{cases}1 & \text{for} \quad l=m\\ 0 & \text{for} \quad l\neq m\end{cases} \quad (2.24)$$

The partial structure factors $S_{11}(k)$, $S_{22}(k)$ and $S_{12}(k)$ were solved by taking the Fourier transformation of $h_{lm}(k)$ given by (Gopala Rao and Satpathy, 1990)

$$S_{11}(k)=\left\{1-\rho_1 C_{11}(k)\rho_1\rho_2 C_{12}^2(k)/\left[1-\rho_2 C_{22}(k)\right]\right\}^{-1} \quad (2.25)$$

$$S_{22}(k)=\left[1-\rho_1 C_{11}(k)\right]S_{11}(k)/\left[1-\rho_2 C_{22}(k)\right] \quad (2.26)$$

$$S_{12}(k)=(\rho_l\rho_m)^{1/2}C_{12}(k)S_{11}(k)/\left[1-\rho_2 C_{22}(k)\right] \quad (2.27)$$

$$C_{lm}(r)=-[a_1+b_1 r+dr^3] \;; \qquad r<\sigma_l \quad (2.28)$$

$$C_{12}(r)=-a_1 \;; \qquad r<\lambda \quad (2.29)$$

$$=-\left[a_1+\left\{b(r-\lambda)^2+4\lambda d(r-\lambda)^3+d(r-\lambda)^4\right\}/r\right] \quad ; \quad \lambda<r<\sigma_{12} \tag{2.30}$$

$$=0 \quad ; \quad r>\sigma_{12} \tag{2.31}$$

$$\lambda=(\sigma_2-\sigma_1)/2 \tag{2.32}$$

$$\eta_l = \frac{\pi \rho_l \sigma_l^3}{6} \tag{2.33}$$

$$\eta = \eta_1+\eta_2 \tag{2.34}$$

$$\alpha = \sigma_1/\sigma_2 \tag{2.35}$$

$$a_1=\{(\eta_1+a^3\eta_2)(4+4\eta+\eta^2)-3\eta_2(1-\alpha)^2\left[1+\eta_1+\alpha(1+\eta_2)\right](1+2\eta_1+\eta_2) +(1-\eta^3)-3\eta_1\eta_2(1-\eta)(1-\eta)^2(1-\alpha)^2\}(1-\eta)^{-4} \tag{2.36}$$

$$\alpha^3a_2=\{(\eta_1+a^3\eta_2)(4+4\eta+\eta^2)-3\eta_1(1-\alpha)^2\left[1+\eta_1+\alpha(1+\eta_2)\right](1-\eta_1+2\eta_2) +(1-\eta^3)\alpha^3-3\eta_1\eta_2(1-\eta)(1-\eta)^2(1-\alpha)^2\alpha\}(1-\eta)^{-4} \tag{2.37}$$

$$\beta_1=b_1\sigma_1=-6\left[\eta_1g_{11}^2+\eta_2(1+\alpha)^2\alpha g_{12}^2/4\right] \tag{2.38}$$

$$\beta_2=b_2\sigma_2=-6\left[\eta_2g_{22}^2+\eta_1(1+\alpha)^2\alpha g_{12}^2/4\alpha^3\right] \tag{2.39}$$

$$\gamma_1=d\sigma_1^3=\left[\eta_1a_1+\alpha^3\eta_2a_2\right]\Big/2=\alpha^3\gamma_2 \tag{2.40}$$

$$b\sigma_2=-3(1+\alpha)\left[\eta_1g_{11}/\alpha^2+\eta_2g_{22}\right]g_{12} \tag{2.41}$$

$$g_{11}=\left[(1+\eta/2)+3\eta_2(\alpha-1)/2\right](1-\eta)^{-2} \tag{2.42}$$

$$g_{22}=\left[(1+\eta/2)+3\eta_1(\alpha-1)/2\alpha\right](1-\eta)^{-2} \tag{2.43}$$

$$g_{12}=\left[(1+\eta/2)+3(1-\alpha)(\eta_1-\eta_2)/2(1+\alpha)\right](1-\eta)^{-2} \tag{2.44}$$

And finally obtaining the total structure factor

$$S(k)=\sum_{l=1}^{2}\sum_{m=1}^{2}(C_lC_m)^{1/2}\frac{f_l(k)f_m(k)}{C_1f_1^2(k)+C_2f_2^2(k)}S_{lm}(k) \tag{2.45}$$

where $f_l(k)$ and $f_m(k)$ are the atomic scattering factors taken from literature (Venkatesh *et al.*, 2003) and C_l and C_m are the atomic fractions of the l^{th} and m^{th} species respectively.

Thus for the binary alloy, the total structure factor can be written as

$$S(k)=\left[C_1f_1^2S_{11}(k)-2(C_1C_2)^{1/2}f_1f_2S_{12}(k)+C_2f_2^2S_{22}(k)\right]\times\left[C_1f_1^2+C_2f_2^2\right]^{-1} \quad (2.46)$$

The Fourier analysis of partial and total correlation functions gives their corresponding partial and total radial distribution function, which can be defined by the following equation

$$g_{lm}(r) - 1 = \frac{1}{2\pi^2(\rho_l\rho_m)^{1/2}}\int_0^\infty [S_{lm}(k)-\delta_{lm}]\, k \sin(kr)\, dr \quad (2.47)$$

Here, δ_{lm} is the Kronecker delta and is given in Eqn. (2.24)

Co-ordination numbers in liquid binary alloys were obtained by integrating the pair correlation functions $g_{lm}(r)$ up to the first minimum (r_{min})

$$\psi_{lm}=4\pi\rho_{lm}\int_0^{r_{min}} g_{lm}(r)\, r^2 dr \quad (2.48)$$

2.3. RESULTS AND DISCUSSIONS

2.3.1. Concentration dependent structural characteristics in Cu-In alloys

2.3.1.1. *Partial and Total Structure factors in Cu-In alloys:*

Table 2.1. Input parameters of liquid Cu-In alloys with σ as the diameter, ε/k_B as the depth, λ as the breadth of the square well and ρ_n as the number density

Metals	σ(Å)	ε/k_B	λ	ρ_n
Cu	2.36	300.00	1.60	0.07408
In	2.83	173.76	1.65	0.03686

As seen from Table 2.2, the first peak positions of partial and total structure factors are invariant of In and Cu atoms in the melts. However, the first peak height of S(k) decreases by around 7.5 % with increasing concentration of In from 25% to 34% In, whereas Cu-Cu partial correlation decreases by about 11% with increasing In composition in the melts.

Table 2.2. Partial and total structure factors with the first peak position, k and peak heights S(k) of Cu-In alloys at different compositions of In

% In in Cu-In	Temp (K)	k_{Cu-Cu} $(\dot{A}^{-1})$	$S_{Cu-Cu}(k)$	k_{In-In} $(\dot{A}^{-1})$	$S_{In-In}(k)$	k_{Cu-In} $(\dot{A}^{-1})$	$S_{Cu-In}(k)$	k $(\dot{A}^{-1})$	S(k)
25	950	2.80	2.33	2.60	1.57	2.70	0.93	2.70	2.78
27	950	2.80	2.25	2.60	1.61	2.70	0.93	2.70	2.75
29	950	2.70	2.18	2.60	1.65	2.70	0.92	2.70	2.71
32	963	2.70	2.11	2.60	1.70	2.70	0.90	2.70	2.63
34	963	2.70	2.07	2.60	1.72	2.70	0.88	2.70	2.57

It means that increasing Cu-Cu correlation with increasing percent of In is controlling the total correlation functions. Further, the first peak height of pure liquid Cu and In are 2.5 and 2.7 respectively, however, the first peak height of the total structure factor of liquid Cu-In alloys was observed in between 2.6 to 2.8 for investigated compositions. This is a clear indication of the mixing of components at the atomic level in liquid Cu-In alloys.

Extensive computations have been carried out for the liquid Cu-In alloys at five different atomic fractions of In at two different temperatures (950 K and 963 K) with SW parameters of pure components as given in Fig. 2.1. These temperatures and compositions were taken under investigation based on the estimation of atomic structures via X-ray diffraction by Mudry *et al.* (Mudry *et al.*, 2013). Three Partial structure factors required for a full description of total atomic structures in liquid Cu-In are determined by Eqns. (2.25) to (2.27) and are illustrated in Figs. 2.1 (a) to (c).

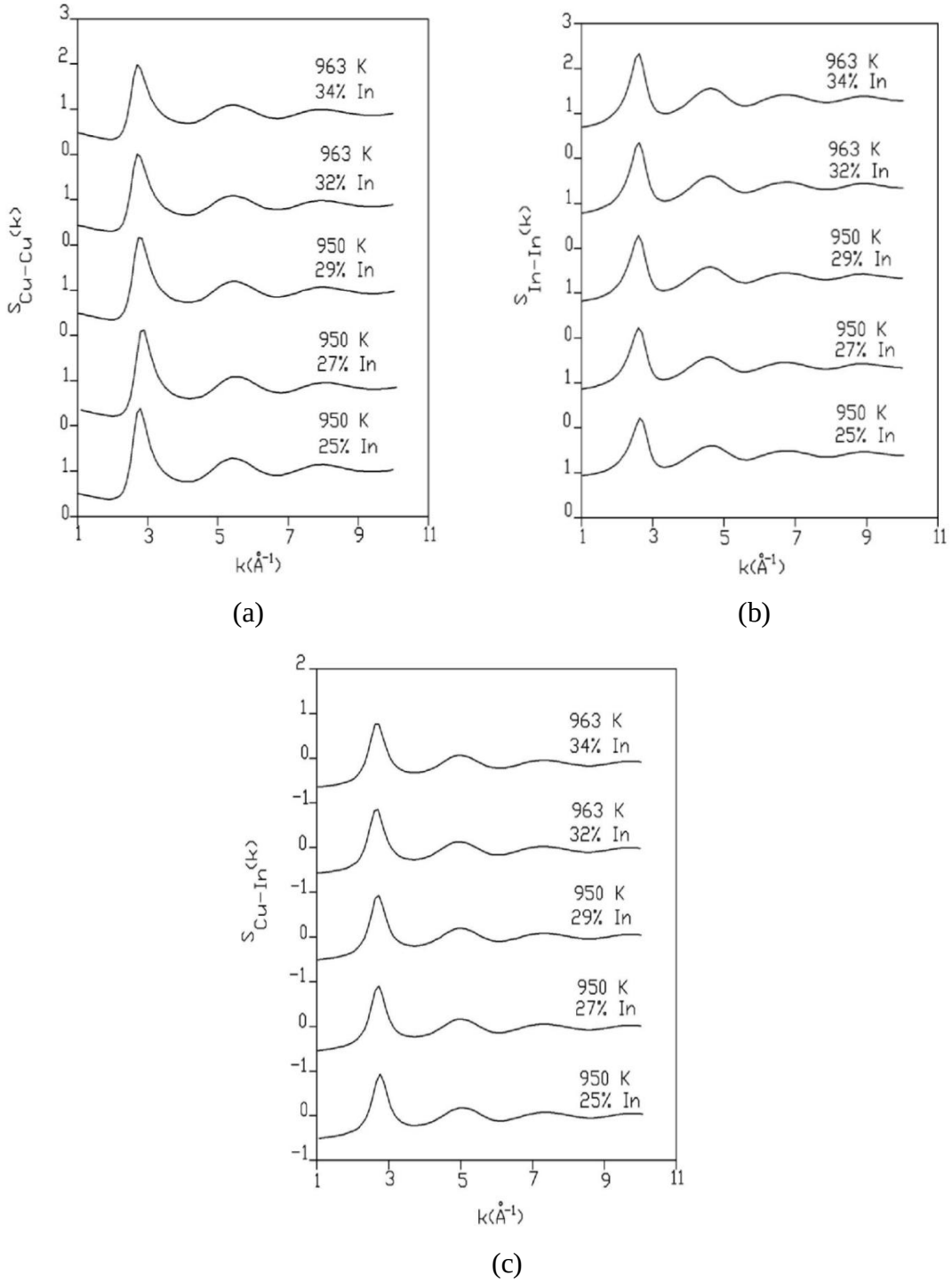

Figure 2.1: Partial structure factors of liquid Cu-In alloys, (a) $S_{Cu\text{-}Cu}(k)$, (b) $S_{In\text{-}In}(k)$, (c) $S_{Cu\text{-}In}(k)$

We observe from Fig. 2.1 (a) to (c) that with an increasing concentration of In, the first peak intensity of $S_{Cu\text{-}Cu}(k)$ decreases where as that of $S_{In\text{-}In}(k)$ increases, which may be due to larger size of In. Very small fluctuations in $S_{Cu\text{-}In}(k)$ were observed and its first peak intensity decreases from 0.93 to 0.88 with an increasing composition of In from 25% to 34 %. It must be noted that no experimental data of PSFs of liquid Cu-In alloys have been reported till now in the literature.

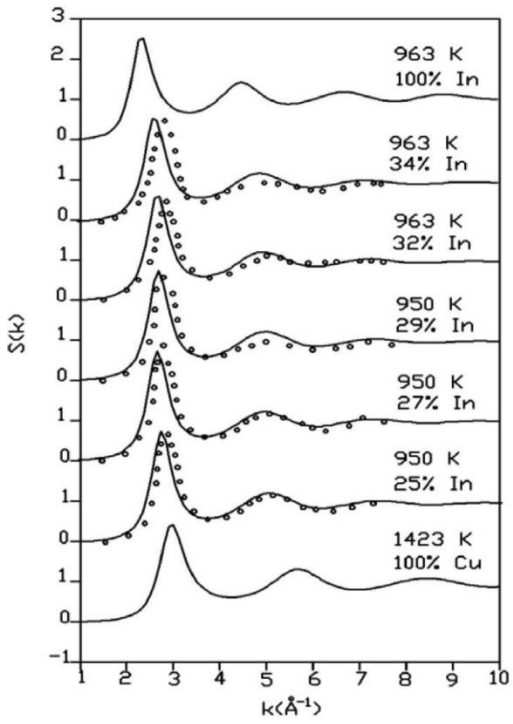

Figure 2.2: Composition dependent total structure factor of liquid Cu-In alloys; (——) theoretical values; (o o o o) experimental values (Mudry *et al.*, 2013).

Mudry *et al.* (Mudry *et al.*, 2013) recently reported the total structure factor S(k) and pair correlation function g(r) of liquid Cu-In alloys at five different compositions of In using X-ray diffraction technique. In Fig. 2.2 we illustrate the comparison between the computed and experimental values (Mudry *et al.*, 2013) of total structure factor as a function of In compositions in the considered liquid alloys. The computed values of total structure factors are in fair agreement with experimental values. In addition, the computed values of the structure factor of pure liquids are also given in Fig. 2.2 to understand the change in atomic-level structural features of the melts on alloying

It should be noted that the position of the principal peak of the partial and total structure factors are independent of both composition and temperature. Fig. 2.2 also indicates that the shifting of binary peaks towards pure In peak with increasing In concentration in Cu-In mixtures. The position and intensity of the principal peak are the main structural parameters of considered alloys are given in Table 2.2.

2.3.1.2. *Partial and Total radial distribution functions in Cu-In alloys:*

In Fig. 2.3 we compare the computed and experimental values (Mudry *et al.*, 2013) of total radial distribution function (RDF) as a function of In compositions at two temperatures as obtained from Fourier transform of total structure factors of respective alloys.

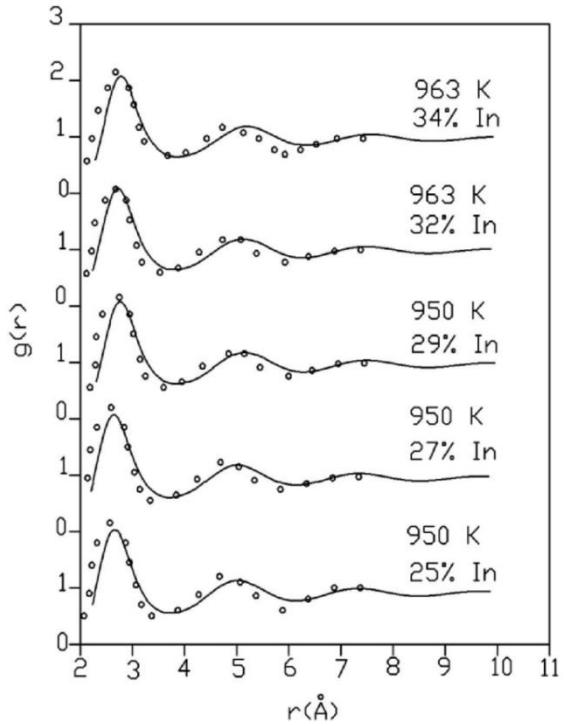

Figure 2.3: Composition dependent radial distribution function g(r) of liquid Cu-In alloys; (——) theoretical values; (o o o o) experimental values (Mudry *et al.*, 2013).

It can be seen that the computed values of the pair correlation function reproduce the shape and position of the X-ray measured data (Mudry *et al.*, 2013).

Since the microscopic structural features are mainly characterized by the principal peak of structure factor and RDF hence these features of the investigated

alloys are given in Table 2.3 The separation between Cu-Cu, In-In, and Cu-In pairs in the considered alloys, $r_{Cu\text{-}Cu}$, $r_{In\text{-}In}$ and, $r_{Cu\text{-}In}$ were estimated from the first peak of each partial pair correlation function and are shown in Table 2.3.

Table 2.3. Partial and total radial distribution functions with the first peak position, r and peak heights g(r) of Cu-In alloys at different compositions of In

% In in Cu-In	Temp (K)	$g_{Cu-Cu}(r)$	r_{Cu-Cu} (Å)	$g_{In-In}(r)$	r_{In-In} (Å)	$g_{Cu-In}(r)$	r_{Cu-In} (Å)	g(r)	r_{max}(Å)
25	950	2.78	2.54	2.99	3.00	2.86	2.77	2.13	2.76
27	950	2.77	2.54	2.98	3.01	2.84	2.77	2.12	2.78
29	950	2.76	2.54	2.96	3.00	2.83	2.77	2.12	2.82
32	963	2.74	2.54	2.94	3.00	2.81	2.77	2.11	2.83
34	963	2.73	2.54	2.92	3.00	2.80	2.78	2.11	2.85

It can be observed from Table 2.3 that the principal peak height of the partial and pair correlation functions are changeable with In concentration whereas peak positions are independent of concentration and temperature. The nearest neighbor distance for Cu-Cu varies between 2.52 and 2.54 Å while In-In varies between 2.88 to 2.90 Å can be interpreted as the larger size of In atom in comparison of liquid Cu atom.

It must be noted that inter-atomic separation in liquid alloys also infers the average distance between atoms in the first coordination shell. The average value of inter-atomic separation between Cu and In is less than the sum of radii of pure Cu and In. It supports the existence of chemical ordering between Cu and In in liquid Cu-In alloys.

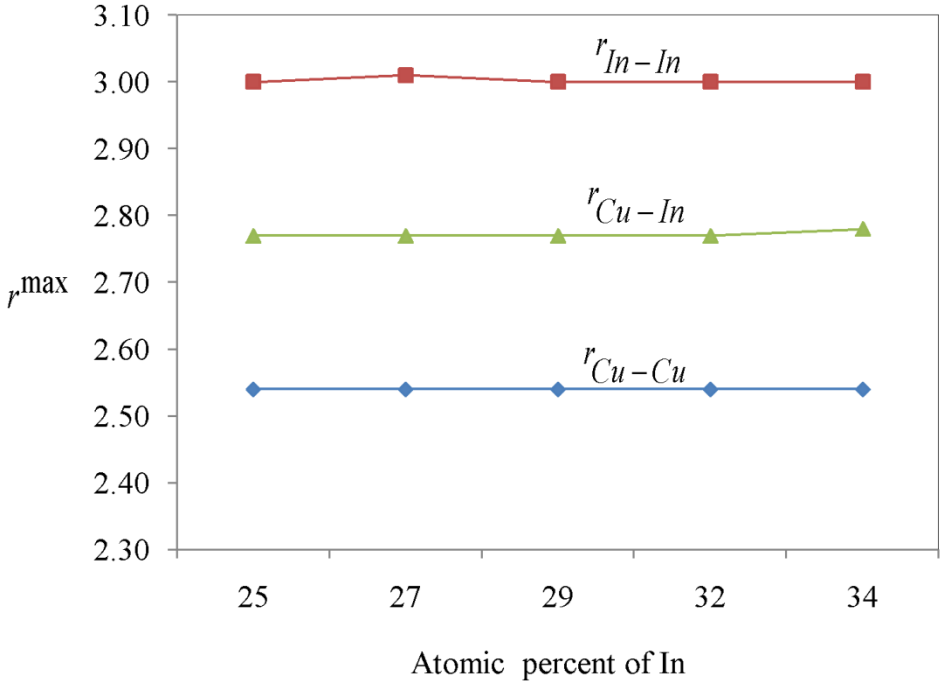

Figure 2.4: The effective radius of first peak position (r^{max}) vs atomic percent of In.

From Fig. 2.4 one can see that In-In separation is always greater than Cu-Cu separation for all considered concentrations. It is interesting to note that, r_{Cu-In} always lies between r_{Cu-Cu} and r_{In-In} whatever the composition and invariant with composition.

2.3.1.3. *Partial and Total Coordination number in Cu-In alloys:*

Coordination numbers of an atom surrounded by similar or different atoms in a binary mixture are obtained by integrated computed of Eqn. (2.48) and are illustrated in Fig. 2.5. Coordination provides atomic-level structural changes in binary liquids through chemical short-range ordering parameters (Trybula, 2016; Trybula *et al.*, 2018; Das *et al.*, 2005). Fig. 2.5 illustrates the number of Cu atoms around Cu, ψ_{Cu-Cu}, the number of In atom around In, ψ_{In-In}, hetero coordination of Cu and In, ψ_{Cu-In} as well as the total coordination number, ψ_{total} computed as a weighted average of atomic composition as a function of In% in liquid Cu-In alloys.

Table 2.4. Partial and total coordination number of Cu-In alloys at different compositions of In

% In in Cu-In	Temp (K)	ψ_{Cu-Cu}	ψ_{In-In}	ψ_{Cu-In}	ψ_{Total}
25	950	9.89	3.47	13.72	13.36
27	950	9.53	3.70	14.06	13.24
29	950	9.18	3.97	13.87	13.13
32	963	8.68	4.36	13.84	13.04
34	963	8.39	4.58	14.10	12.98

One can see that ψ_{Cu-Cu} is always greater than ψ_{In-In} at all investigated compositions and their difference is decreasing with increasing atomic % of In in the melts. ψ_{Cu-In} and ψ_{total} were observed between 13 and 14 and all most unchangeable with composition.

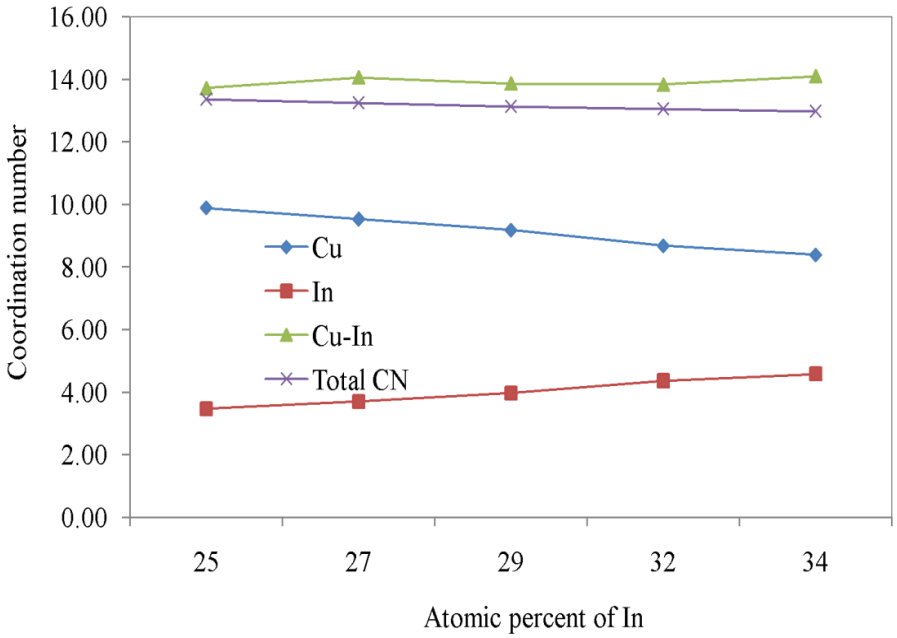

Figure 2.5: Partial and total coordination number of liquid Cu-In alloys at different percentage of In.

Due to the unavailability of experimental or simulation data of coordination numbers of liquid Cu-In alloy yet in literature, comparison of the current data could not be demonstrated.

2.3.2. Concentration dependent structural characteristics in Fe-Al alloy

2.3.2.1. *Partial and total structure factor in Fe-Al alloys:*

S(k) of liquid Fe-Al alloys was computed at four different concentrations of Al, at a temperature of 500 K which is higher than the corresponding liquidus temperature. All the input parameters for the present calculations are given in Table 2.5.

Table 2.5. Potential parameters of liquid Fe and Al.

Metals	$\sigma(\mathring{A})$	ε/k_B	λ	ρ_n
Fe	2.18	425.67	1.76	0.07560
Al	2.32	160.00	1.30	0.06459

σ_{ll} and σ_{mm} corresponds to the diameter of Fe and Al respectively.

As seen from Table 2.6, the first peak positions of partial and total structure factors are invariant of Fe and Al atoms in the melts. However, the first peak height of S(k) increases by around 2.4 % with increasing concentration of Al from 70% to 86% Al, whereas Al-Al partial correlation increases by about 9.8% with increasing Al composition in the melts.

Table 2.6. Partial and total structure factors with the first peak position, k and peak height, S(k) of Fe-Al alloys at different compositions of Al

% Al in Fe-Al	Temp (K)	k_{Fe-Fe} $(\mathring{A}^{-1})$	$S_{Fe-Fe}(k)$	k_{Al-Al} $(\mathring{A}^{-1})$	$S_{Al-Al}(k)$	k_{Fe-Al} $(\mathring{A}^{-1})$	$S_{Fe-Al}(k)$	k $(\mathring{A}^{-1})$	S(k)
70	1493	2.90	1.38	2.90	2.10	2.90	0.68	2.90	2.42
78	1453	2.90	1.29	2.90	2.22	2.90	0.62	2.90	2.46
82	1463	2.90	1.23	2.90	2.27	2.90	2.57	2.90	2.46
86	1433	2.90	1.18	2.90	2.33	2.90	0.52	2.90	2.48

It means that increasing Al-Al correlation with increasing percent of In is controlling the total correlation functions. Further, the first peak height of pure liquid Fe and Al are 2.85 and 2.38 respectively, however, the first peak height of the total structure factor of liquid Fe-Al alloys was observed in between 2.42 to 2.48 for investigated compositions. This is a clear indication of the mixing of components at the atomic level in liquid Fe-Al alloys.

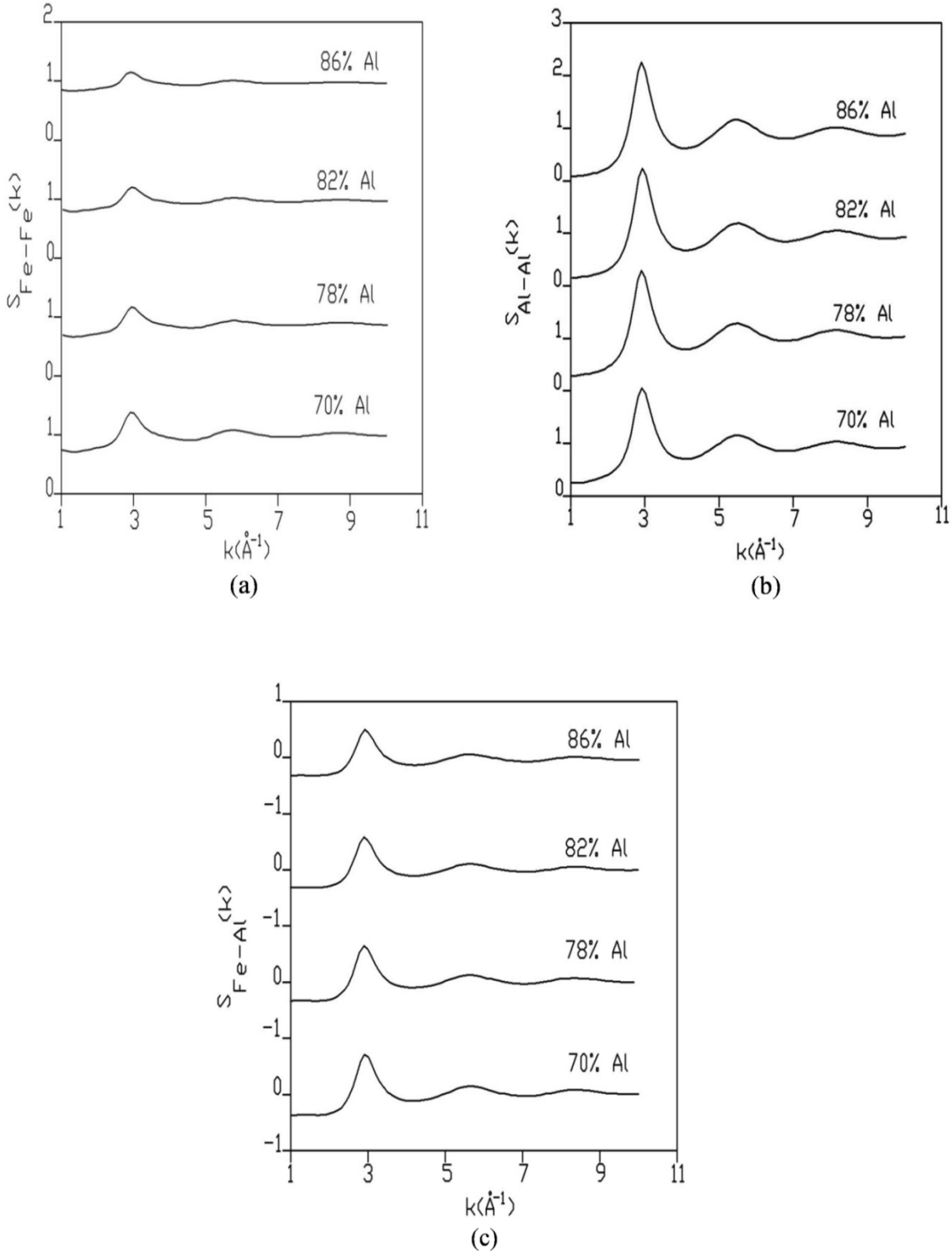

Figure 2.6: PSFs against k at different atomic % of Al: (a) $S_{Fe\,-\,Fe}(k)$, (b) $S_{Al\,-\,Al}(k)$ and, (c) $S_{Fe\,-\,Al}(k)$.

Fig. 2.6 (a) to (c) show the PSFs of liquid Fe-Al alloys at different concentrations of Al from 70 to 86 %. We observe that the first peak intensities of $S_{Fe - Fe}(k)$ and $S_{Fe - Al}$ decreases whereas that of $S_{Al - Al}(k)$ increases, which may be due to the larger size of Al.

Fig. 2.7 shows the total structure factor S(k) which was derived through the computed values of PSFs. We find a fair agreement between computed values with experimentally observed S(k) using X-ray diffraction studies(Roik *et al.*, 2014). The S(k) values of pure Fe and Al are also plotted to understand the change in atomic-level structural features of the melts on alloying. It can be seen from Fig. 2 that the first peak position of pure Al at 973 K occurred at a lower momentum vector than pure Fe at 1833 K. Roik *et al.* experimentally (Roik *et al.*, 2014) observed the same pattern for pure liquid Fe and Al.

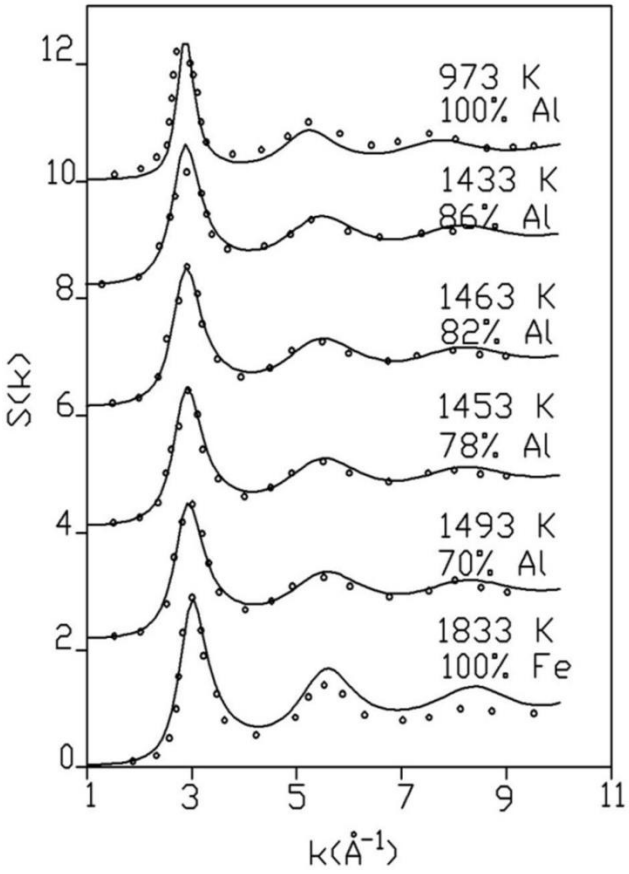

Figure 2.7: Total structure factor against *k* at different atomic % of Al; (——) theoretical values; (o o o o) experimental values (Roik *et al.*, 2014).

Fig. 2.7 shows that the intensity of the first peak and its positions are almost independent of concentrations and temperatures, however, the intensity of the first peak of S(k) increases by around 2.4 % with increasing concentration of Al from 70% Al to 86% Al, whereas the first peak height of Al-Al partial correlation increases by about 9.8% with increasing Al composition in the melts. X-ray diffraction data (Roik *et al.*, 2014), and our computed values of liquid Fe and Al show that the first peak intensity of these two are 2.90 and 2.20 respectively whereas, the first peak of mixture was observed in between 2.42 to 2.48.

2.3.2.2. *Partial and total radial distribution function in Fe-Al alloys:*

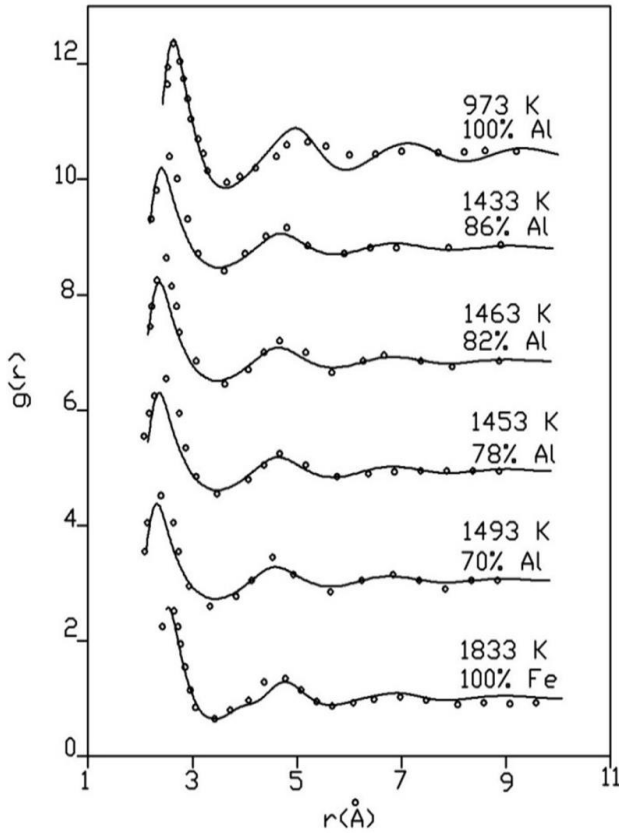

Figure 2.8: Composition dependent radial distribution function g(r) of Fe-Al liquid alloys; (——) theoretical values; (o o o o) experimental values (Roik *et al.*, 2014).

Fig. 2.8 shows that the first peak position for partial radial distribution function of $g_{Fe-Fe}(r)$ and $g_{Al-Al}(r)$ occurs at 2.37 and 2.51Å respectively while first

peak position for pure Fe and Al occurs at 2.57 and 2.83Å respectively. This shows that the peak position in alloy corresponds to that of the pure component i.e. the nearest neighbor distance between Fe-Fe atoms is 2.37 Å and that of Al-Al atoms is 2.51 Å.

Table 2.7 indicates that the positions of the first peak of partial and total pair correlation functions are independent of composition and temperature in binary Fe-Al alloys. The first peak position of the partial radial distribution function, $g_{Fe-Fe}(r)$ and $g_{Al-Al}(r)$ occurs at 2.37 Å and 2.51Å respectively, whereas the first peak position of the radial distribution function of pure Fe and Al occur at 2.57 Å and 2.83Å respectively. Al-Al correlation in all the investigated alloys is independent of composition and temperature, whereas Fe-Fe, Fe-Al, and total correlations are changing in the same pattern in the formation of liquid Fe-Al alloys.

Table 2.7 Pair correlation functions characteristics as function of atomic % of Al.

% Al in Fe-Al	Temp (K)	r_{Fe-Fe} (Å)	$g_{Fe-Fe}(r)$	r_{Al-Al} (Å)	$g_{Al-Al}(r)$	r_{Fe-Al} (Å)	$g_{Fe-Al}(r)$	r (Å)	g(r)
70	1493	2.37	2.38	2.51	2.43	2.44	2.36	2.48	2.33
78	1453	2.37	2.39	2.51	2.43	2.44	2.37	2.48	2.35
82	1463	2.37	2.40	2.51	2.43	2.44	2.37	2.48	2.36
86	1433	2.37	2.40	2.51	2.43	2.44	2.38	2.48	2.37

The average value of inter-atomic separation between Fe and Al is less than the sum of radii of pure Fe and Al. It supports the existence of chemical ordering between Fe and Al in liquid Fe-Al alloys.

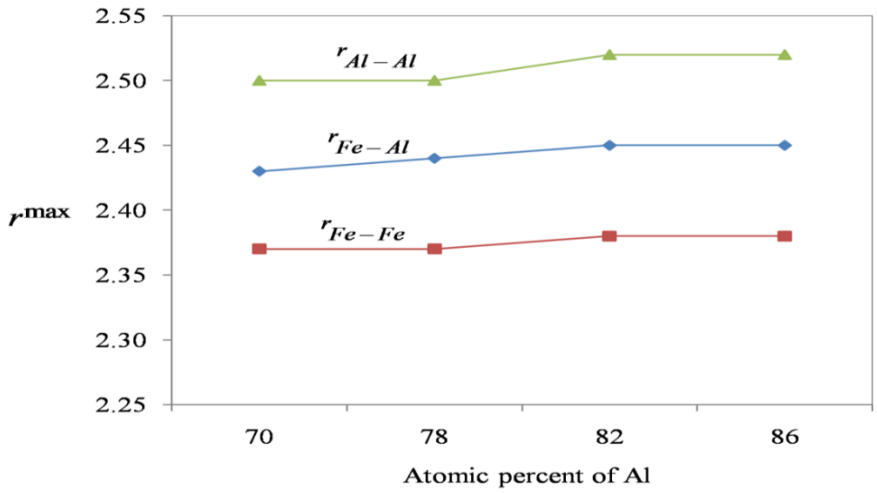

Figure 2.9: Effective radius of first peak position (r^{max}) vs atomic percent of In.

From Fig. 2.9 one can see that Al-Al separation is always greater than Fe-Fe separation for all considered concentrations. It is interesting to note that, $r_{Fe\text{-}Al}$ always lies between $r_{Fe\text{-}Fe}$ and $r_{Al\text{-}Al}$ whatever the composition and invariant with composition.

2.3.2.3. *Partial and total coordination number in Fe-Al alloys:*

Fe in solid state has a coordination number of 6. From Table 2.8 and Fig. 2.10, it can be seen that the partial coordination number of Fe-Fe varies from 3.29 to 1.06 at 1873 K. This shows that there is a good miscibility of Fe in Fe-Al alloy at this working temperature. The partial coordination number of Al-Al increases from 8.13 to 10.03 with increase in Al concentration.

Table 2.8. Coordination numbers of pure component and alloys of Fe-Al as a function of atomic % of Al.

% Al in Fe-Al	Temp (K)	Ψ_{Fe-Fe}	Ψ_{Al-Al}	Ψ_{Fe-Al}	Ψ_{Total}
70	1873	3.29	8.13	11.88	11.42
78	1873	2.34	8.84	11.81	11.19
82	1873	1.96	9.24	11.68	11.20
86	1873	1.47	9.64	11.87	11.12
90	1873	1.06	10.03	11.70	11.11

One can assume that Al which has a coordination number of 12 and a face center cubic structure (fcc) in its solid-state also shows a good miscibility nature and retains a fraction of its fcc lattice in Fe-Al alloy.

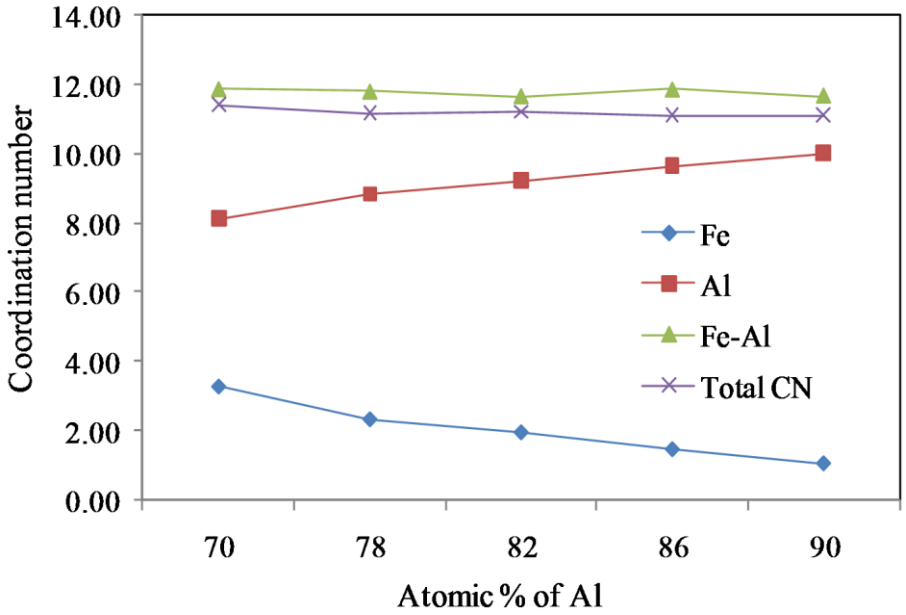

Figure 2.10: Coordination numbers of pure component and alloys as a function of atomic % of Al.

The total coordination number varies between 11.42 to 11.11 throughout the whole concentration range, which is very close to coordination number equal to12 used in quasi-lattice (QL) formalism (Akinlade *et al*., 2000).

BHATIA-THORNTON FLUCTUATIONS AND ASSOCIATED PROPERTIES OF LIQUID BINARY ALLOYS

3.1. INTRODUCTION

The knowledge of structure functions, atomic dynamics, and thermophysical properties of metallic melts are important for two fundamental reasons. Firstly, to understand the metallurgical processing of solid alloys and secondly, to model new materials required for sophisticated purposes. During alloying of metallic melts at different compositions and temperatures, some structural changes and properties of individual metals get suppressed and evolve with new properties. Various authors investigated the composition-dependent thermodynamic and surface properties of the compound forming liquid binary alloys (Meyer *et al*., 2019; Ning *et al*., 2010; Gruner and Hoyer, 2008; Bossa *et al*., 2017; Hultgren *et al*., 1973; Okamoto, 2005; Knott and Mikula, 2006; Itabashi *et al*., 2001;). However, there are very few manuscripts on the microscopic structure functions of liquid binary alloys either in theoretical or experimental studies.

Recently, Mudry *et al.*(Mudry *et al*., 2013) reported X-ray diffraction studies on liquid Cu-In alloys at five different compositions and confirmed the existence of Warren-Cowley chemical short-range order (CSRO) parameter, α' in Cu-In alloys. Investigations in free energy of mixing and composition fluctuations in the long-wavelength limit using quasi-lattice (QL) theory by Akinlade and Singh (Akinlade and Singh, 2002) suggest clearly that the hetero coordination occurs in Cu rich region, where as homo coordination is favorable in indium rich region of Cu-In melts. Roik *et al.* (Roik *et al.*, 2014) and Il'inskii *et al.* (Il'inskii *et al.*, 2002) reported X-ray diffraction studies on liquid Fe-Al alloys. Akinlade *et al.* (Akinlade *et al.*, 2000) reported the existence of CSRO, α' in Fe-Al alloys.

A well-established statistical mechanics model using Percus-Yevick (PY) hard-sphere reference system invoked with square-well (SW) attractive part has been successfully applied to investigate structure functions, transport coefficients, thermodynamic and thermophysical properties of liquid metals and binary liquid

alloys (Gopala Rao and Venkatesh,1989; Gopala Rao and Venkatesh, 1989; Dubinin *et al*., 2014; Dubinin, 2019; Mishra *et al*., 2015; Mishra and Venkatesh, 2008; Lalneihpuii *et al*. 2019; Mishra and Shrivastava *et al*., 2017). SW model calculation is an efficient method to study the complexities in binary liquids (Lalnuntluanga *et al*., 2021; Mishra and Venkatesh, 2008; Mishra *et al*., 2020). $S_{CC}(0)$ and α' have been derived through the long-wavelength limit of partial structure factors to analyze the chemical ordering binary melts. Bhatia and Thornton (BT) (Bhatia and Thornton, 1970; Bhatia *et al*., 1974; Bhatia, 1977) proposed thermodynamically important three correlation functions which depend on the fluctuations in number and concentration using a linear combination of Ashcroft-Langreth (AL) partial structure factors (PSFs) (Ashcroft and Langreth, 1967)

In this chapter, we compute the detailed analysis of the BT structure factors for Cu-In and Fe-Al liquid binary alloys using AL-PSFs derived by considering SW interatomic interactions between the particles (Venkatesh *et al*., 2003) The composition-dependent concentration fluctuation at zero momentum vector i.e., $S_{CC}(0)$ computed from the long-wavelength limit of partial structure factors (Akinlade and Singh, 2002; Akinlade *et al*., 2000; Odusote, 2008) is less than the ideal values for both Cu-In and Fe-Al alloys within the investigated compositions. This indicates the formation of a chemical bond between unlike atoms and the existence of strong chemical ordering in the investigated alloys (Dubinin, 2019; Mishra and Venkatesh, 2008). The direct investigation of thermodynamically important $S_{CC}(0)$ using molecular dynamic simulations has not been given till now, and its experimental determination is not an easy task. Thus, theoretical derivation and computation of $S_{CC}(0)$ for such compound forming alloys is important information to analyze the complexities in the investigated alloys.

3.2. THEORY

The BT partial structure factor were calculated using AL type partial structure factors of Cu-In and Fe-Al liquid alloys. The BT correlation functions in binary alloys are linearly relate to the partial structure factors $S_{lm}(k)$(Gopal Rao and Satpathy, 1990; Venkkatesh *et al*., 2003) as follows

$$S_{NN}(k) = \left[C_1 S_{12}(k) + C_1 S_{22}(k) + 2 (C_1 C_2)^{1/2} S_{12}(k) \right] \tag{3.8}$$

$$S_{CC}(k) = C_1 C_2 \left[C_1 S_{11}(k) + C_1 S_{22}(k) - 2 (C_1 C_2)^{1/2} S_{12}(k) \right] \tag{3.9}$$

$$S_{NC}(k) = \left[C_1 C_2 S_{11}(k) - C_1 C_2 S_{22}(k) - (C_2 - C_1) (C_1 C_2)^{1/2} S_{12}(k) \right] \tag{3.10}$$

where C_1 and C_2 are the atomic fractions of the component 1 and 2 respectively.

The concentration fluctuation, $S_{CC}(0)$, which is an important parameter to understand the structure and the binding of atoms at the microscopic level, is related to ordering effetcs in binary liquid alloys (Singh, 1987; Singh, 1993). Further $S_{CC}(0)$ can be calculated through the computed PDFs in the long wavelength limits.

$$S_{CC}(0) = C_1 C_2 [C_2 S_{11}(0) + C_1 S_{22}(0) - 2 (C_1 C_2)^{1/2} S_{12}(0)] \tag{3.11}$$

Here $S_{11}(0)$, $S_{22}(0)$ and, $S_{12}(0)$ are the long wavelength limit of AL type correlation functions presented in chapter 2 by Eqns. (2.25) to (2.27) in the limit of $k \to 0$

$$S_{11}(0) = \left[\frac{[1 - \rho_{11} C_{11}(0) - \rho_1 \rho_2 C_{12}^2(0)]}{1 - \rho_2 C_{22}(0)} \right]^{-1} \tag{3.12}$$

$$S_{22}(0) = \frac{[1 - \rho_1 C_{11}(0)] S_{11}(0)}{1 - \rho_2 C_{22}(0)} \tag{3.13}$$

$$S_{12}(0) = \frac{(\rho_1 \rho_2)^{1/2} C_{12}(0) S_{11}(0)}{1 - \rho_2 C_{22}(0)} \tag{3.14}$$

where

$$\rho_1 C_{11}(0) = -24\eta_1 \left[\frac{a_1}{3} + \frac{b_1\sigma_1}{4} + \frac{d\sigma_1^3}{6} \right] + \frac{8\eta_1 \varepsilon_{11} (\lambda_{11}^3 - 1)}{k_B T} \tag{3.15}$$

$$\rho_2 C_{22}(0) = -24\eta_2 \left[\frac{a_2}{3} + \frac{b_2\sigma_2}{4} + \frac{d\sigma_2^3}{6} \right] + \frac{8\eta_2 \varepsilon_{22} (\lambda_{22}^3 - 1)}{k_B T} \tag{3.16}$$

$$C_{12}(0) = \frac{-4\pi\varepsilon_{12}\sigma_{12}^3 (\lambda_{12}^3 - 1)}{3k_B T} - \frac{4\pi a_1 \sigma_{12}^3}{3} - 4\pi\sigma_1^3 \left\{ \frac{b(\sigma_1 + 2\sigma_2)}{12} + \frac{\pi d\sigma_1 (3\sigma_1 + 5\sigma_2)}{10} + \frac{d\sigma_1^2 (2\sigma_1 + 3\sigma_2)}{30} \right\} \tag{3.17}$$

Warren-Cowley CSRO parameter, α' indicates chemical ordering or segregating behavior in binary liquid alloys. An interesting relationship between $S_{CC}(0)$ and α' for the first neighbor shell can be given as

$$\alpha' = \frac{S_{CC}(0) - S_{CC}^{id}(0)}{\psi S_{CC}(0) - S_1} = \frac{S_1}{\psi S_{CC}(0) - S_1} \tag{3.18}$$

Here $S_{CC}^{id}(0) = C_1 \times C_2$ and S_1 is the deviation of the $S_{CC}(0)$ from its ideal value, Z is the total coordination number.

The concentration dependent isothermal compressibility χ_T has been calculated through the Kirkwood-Buff's equation (Mishra and Venkatesh, 2008), which is given by

$$\rho k_B T \chi_T = [1 - C_1 \rho_{11} C_{11}(0) + C_2 \rho_{22} C_{22}(0) - 2 C_1 C_2 (\rho_1 \rho_2)^{1/2} C_{12}(0)]^{-1} \tag{3.19}$$

3.3. RESULTS AND DISCUSSIONS

We compute Bhatia-Thornton (BT) correlation functions namely number-number $S_{NN}(k)$, concentration-concentration $S_{CC}(k)$ and number-concentration $S_{NC}(k)$ using AL PSFs with SW model potential function. $S_{NN}(k)$ and $S_{CC}(k)$ are thermodynamically important functions to understand complexities of binary mixtures. Thus, the BT structure factors can be derived from theoretically or experimentally generated AL or Faber-Ziman (FZ) types partial structure factors using Eqns. (3.8) to (3.10). These correlation functions are very useful in binary liquids because they are directly linked with various thermodynamic parameters.

$S_{NN}(k)$ gives the overall static structure factor of the melts and which can be measured directly. It means that $S_{NN}(k)$ deals with the number of scattering sites present in the melts and does not concern with the chemical identity of those sites.

$S_{CC}(k)$ and its Fourier transform provide information on the segregation or chemical ordering of constituent chemical species in the melts. $S_{CC}(k)$ fluctuates around the product of the concentrations in binary melts and can be measured directly in a neutron diffraction experiment.

$S_{NC}(k)$ and its Fourier transform is the correlation between sites of the scattering nuclei and the constituting elements which occupy those sites. For an ideal solution $S_{NC}(k)=0$ and global structure of binary melts is present in $S_{NN}(k)$. Long wavelength limit of BT correlation functions are readily linked with the important thermodynamic parameters of the alloys and also helpful to explain the chemical complexities in the binary mixture.

3.3.1. Cu–In alloys

The potential parameters of the pure components for the evaluation of partial structure factors are given in Table 2.1 in Chapter 2. The computed values of BT correlation functions as a function of In composition are given in Figs. 3.1 (a-c).

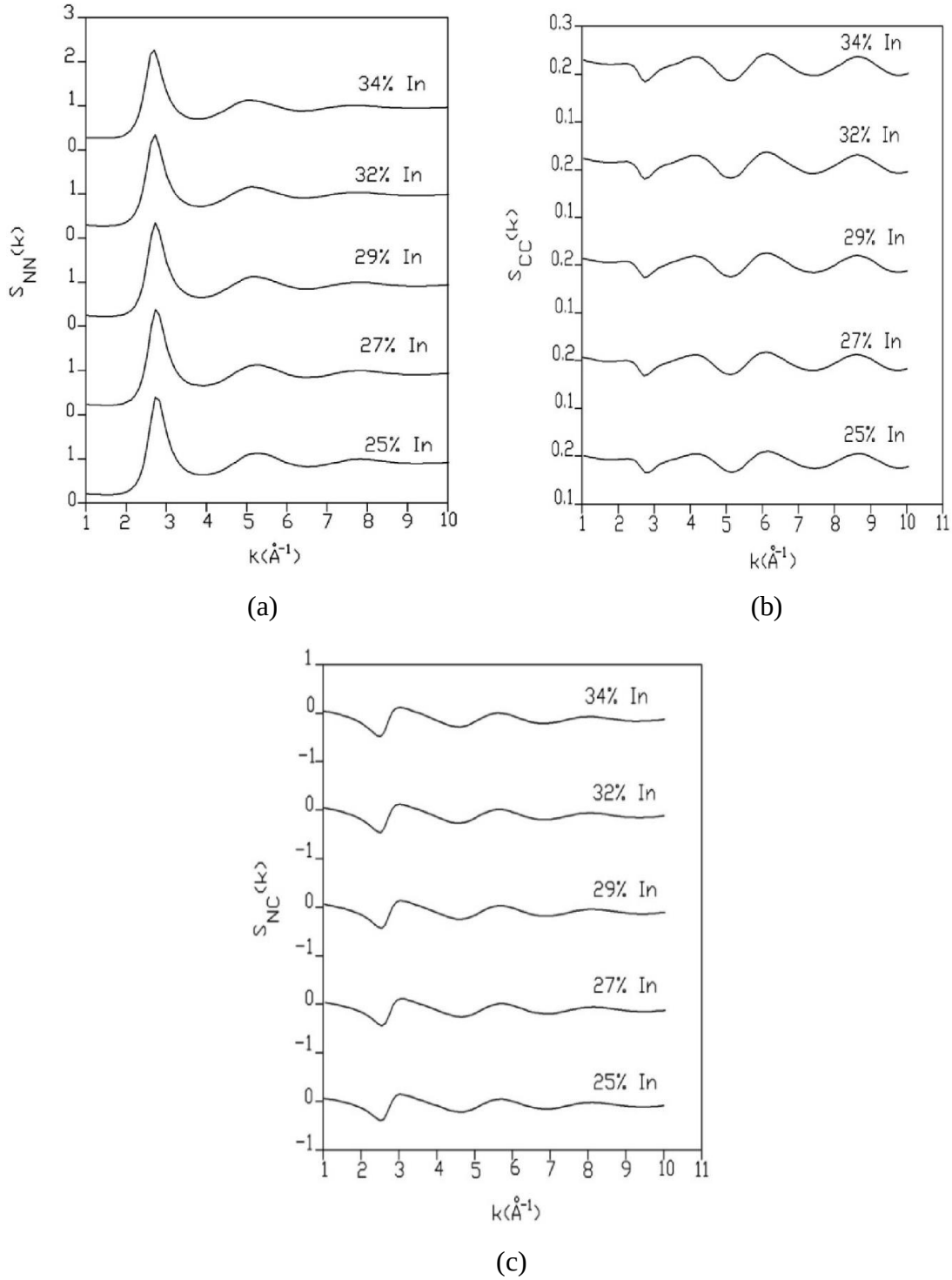

Figure 3.1: Bhatia-Thornton correlation functions; (a) $S_{NN}(k)$ versus k (b) $S_{CC}(k)$ versus k (c) S_{NC} (k) versus k

$S_{NN}(k)$ provides global non-crystalline structural functions. The values of $S_{NN}(k)$ varies comparably as the total structure factor $S(k)$ such that their first peak position occurs at the same position i.e., $2.70\mathring{A}^{-1}$, and the intensities of the first peak of $S_{NN}(k)$ decreases with increasing In concentration as in $S(k)$ (Mudry *et al*., 2013) The $S_{CC}(k)$ oscillates about the product of the concentration of Cu and In i.e., $C_{Cu}C_{In}$ as shown in Fig.3.1 (b).The ideal values of $S_{CC}(k)$ is equal to $C_{Cu}C_{In}$ and as is observed from Fig. 3.1 (b), it is found that at around 2.7Å^{-1} the graph show minimum deviation from ideal behavior for all investigated melts. $S_{CC}(k)$ is also related to charge-charge structure factors in ionic liquids and which is also linked with $S_{NC}(k)$ (Venkatesh and Mishra, 2005)

$$S_{CC}(k)=C_M C_X S_{qq}(k), \tag{3.20}$$

$$S_{NC}(k)=(C_X/Z_M)S_{Nq}(k) \tag{3.21}$$

here q is the charge on chemical species

From Fig.3.1 (c) it can be inferred that $S_{NC}(k)$ oscillates around zero. Further, $S_{NC}(k)$ shows a significant decrease at or around the first peak position of $S(k)$ for liquid Cu-In alloys. The small fluctuation in $S_{NC}(k)$ around zero indicates weak correlation between number-concentration fluctuations in the melts.

Thus, from Fig. 3.1(a), (b), and (c) it can be concluded that the values of $S_{NN}(k)$ have been the highest weighing factor amongst BT correlations in the expression of the total structure factor $S(k)$.

$S_{CC}(k)$ has been computed for various liquid Cu-In alloys for entire k region and especially in the long-wavelength limit at k tends to zero, $S_{CC}(0)$ provides important information on Cu-Cu co-ordination, In-In co-ordination and Cu-In co-ordination in the Cu-In melts. This information cannot be withdrawn from the X-ray scattering studies of the melts (Salmon and Zeidler, 2013). $S_{CC}(0)$ can be

obtained experimentally (Akinlade and Singh, 2002) through activity data of liquid binary alloys. The computed values of concentration-concentration fluctuation at the long wavelength limit, $S_{CC}(0)$ and $S^{id}_{CC}(0)$ at different atomic fractions of In in Cu-In melts are given in Table 3.1.

Table 3.1 The concentration-concentration fluctuation at the long wavelength limit $S_{CC}(0)$ and its ideal value, $S^{id}_{CC}(0)$, Co-ordination number, ψ and Chemical short range order parameter, α' of Cu-In alloys at different compositions of In.

% In	$S_{CC}(0)$ (Cal.)	$S_{CC}(0)$ (Exp.)	$S^{id}_{CC}(0)$	ψ	α' (Square-Well)	α' (Quasi-Lattice)
25	0.098	0.102	0.187	11.420	-0.064	-0.071
27	0.107	0.114	0.197	11.190	-0.061	-0.062
29	0.114	0.122	0.205	11.208	-0.058	-0.054
32	0.124	0.131	0.217	11.123	-0.055	-0.042
34	0.130	0.143	0.224	11.110	-0.053	-0.034

Table 3.1 shows an excellent agreement between the computed values of $S_{CC}(0)$ with experimental values (Akinlade and Singh, 2002). Further, a compound forming tendency between Cu and In atoms at all investigated compositions can also be observed from Table 3.1.

Deviation of $S_{CC}(0)$ from its ideal value i.e., $S^{id}_{CC}(0) > S_{CC}(0)$ indicates the formation of chemical compound between Cu and In atoms in Cu rich Cu-In melts. The computed results of the composition dependent $S_{CC}(0)$, its ideal values $S^{id}_{CC}(0)$ and experimental value derived from activity data (Akinlade and Singh, 2002) are plotted in Fig.3.2. The results obtained by using our theoretical model calculations without any experimental parameters unlike others (Akinlade and Singh, 2002) show a very close agreement with the experimental values

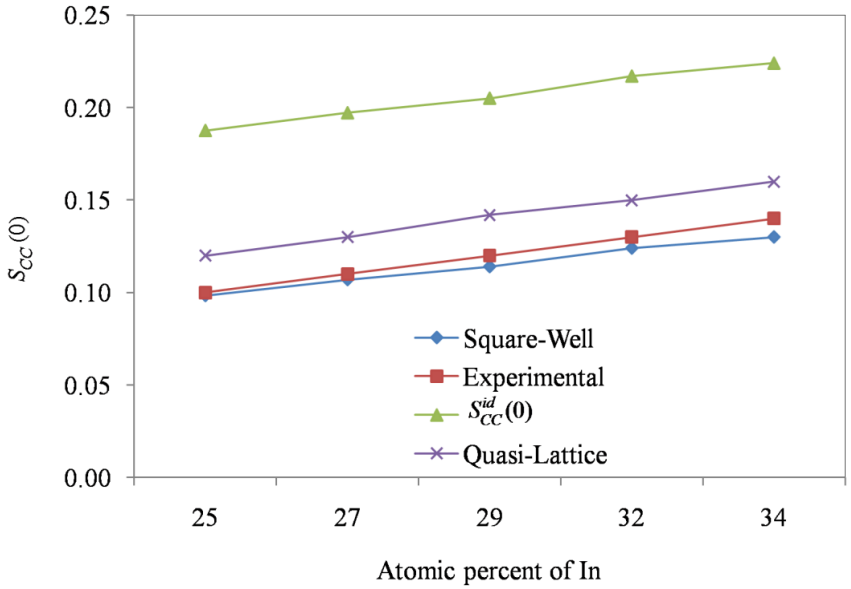

Figure 3.2: Theoretical, ideal, Quasi-Lattice and experimental (Akinlade and Singh, 2002) values of concentration dependence of $S_{CC}(0)$ in Cu-In melts

Fig. 3.2 shows the comparison between α' obtained through SW model and QL model (Akinlade and Singh, 2002). The negative values of α' show the existence of chemical ordering in liquid Cu-In alloys at all the investigated compositions.

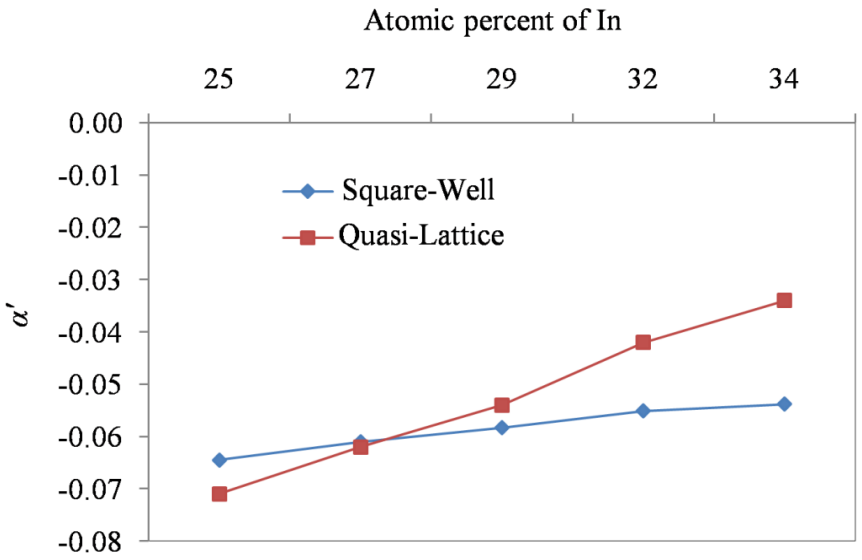

Figure 3.3: Warren-Cowley short range order parameter, α' versus atomic percent of In at 1073 K

The values of α' can be used as a scale to measure the complex forming or segregating nature of the alloy. The values of $\alpha' < 0$ refers to the complex forming nature of the alloy i.e. pairing of unlike atoms as the nearest neighbors whereas the values of $\alpha' > 0$ refer to the segregating nature of the alloy i.e. pairing of like atoms as the nearest neighbors.

The isothermal compressibility, (χ_T) at different composition of the melts has been computed from the well-known Kirkwood-Buff's equation using a long wavelength limit of partial structure factors $S_{lm}(k \to 0)$. The computed values of $S_{Cu\text{-}Cu}(0)$, $S_{In\text{-}In}(0)$, $S_{Cu\text{-}In}(0)$ and χ_T are shown in Table 3.2.

Table 3.2. $S_{Cu\text{-}Cu}(0)$, $S_{In\text{-}In}(0)$ and $S_{Cu\text{-}In}(0)$, and isothermal compressibility, χ_T of Cu-In alloys at different compositions of In

% In	$S_{Cu\text{-}Cu}(0)$	$S_{In\text{-}In}(0)$	$S_{Cu\text{-}In}(0)$	$\chi_T (10^{-12} m^2 Nm^{-1})$
25	0.507	0.614	-0.538	2.832
27	0.535	0.588	-0.541	2.929
29	0.562	0.561	-0.542	3.024
32	0.600	0.524	-0.540	3.160
34	0.624	0.500	-0.537	3.249

The computed values of the isothermal compressibility (χ_T) increases linearly with atomic percent of In beyond liquidus temperature. This implies that as the concentration of In increases in the melts, the void space between the particles increase or the existence of deform nature of the alloy is indicated.

3.3.2. Fe-Al alloys

The potential parameters of the pure components of Fe-Al liquid binary alloys for the evaluation of partial structure factors are given in Table 2.5 in Chapter 2. The computed values of BT correlation functions as a function of Al composition are given in Figs. 3.4 (a-c).

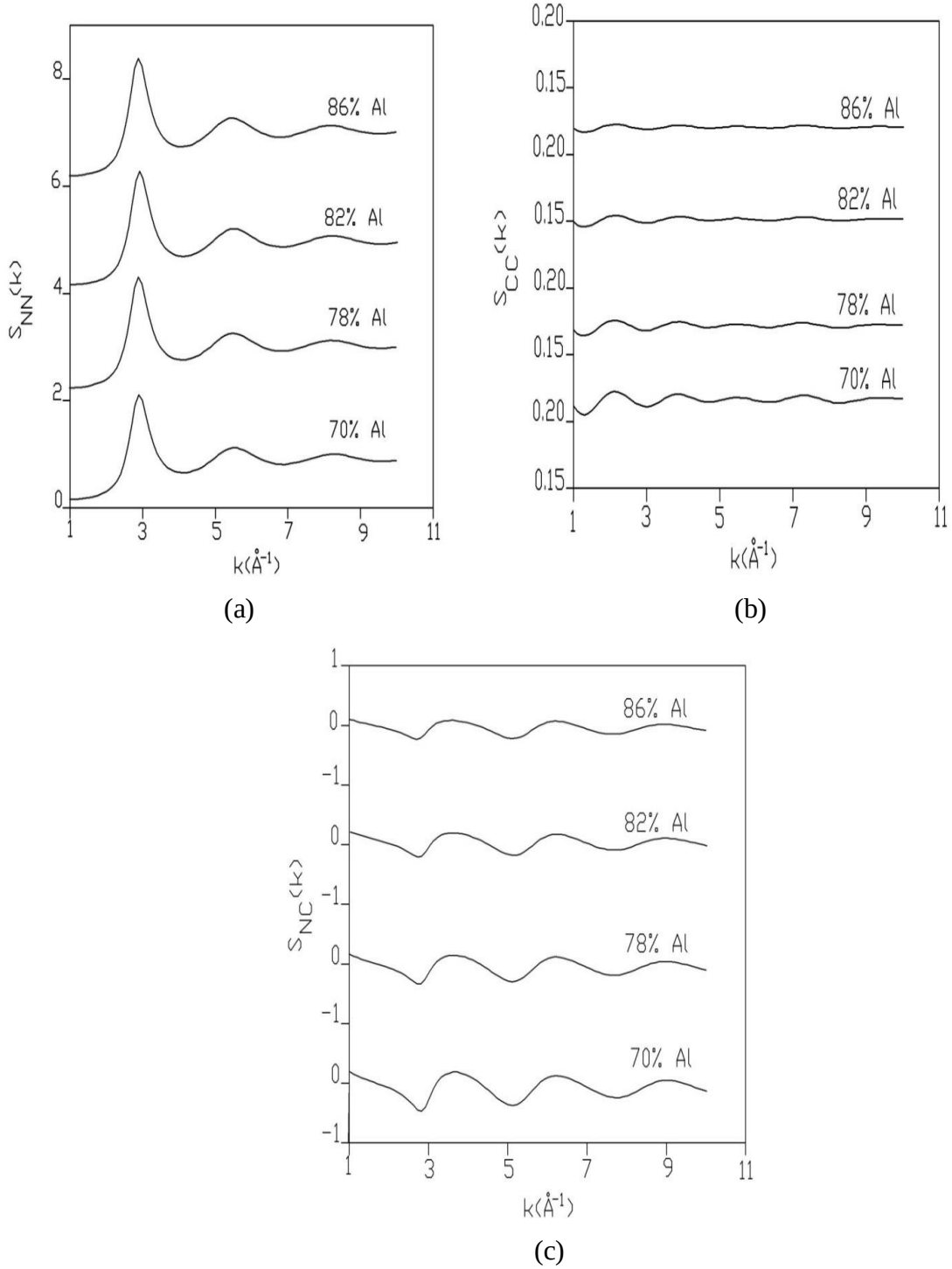

Figure 3.4: Bhatia-Thornton correlation functions; (a) $S_{NN}(k)$ versus k, (b) $S_{CC}(k)$ versus k and (c) S_{NC} (k) versus k

$S_{NN}(k)$ fluctuates in resemblance to the total structure factor $S(k)$, their peak intensity increases with increase in concentration of Al and their first peak position occurs at the same position i.e. 2.90 $\dot{A}^{-1}$. $S_{CC}(k)$ oscillates about the product of pure components concentration i.e., $C_{Fe}C_{Al}$. As is observed from Fig. 3.5 (b) the ideal value i.e. $C_{Fe}C_{Al}$ shows a maximum deviation from ideal behavior at around 1.60 $\dot{A}^{-1}$. Massobrio *et al.*(Massobrio *et al.*, 2004) shows that $S_{CC}(k)$ is proportional to charge-charge structure factor, $S_{qq}(k)$ when point like charge (PLC) approximation is adopted in a binary system.

$$S_{qq}^{PLC}(k)=(C_M C_X)^{-1} S_{CC}(k) \tag{3.22}$$

here *q* is the charge on chemical species.

The cross correlation function $S_{NC}(k)$ oscillates around zero. Fig. 3.4 (c) display that $S_{NC}(k)$ shows a significant decrease at or around the first peak position of $S(k)$ for liquid Fe-Al alloys. The small fluctuation in $S_{NC}(k)$ around zero indicates weak correlation between number-concentration fluctuations in the melts. Based on the observations from Fig. 3.4 (a), (b) and (c), we conclude that amongst the three BT partial correlation functions, $S_{NN}(k)$ is the highest weighing factor contributing to the total structure factor $S(k)$.

$S_{CC}(k)$ has been computed for various liquid Fe-Al alloys for entire k region and especially in the long-wavelength limit as k tends to zero, $S_{CC}(0)$ provides important information on Fe-Fe coordination, Al-Al coordination and Fe-Al coordination in the Fe-Al melts. This information cannot be withdrawn from the X-ray scattering studies of the melts (Salmon and Zeidler, 2013). $S_{CC}(0)$ can be obtained experimentally (Akinlade *et al.*, 2000) through activity data of liquid binary alloys. The computed values of partial structure factors in the long wavelength limit

of ($S_{Fe\text{-}Fe}(0)$, $S_{Al\text{-}Al}(0)$ and $S_{Fe\text{-}Al}(0)$) along with $S_{CC}(0)$ and $S^{id}_{CC}(0)$ at different atomic fractions of Al in Fe-Al melts are given in Table 3.3.

Table 3.3 The concentration-concentration fluctuation at the long wavelength limit $S_{CC}(0)$ and its ideal value, $S^{id}_{CC}(0)$, Co-ordination number, ψ and Chemical short range order parameter, α' of Fe-Al alloys at different compositions of Al.

% Al	$S_{CC}(0)$ (Cal.)	$S_{CC}(0)$ (Exp.)	$S^{id}_{CC}(0)$	ψ	α' (Square-Well)	α' (Quasi-Lattice)
70	0.129	0.090	0.21	11.420	-0.052	-0.050
78	0.074	0.075	0.17	11.190	-0.103	-0.090
82	0.051	0.052	0.14	11.208	-0.147	-0.120
86	0.031	0.040	0.12	11.123	-0.205	-0.194
90	0.020	0.039	0.09	11.110	-0.239	-0.219

Table 3.3 shows a good agreement between the computed values of $S_{CC}(0)$ with experimental values (Akinlade *et al*., 2000). Further, it can observe from Table 3.3 that the compound forming tendency between Fe and Al atoms increases with increase in Al concentration. Deviation of $S_{CC}(0)$ from its ideal value i.e., $S^{id}_{CC}(0) > S_{CC}(0)$ indicates the formation of chemical compound between Fe and Al atoms in Al rich Fe-Al melts.

In order to determine thermodynamic contribution of interdiffusion coefficient, we derive $S_{CC}(0)$ as a function of Al concentration in liquid Fe-Al alloys. Our model calculations gave quite similar $S_{CC}(0)$ function behavior as that of quasi-lattice (QL) model and experimental values (Akinlade *et al*., 2000).

The comparison between computed results of the composition dependent $S_{CC}(0)$, its ideal values $S^{id}_{CC}(0)$, Quasi-Lattice (QL) and experimental value derived from activity data (Akinlade *et al*., 2000) are plotted in Fig.3.5.

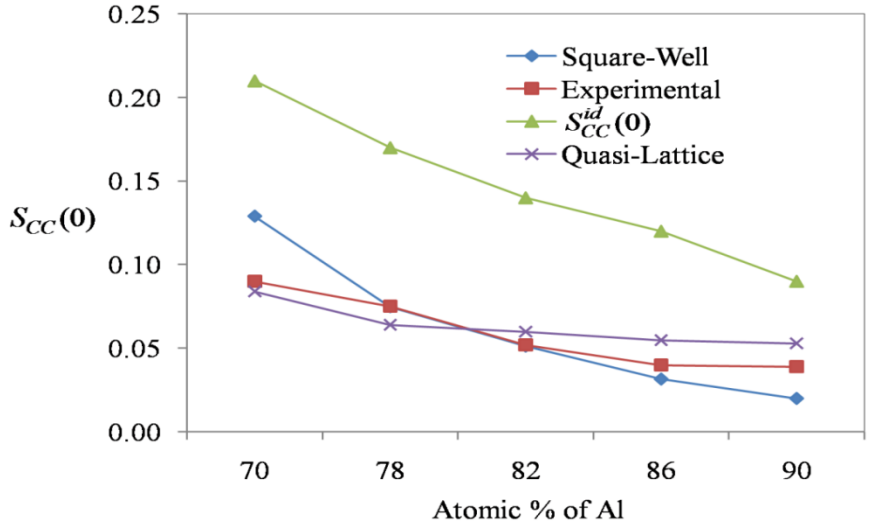

Figure 3.5: Square-well, quasi-lattice, experimental (Akinlade *et al*., 2000) and, ideal values of $S_{CC}(0)$ as a function of atomic % of Al.

It can be seen from Fig. 3.5 that the computed values of $S_{CC}(0)$ at all investigated concentrations are lower than their corresponding ideal values, $S_{CC}^{id}(0)$, which suggest hetero-coordination is more favorable than homo-coordination in the considered melts.

. Fig. 3.6 shows the comparison between α' obtained through SW model and QL model (Akinlade *et al*., 2000). The negative values of α' show the existence of chemical ordering in liquid Fe-Al alloys at all the investigated compositions

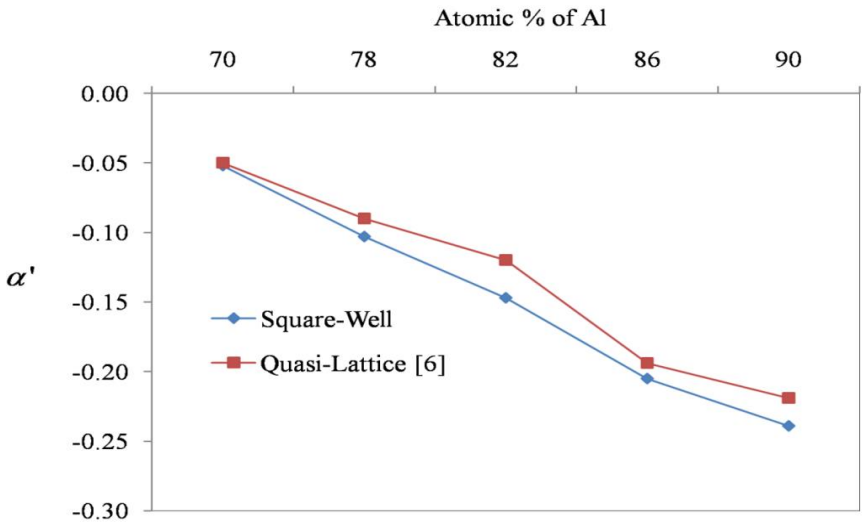

Figure 3.6: α' versus atomic % of Al at 1873 K.

Our study on Cowley-Warren short range order parameter, α' and $S_{CC}^{id}(0) > S_{CC}(0)$ confirm the compound forming behavior in the liquid Fe-Al alloys. Fig. 3.6 illustrates that the minimum value of $\alpha'_{min} \approx -0.052$, while the lowest possible value of $\alpha'_{min} = -1$, which is an indication of chemical ordering where as the maximum possible value of $\alpha'_{max} = 1$ indicates segregation in the liquid binary alloys. $\alpha' = 0$ implies an irregular distribution of atoms.

The partial structure factors in the long wavelength limit $S_{lm}(k \to 0)$ were used to obtain isothermal compressibility, (χ_T). The computed values of $S_{Fe\text{-}Fe}(0)$, $S_{Al\text{-}Al}(0)$, $S_{Fe\text{-}Al}(0)$ and χ_T are presented in Table 3.4.

Table 3.4. $S_{Fe\text{-}Fe}(0)$, $S_{Al\text{-}Al}(0)$ and $S_{Fe\text{-}Al}(0)$, and isothermal compressibility, χ_T of Fe-Al alloys at different compositions of In

% Al	$S_{Fe\text{-}Fe}(0)$	$S_{Al\text{-}Al}(0)$	$S_{Fe\text{-}Al}(0)$	$\chi_T(10^{-11}m^2Nm^{-1})$
70	1.107	0.352	-0.583	0.249
78	1.097	0.243	-0.471	0.241
82	1.085	0.195	-0.411	0.235
86	1.070	0.152	-0.350	0.228
90	1.052	0.113	-0.284	0.221

The computed values of the isothermal compressibility (χ_T) decreases linearly with atomic percent of Al beyond liquidus temperature. This shows that the void space between the particles decrease and the existence of compact nature of the alloy as the concentration of Al increases.

TRANSPORT, SURFACE AND SCALING PROPERTIES OF LIQUID BINARY ALLOYS

4.1. INTRODUCTION

The concentration dependent self and mutual diffusion coefficients of liquid binary alloys also provide important information on various structural changes like crystal nucleation, crystal growth rate and glass transition (Liu *et al*., 2010; Wang *et al*., 2015). The concentration dependent inter diffusion coefficients were determined by using kinetic contribution as discussed by Mishra and Venkatesh (Mishra and Venkatesh, 2008) and thermodynamic contribution through $S_{CC}(0)$ in modify Darken's equation (Trybula et al., 2018; Jakse and Pasturel, 2016; Souto *et al*., 2013; Zhang *et al*., 2010). It is interesting to study the influence of chemical ordering on atomic dynamics in binary liquid alloys (Meyer *et al*., 2019; Yan *et al*., 2018; Das *et al*., 2005). Speedy *et al*. (Speedy *et al*., 1988) noticed the differences in self diffusivity of liquids using a square-well (SW) and hard-sphere potential functions. Thus, to study the liquid binary alloys, using SW attractive part as a perturbation over hard sphere reference system is more convincing to predict the structure functions and their associated properties.

It has been reported that the concentration dependent viscosity is related with intermetallic compounds present in various metallic systems (Mudry *et al*., 2013). There are few articles with theoretical/computational or experimental data of atomic structures and transport coefficients measurements of liquid Cu-In alloy. The diffusion coefficient of Brownian particles and the shear viscosity of fluids can be related through the SE relation (Meyer *et al*., 2019; Trybula, 2016; Souto *et al*., 2013). In fact, it works for many metallic melts (Wang *et al*., 2015; Trybula, 2016; Trybula *et al*., 2014; Brillo *et al*., 2008; Trybula *et al*., 2018; Lalneihpuii *et al*., 2019). We use SE relation to compute the shear viscosity at five compositions in particular Cu-rich composition region of the Cu-In melts. Our computed results indicate a non linear dependence of the shear viscosity as a function of composition and in fair agreement with available experimental data (Mudry *et al*., 2013) in particular beyond 31% of In in Cu-In system. Also, we find the difference of our computed values from

experimental values decreases with increase of In composition in the melts. Thus, we illustrate that this breakdown of the SE relation can be related to the detailed discussion of local microscopic chemical ordering of unlike atoms in the high Cu-rich composition range which become feeble with increase of In atoms in the liquid Cu-In alloys

Knowledge of transport coefficients like diffusivity and viscosity of liquid metals and alloys in the bulk state has been improved dramatically over the past decades (Roik *et al*., 2014; A.L. Bel'tyukov *et al*., 2015; Lihl *et al*., 1964; Trybula *et al*., 2014; Peng *et al*., 2015; Van der Ven and Ceder, 2005; Wang *et al*., 2015; Jakse and Pasturel, 2015; Lalnuntluanga *et al*., 2021; Jakse and Pasturel, 2016). Akinlade *et al.* (Akinlade *et al*., 2000) have reported interdiffusion coefficients of Fe-Al melts using complex formation approximation which gives based on a thermodynamic contribution only (Jakse and Pasturel, 2015). Thus, detailed knowledge of self diffusivity of pure components and interdiffusion coefficients of liquid Fe-Al alloys is required to understand atomic interaction at a microscopic level and rate a mechanism of non-equilibrium phenomena in such alloys (Van der Ven and Ceder, 2005).

The investigation of transport coefficients has been reported based on Stokes-Einstein (SE) relation, which is given as $D = k_B T / 2\pi r^{\max} \eta$, where η is the shear viscosity, k_B is the Boltzmann constant, T is the working temperature, and $r^{\max}$ is the first peak position of the pair correlation function (Jakse and Pasturel, 2016). The validity of the SE relation has been successfully reported for monoatomic liquids (Hansen and McDonald, 1986), binary liquid alloys (Jakse and Pasturel, 2016), and molecular liquids (Jonas and Akaii, 1997). We agree with Jakse and Pasturel (Jakse and Pasturel, 2016) that the SE relation must be tested for many liquid alloys to get a clear understanding of its applicability in dense liquids.

4.2. THEORY

4.2.1. Evaluation of diffusion coefficients in liquid binary alloys

We define composition-dependent mutual diffusion coefficient D_{lm} using BT structure factors (Lalneihpuii *et al*., 2019) as follows:

$$D_{lm} = \frac{\left(C_l\xi_l + C_m\xi_m\right)}{k_B T} \times D_l D_m \phi \tag{4.10}$$

Here, D_{lm} is the interdiffusion or mutual diffusion coefficient, D_l and D_m are the self-diffusivity of l and m species respectively in the liquid binary alloys and ϕ is the thermodynamic factor due to the second derivative of Gibb's free energy.

Here,

$$\frac{1}{\phi} = \frac{S_{CC}^{id}(0)}{k_B T}\frac{\partial^2 G^{mix}}{\partial C_l \partial C_m} = \frac{S_{CC}^{id}(0)}{S_{CC}(0)} \tag{4.11}$$

where G^{mix} is the Gibbs free energy of mixings. $C_l\xi_l + C_m\xi_m$ can be computed as follows (Lalneihpuii *et al*., 2019)

$$C_l\xi_l + C_m\xi_m = \frac{1}{6(2\pi^3 k_B T)^{1/2}}\left[\int_0^\infty k^3 \phi_{NN}(k)[S_{NN}(k) - 1]dk + \int_0^\infty k^3 \phi_{CC}(k)[S_{CC}(k) - 1]dk + 2\int_0^\infty k^3 \phi_{NC}(k) S_{NC}(k)\,dk\right] \tag{4.12}$$

where $\phi_{CC}(k)$ is the Fourier transform of the ordering potential. $\phi_{NN}(k)$ and $\phi_{NC}(k)$ are computed as given by (Nath and Joarder, 2005).

The self diffusivities D_l and D_m were determined using the famous Einstein equation linear trajectory (LT) approximation given by the equation

$$D = \frac{k_B T}{\xi} \tag{4.13}$$

where ξ is the friction coefficient experienced by the particles. In a binary melts under SW interatomic interaction ξ can be estimated from contributions due to the

repulsive part (ξ^H), attractive well (ξ^S) and beyond the attractive well called as hard-soft part (ξ^{HS}).

The friction coefficients were computed by solving time integral function under linear trajectory principle. Thus,

$$\xi=\frac{1}{3k_BT}\left[\int_0^t ds\left\langle F_H(t).F_H(t+s)\right\rangle+\left\{\int_0^t ds\left\langle F_S(t).F_S(t+s)\right\rangle+\int_0^t ds\left\langle F_S(t).F_H(t+s)\right\rangle\right\}\right] \tag{4.14}$$

$$=\xi^H+\xi^S+\xi^{HS} \tag{4.15}$$

Here, ξ^H, ξ^S and ξ^{HS} are the friction coefficient due to hard sphere, soft and hard-soft part respectively (Gopala Rao and Sathpathy, 1990; Gopala Rao and Velkatesh, 1989). The friction coefficients arise due to hard and soft part of the force under SW interaction were solved under linear trajectory principle (Helfand, 1961).

Thus the interparticle pair potential $U_{lm}(r)$ for model potential is assumed to be seperable into two parts (Gopala Rao and Das, 1987; Mishra and Venkatesh, 2008) i.e. as a pair potential for hard spheres and other for the attractive part (soft part).

$$U_{lm}(r)=U^H_{lm}(r)+U^S_{lm}(r) \tag{4.16}$$

Where $U^H_{lm}(r)$ is the contribution from the hard spheres and $U^S_{lm}(r)$ from the soft part.

These are represented as

$$U^H_{lm}(r)=\begin{cases}\infty & ; \quad r<\sigma_{lm}\\ 0 & ; \quad r>\sigma_{lm}\end{cases} \tag{4.17}$$

and

$$U^S_{lm}(r)=\begin{cases}0 & ; \quad r<\sigma_{lm}\\ U_{lm}(r) & ; \quad r>\sigma_{lm}\end{cases} \tag{4.18}$$

Similarly, the force can also be divided into two parts

(a) $F_{H'}$ the hard sphere contribution

(b) $F_{S'}$ the soft potential contribution

Thus,

$$\xi_l^H = \sum_{b=1}^{2} \frac{8}{3} \sigma_{lm}^2 g_{lm}(\sigma_{lm}) \rho_m (2\pi\mu_{lm} k_B T)^{1/2} \tag{4.19}$$

The contribution from the soft part is given by (Shimoji and Itami, 1986; Gopala Rao and Satpathy, 1982; Polyvos and Davis, 1967)

$$\xi_l^S = -\sum_{b=1}^{2} \frac{\rho_m}{3} \left[\frac{2\pi\mu_{lm}}{k_B T}\right] \frac{1}{(2\pi)^2} \int_0^\infty k^3 U_{lm}^S(k) h_{lm}(k) dk \tag{4.20}$$

While ξ_l^{HS}, the cross contribution (Polyvos and Davis, 1967) is given by

$$\xi_l^{HS} = -\sum_{b=1}^{2} \frac{\rho_m}{3} g_{lm}(\sigma_{lm}) \left[\frac{2\mu_{lm}}{\pi k_B T}\right]^{1/2} \int_0^\infty \left[k\sigma_{lm}\cos(k\sigma_{lm}) - \sin(k\sigma_{lm})\right] U_{lm}^S(k) dk \tag{4.21}$$

Here ρ_m is the number density of the bth species, $h_{lm}(k)$ and $U_{lm}^S(k)$ are the Fourier transform s of the total correlation function $h_{lm}(r)$ and the soft part of the potential $U_{lm}^S(r)$ respectively. Further μ_{lm} is the reduced mass and is given by

$$\mu_{lm} = \frac{m_l m_m}{m_l + m_m} \tag{4.22}$$

The quantities $h_{lm}(k)$ and $U_{lm}^S(k)$ are given by

$$h_{lm}(k) = \left[S_{lm}(k) - \delta_{lm}\right] \left(\rho_l \rho_m\right)^{-1/2} \tag{4.23}$$

$$U_{lm}^S(k) = \frac{4\pi\varepsilon_{lm}}{k^3} \left[A_{lm} k\sigma_{lm} \cos(A_{lm} k\sigma_{lm}) - \sin(A_{lm} k\sigma_{lm}) - k\sigma_{lm}\cos(k\sigma_{lm}) + \sin(k\sigma_{lm})\right] \tag{4.24}$$

Here δ_{lm} is the Kronecker delta function already defined in Chapter-2, σ_{lm}, ε_{lm} and A_{lm} are the cross correlation due to hard core diameter, depth and breadth of

the square well potential. The mixed parameters are discussed in Chapter-2. The partial structure factors which were already discussed in Chapter-2 for Cu-In and Fe-Al alloys are used in the evaluation of the friction coefficients. According to Darken's thermodynamic formalism, the diffusion is directly related to $S_{CC}(0)$ as

$$\frac{D_{lm}}{D_{id}} = \frac{S_{CC}^{id}(0)}{S_{CC}(0)} \tag{4.24}$$

Here $S_{CC}^{id}(0)$ and $S_{CC}(0)$ are concentration-concentration correlations in the limit $k \to 0$. D_{lm} is the mutual diffusion and D_{id} is the intrinsic diffusion can be defined as

$$D_{id} = c_l D_m + c_m D_l \tag{4.25}$$

Here, D_l and D_m are the self-diffusivity of l and m species respectively in the melts.

4.2.2. Evaluation of viscosity coefficients in liquid binary alloys

Further, the viscosity coefficients of pure components in liquid binary alloys can be determined by assuming Stokes-Einstein (SE) form of equations where hydrodynamic length is replaced by the first peak position of the partial correlation function of the pure component in binary melts (Mishra *et al*., 2020) as follow:

$$\eta_l = \frac{k_B T}{2\pi r_{ll}^{max} D_l} \tag{4.25}$$

$$\eta_m = \frac{k_B T}{2\pi r_{mm}^{max} D_m} \tag{4.26}$$

Here $k_B T$ is product of Boltzmann constant and the working temperature, r_{ll}^{max} and r_{mm}^{max} are the first peak positions of the PCFs, $g_{ll}(r)$ and $g_{mm}(r)$ in Fe-Al binary melts

Hence, the total shear viscosity coefficient of the binary melts can be written in terms of partial viscosity coefficient of the constituent atoms (η_l and η_m) as

$$\eta_{lm} = C_l \eta_m + C_m \eta_l \tag{4.27}$$

4.2.3. Evaluation of surface tension in liquid binary alloys

Prasad *et al*. considered the existence of layer structure near the surface of binary liquid alloys in their structural mechanical formalism (Prasad *et al*., 1998; Prasad *et al*., 1991). They also pointed out that the surface of binary liquid alloys is in thermodynamically equilibrium with the bulk and, surface properties are influenced by thermodynamic properties of the bulk.

Detailed studies of the surface properties of condensed matter help in understanding their metallurgical processing. The surface tension, γ for series of liquid metals has been studied by statistical mechanical approach under zeroth order approximation (Fowler, 1937). It is further extended for binary alloys. In present work, γ in binary melts has been computed by using mutual diffusion coefficient values at different concentrations.

Transport and surface properties are useful parameters in metallurgical science and surface tension in particular contributes significantly in crystal growth (Sharma *et al*., 2014). Recently authors have reported surface tension of binary square-well liquid in terms of interdiffusion coefficient which can be given as (Mishra *et al*., 2020)

$$\gamma_{\text{Alloy}} = \frac{15}{16}\left(\frac{k_B T}{\mu_{lm}}\right)^{\frac{1}{2}} \times \frac{k_B T}{2\pi r_{lm}^{max} D_m} \tag{4.28}$$

where D_m is the mutual diffusion coefficient, μ_{lm} is the reduced atomic mass, r_{lm}^{max} is the first peak position of the pair correlation function and $k_B T$ is the Boltzmann constant times temperature.

4.2.4. Scaling properties in liquid binary alloys

Atomic dynamics in metallic melts depends on structural relaxation and its chemical thermodynamics. Recently Dzugutov (Dzugutov, 1996) advances our present knowledge of transport coefficients by proposing entropy-diffusion scaling law through pair correlation function g(r). The universality of proposed law have been investigated for series of metallic liquids by using molecular dynamic simulation with embedded atomic model potential function (Dzugutov, 1996; Hoyt *et al*., 2000 ; Samanta *et al*., 2004 ; Pasturel and Jakse, 2015) and with SW model potential (Mishra and Lalneihpuii, 2016; Mishra and Shrivastava, 2017).

The reduced inter diffusion in binary mixture can be defined using self diffusivity of pure component (Hoyt *et al*., 2000; Pasturel and Jakse, 2015) as:

$$D^{*} = \left(\frac{D_l}{\chi_l}\right)^{C_l}\left(\frac{D_m}{\chi_m}\right)^{C_m} \tag{4.29}$$

where χ_l and χ_m are the scaling factors (Kanibolotsky *et al*., 2002; Yang *et al*., 2008; Dzugutov, 1996) defined as

$$\chi_l = 4(r_{ll}^{max})^4\rho_l x_l g_{ll}(r^{max})\sqrt{\frac{\pi k_B T}{m_l}} + 4(r_{lm}^{max})^4\rho_l x_m g_{lm}(r^{max})\sqrt{\frac{\pi(m_l+m_m)k_B T}{m_l m_m}} \tag{4.30}$$

$$\chi_m = 4(r_{mm}^{max})^4\rho_m x_m g_{mm}(r^{max})\sqrt{\frac{\pi k_B T}{m_m}} + 4(r_{lm}^{max})^4\rho_l x_l g_{lm}(r^{max})\sqrt{\frac{\pi(m_l+m_m)k_B T}{m_l m_m}} \tag{4.31}$$

where r^{max} is the first peak position of the corresponding partial pair-correlation functions, g_{ll}, g_{mm} and g_{lm} respectively. x_l and x_m are the are the atomic fractions of l and m type of species, m_l and m_m are the atomic masses of the constituents of investigated melts.

Two body excess entropies of pure components were obtained through Dzugutov's scaling law as follows

$$S_l^{ex}/k_B = \log \frac{D_l}{0.049\chi_l} \tag{4.32}$$

$$S_m^{ex}/k_B = \log \frac{D_m}{0.049\chi_m} \tag{4.33}$$

Here, χ_l and χ_m are reducing parameters as given in Eqns. (4.30) and (4.31) respectively.

Now the pair wise excess entropy of liquid binary alloys can be computed through the following equation

$$S_M^{ex} = x_l \times S_l^{ex} + x_m \times S_m^{ex} \tag{4.34}$$

where S_l^{ex} and S_m^{ex} are the partial molar entropies of l and m species in the binary melts and S_M^{ex} is the total molar entropy. We define the reduced viscosity in the light of Rosenfeld scaling law of viscosity (Rosenfeld, 1999)

$$\eta^* = \frac{\eta \rho^{\frac{-2}{3}}}{\left(mk_B T\right)^{\frac{1}{2}}} \tag{4.35}$$

$$\eta^* = D^* \frac{\eta}{D\rho m} \tag{4.36}$$

Finally, total reduced viscosity as a function of concentration in liquid binary alloys were computed by incorporating partial reduced viscosities from Eqn. (4.36) into Eqn. (4.27).

4.3. RESULTS AND DISCUSSION

4.3.1. Cu-In alloys

4.3.1.1. *Friction coefficients and diffusion coefficients of Cu-In alloys*

Various friction coefficients (ξ^H,ξ^S and ξ^{HS}) in Cu-In melts as a function of composition at 1073 K were computed through Eqns. (4.19), (4.20) and (4.21) and are given in Table 4.1

Table 4.1. Friction coefficients ξ^H, ξ^S and ξ^{HS} of Cu-In alloys at different compositions of In at 1073 K.

% In in Cu-In	$\xi^H x10^{-13}$(Kg/s)		$\xi^S x10^{-13}$(Kg/s)		$\xi^{HS} x10^{-13}$(Kg/s)	
	Cu	In	Cu	In	Cu	In
25	14.19	20.73	4.06	3.51	5.25	6.08
27	13.94	20.38	4.02	3.48	5.13	5.94
29	13.70	20.04	3.98	3.44	5.01	5.81
32	13.35	19.55	3.92	3.39	4.85	5.62
34	13.14	19.25	3.87	3.36	4.75	5.50

The values of friction coefficients due to hard, soft, and hard-soft parts have been shown in Table 4.1. It illustrates friction coefficient due to hard-sphere repulsive force is much higher than that of the soft part and hard-soft part, which is expected.

Table 4.2. Diffusion coefficients of liquid Cu-In binary alloys at 1073 K

% In in Cu-In	D_{Cu} (10^{-9} m^2/s)	D_{In} (10^{-9} m^2/s)	D_{In}/D_{Cu}	D_m (10^{-9} m^2/s)	D_{id} (10^{-9} m^2/s)	D_m/D_{id}
25	6.29	4.88	0.77	9.93	5.23	1.90
27	6.41	4.96	0.77	9.85	5.35	1.84
29	6.52	5.05	0.77	9.83	5.49	1.79
32	6.69	5.18	0.77	9.90	5.66	1.75
34	6.80	5.26	0.77	9.95	5.78	1.72

D_{In} and D_{Cu} regularly increase with increasing In composition in the investigated alloy whereas the ratio D_{In}/D_{Cu} is independent of In composition. The constant ratio D_{In}/D_{Cu} value (around 0.77) is also reported by other authors for different liquid alloys and attributed as regular solution behavior of alloys (Gopala Rao and Bandyopadhyay, 1989; Mishra and Venkatesh, 2008).

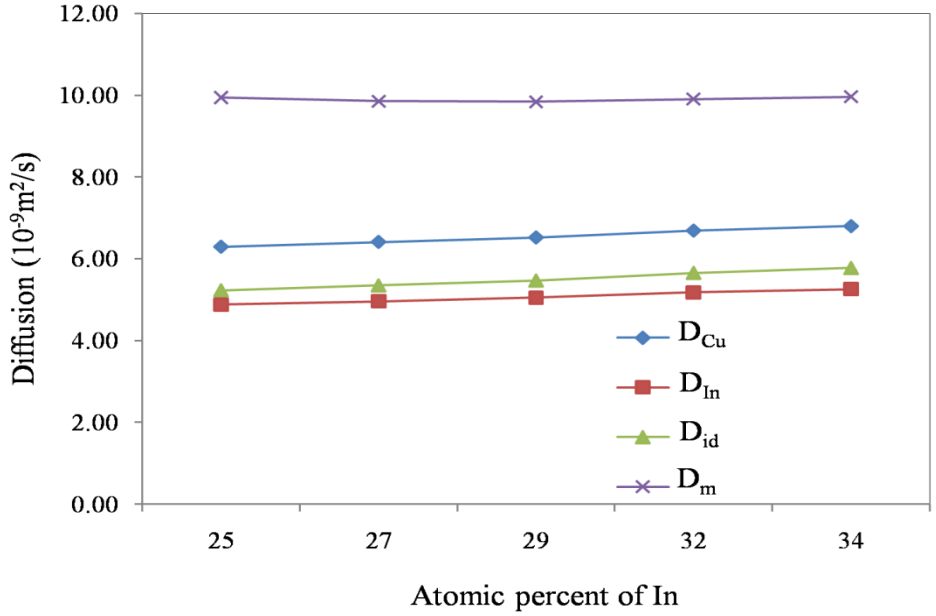

Figure 4.1: Diffusion versus atomic percent of In in Cu-In melts at 1073 K.

The study of mass and momentum transport in liquid alloys is a tedious task due to the existence of atomic level disorders in the system. Thermal transports in liquid alloys propagate heat via vibration between the bonds of the components and thus show complexities. Thermal motion in liquid alloys causes segregation which as is observed (Mudry *et al*., 2013) effect viscosities of liquid alloys. The self, mutual, interdiffusion coefficients and the viscosity coefficients of liquid Cu-In alloys have been computed for a wide range of concentration and temperature through BT correlation functions and are given in Table 4.2 and Table 4.3.

Table 4.3. Diffusion coefficients of Cu-In alloys at 950, 1150, 1350 and 1550 K

% In	Temp(K)	D_{Cu} ($10^{-9}m^2/s$)	D_{In} ($10^{-9}m^2/s$)	D_m ($10^{-9}m^2/s$)	D_{Cu} / D_{In}
25	950	5.60	4.39	4.69	1.28
	1150	6.71	5.17	5.55	1.30
	1350	7.74	5.88	6.34	1.32
	1550	8.70	6.54	7.08	1.33
27	950	5.70	4.47	4.80	1.28
	1150	6.83	5.26	5.68	1.30
	1350	7.88	5.98	6.49	1.32
	1550	8.85	6.65	7.25	1.33
29	950	5.80	4.55	4.91	1.28
	1150	6.95	5.35	5.81	1.30
	1350	8.01	6.09	6.65	1.32
	1550	9.01	6.77	7.42	1.33
32	950	5.95	4.66	5.07	1.28
	1150	7.13	5.48	6.00	1.30
	1350	8.22	6.24	6.87	1.32
	1550	9.23	6.94	7.67	1.33
34	950	6.05	4.74	5.18	1.28
	1150	7.25	5.57	6.14	1.30
	1350	8.35	6.34	7.02	1.32
	1550	9.39	7.05	7.84	1.33

From Table 4.3 we inferred that with the change in composition of investigated liquid Cu-In alloys at a constant temperature, the ratio of self diffusivity of Cu and In remains the same. Further, it can also be seen that self and mutual diffusion coefficients increase with increasing temperature at all investigated compositions. It means that under the cooling effect, these diffusion coefficients will decrease and control the structure of Cu-In alloys in their solid-state. The most striking feature is the continuous increase of self and mutual diffusion coefficients with increase of temperature and concentration of In in the melts.

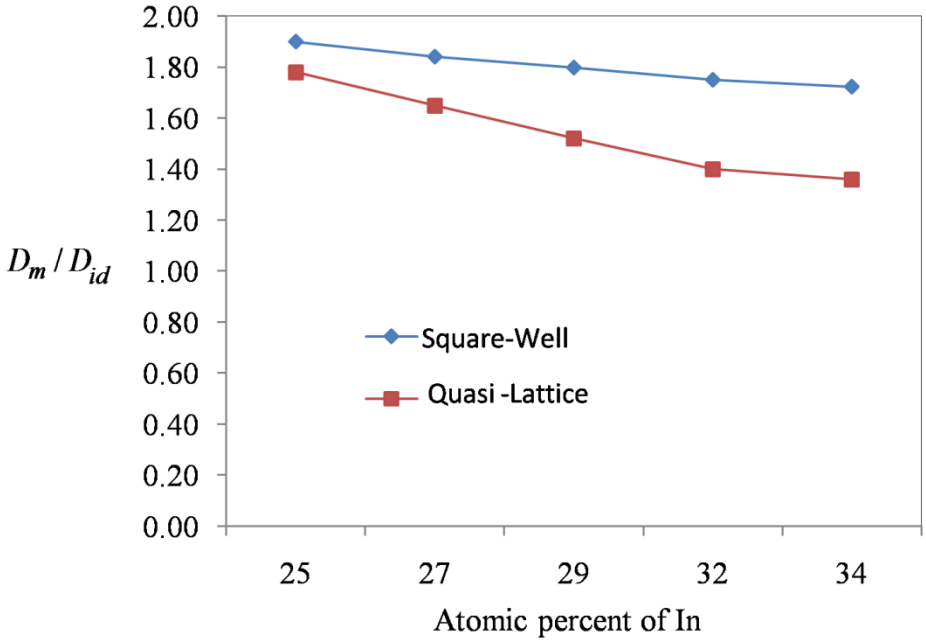

Figure 4.2: Values of the ratio D_m/D_{id} versus atomic percent of In at 1073 K.

Fig. 4.2 shows a constant ratio of mutual diffusion coefficient to the ideal value computed by square-well (SW) model and quasi-lattice (QL) theory (Akinlade and Singh, 2002) in liquid Cu-In alloys at 1073K. Thus, the variation in D_{Cu} and D_{In} with In composition within the investigated range are almost similar as observed by Akinlade and Singh using QL theory (Akinlade and Singh, 2002).

4.3.1.2. *Viscosity coefficients and surface tension of Cu-In alloys*

The composition-dependent partial and total viscosity coefficients of Cu-In liquid alloys were calculated through Eqns. (4.25) to (4.27) at 1173 K and are shown in Table 4.4. It can be observed that the partial, as well as the total shear viscosity coefficients, decreases with an increasing percentage of In. Also, Mudry *et al*. observed a decrease in experimentally measured and theoretically calculated data via the RKP equation for the viscosity of liquid Cu-In alloys (Mudry *et al*., 2013).

Table 4.4. Viscosity coefficients of liquid Cu-In binary alloys at 1173 K.

% In in Cu-In	η_{Cu}	η_{In}	η_{Total}(Computed)	η_{Total}(Experimental)
20	1.55	1.71	3.20	3.68
29	1.42	1.57	2.74	3.20
31	1.40	1.54	2.62	2.80
40	1.30	1.44	2.23	1.98
67	1.09	1.20	1.52	1.20

Fig 4.3 shows the comparison between the computed viscosity data using SE relation with experimental data given in Fig. 3 of reference (Mudry *et al.*, 2013).

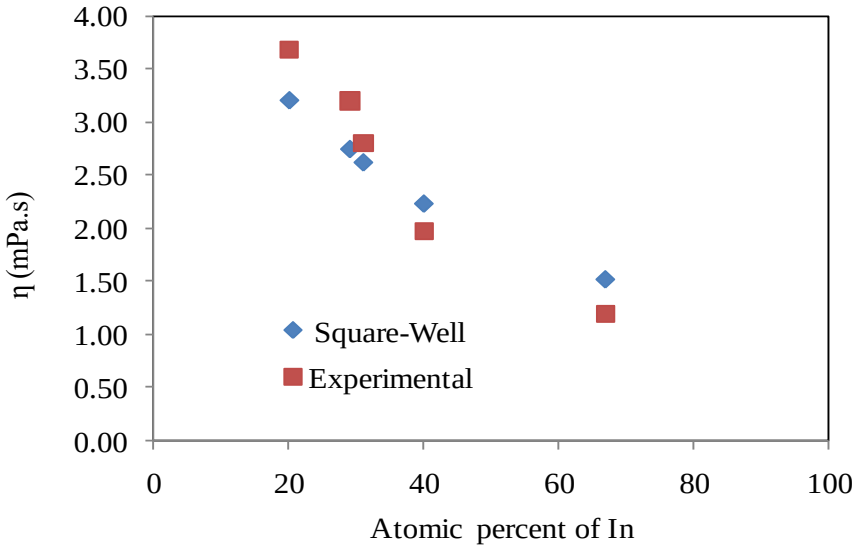

Figure 4.3: Square-Well and experimental (Mudry *et al.*, 2013) values of the concentration dependence of viscosity in liquid Cu-In alloy at 1173 K.

We find a very good agreement between computed and experimental values (Mudry *et al.*, 2013) which also confirms the applicability of SE relation for such dense fluids.

The Fourier inversion of three partial structure factors and total structure factor provide partial and total radial distribution functions of liquid Cu-In alloys. Thus

$$g_{Cu\text{-}In}(r) - 1 = \frac{1}{2\pi^2 (\rho_{Cu}\,\rho_{In})^{1/2}} \int_0^{\infty} [S_{Cu\text{-}In}(k) - \delta_{Cu\text{-}In}]\, k \sin(kr)\, dr \qquad (4.33)$$

Here δ is a Kronecker delta, which takes a value of one for similar components and is equal to zero for different components in a binary system.

In Fig. 4.4 we demonstrate the concentration-dependent first peak position of partial pair correlation functions in the considered melts. It can be seen that the first peak positions of $g_{Cu\text{-}Cu}(r)$, $g_{In\text{-}In}(r)$ and $g_{Cu\text{-}In}(r)$ are independent of composition. This supports the validity of SE relation in the investigated melts.

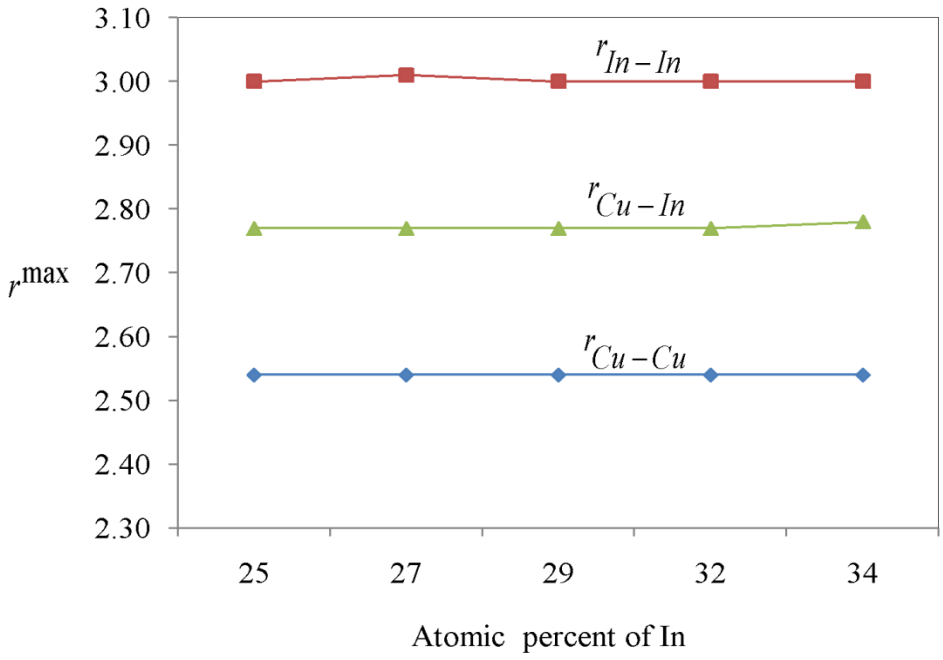

Figure 4.4: Effective radius of first peak position (r^{max}) versus atomic percent of In.

Thus, we use partial inter atomic separation in SE relation $D\eta = \frac{k_B T}{2\pi\, r^{max}}$ to estimate the shear viscosity coefficient of constituent elements using its self-diffusion coefficient data, and finally, the viscosity coefficient of the alloys is obtained by using Eqn. (4.27).

The computed results of coefficient of viscosity as a function of temperatures and compositions in the compound forming Cu-In binary liquids provide various important information like effective size of the particles and changes in liquid

structure at liquidus temperature. The viscosity coefficient of Cu-In liquid alloys as a function of In composition and temperature are listed in Table 4.5. The computed viscosity decreases with increasing In concentration which was also observed by Mudry *et al*. (Mudry *et al*., 2013).

Table 4.5. Viscosity coefficient of Cu-In alloys at 950, 1150, 1350, and 1550 K.

% In	Temp (K)	η_{Cu} (mPa.s)	η_{In} (mPa.s)	η_{Cu-In} (mPa.s)
25	950	1.465	1.581	1.552
	1150	1.480	1.627	1.590
	1350	1.507	1.679	1.636
	1550	1.540	1.733	1.684
27	950	1.439	1.554	1.522
	1150	1.454	1.599	1.559
	1350	1.480	1.650	1.604
	1550	1.513	1.704	1.652
29	950	1.414	1.554	1.513
	1150	1.429	1.572	1.530
	1350	1.455	1.622	1.573
	1550	1.487	1.675	1.620
32	950	1.379	1.490	1.454
	1150	1.394	1.536	1.490
	1350	1.419	1.583	1.530
	1550	1.451	1.634	1.575
34	950	1.356	1.466	1.428
	1150	1.371	1.509	1.462
	1350	1.396	1.557	1.502
	1550	1.427	1.609	1.547

The temperature effect on the viscosities of Cu-In melts is also given in Table 4.5. The viscosity of alloys increase with an increase in temperature at constant composition. It can be seen from Table 4.5 that the viscosity of the melts decreases with an increase of In concentration which indicates the decrease in momentum

transfer as well. It may be due to the increase of chemical ordering in In rich liquid Cu-In alloys.

Mutual diffusion coefficients and shear viscosities of liquid Cu-In alloys at different compositions and temperatures were computed using SW model potential. The product of mutual diffusion coefficient and shear viscosity of liquid Cu-In alloys at different temperatures for five compositions have been plotted in Fig. 4.5 (a to e)

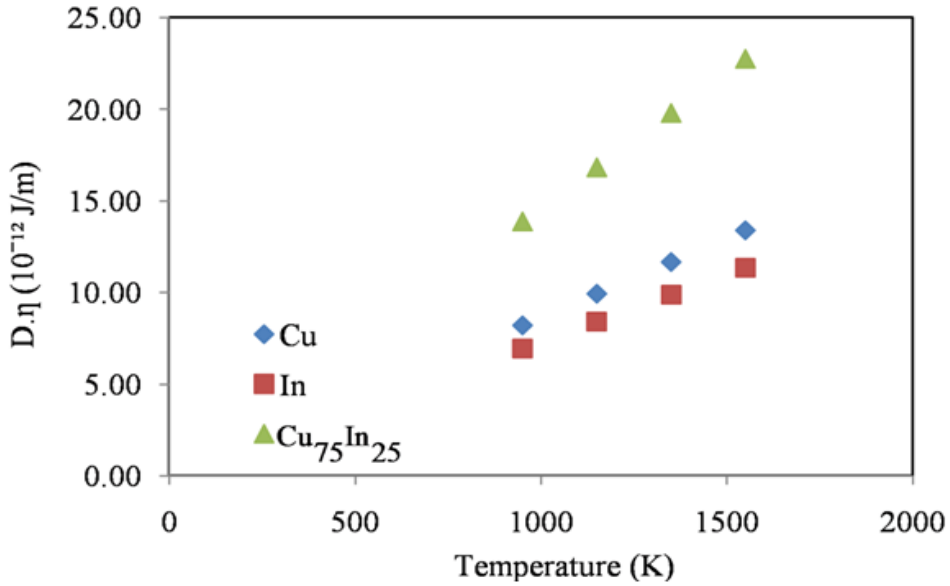

(a)

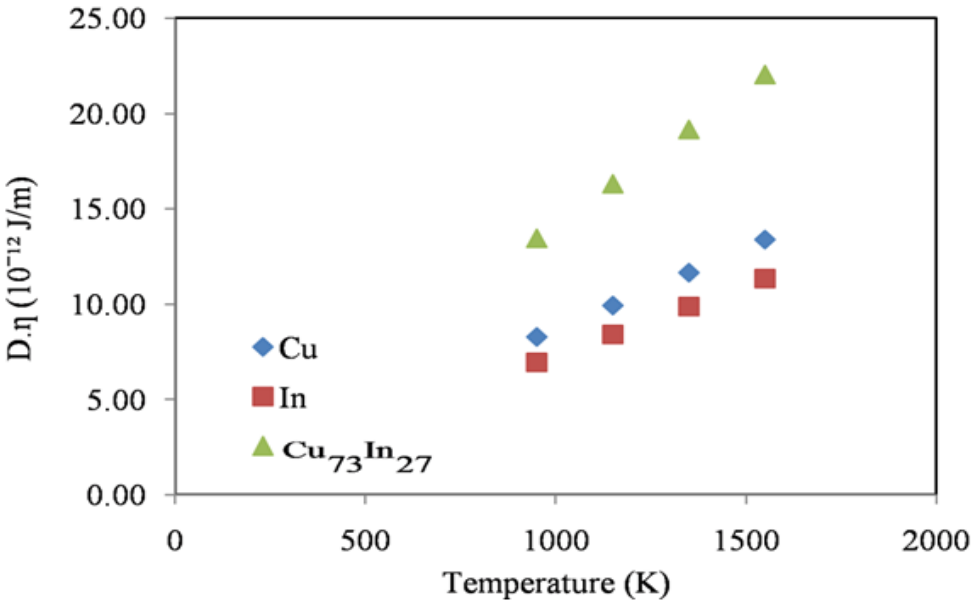

(b)

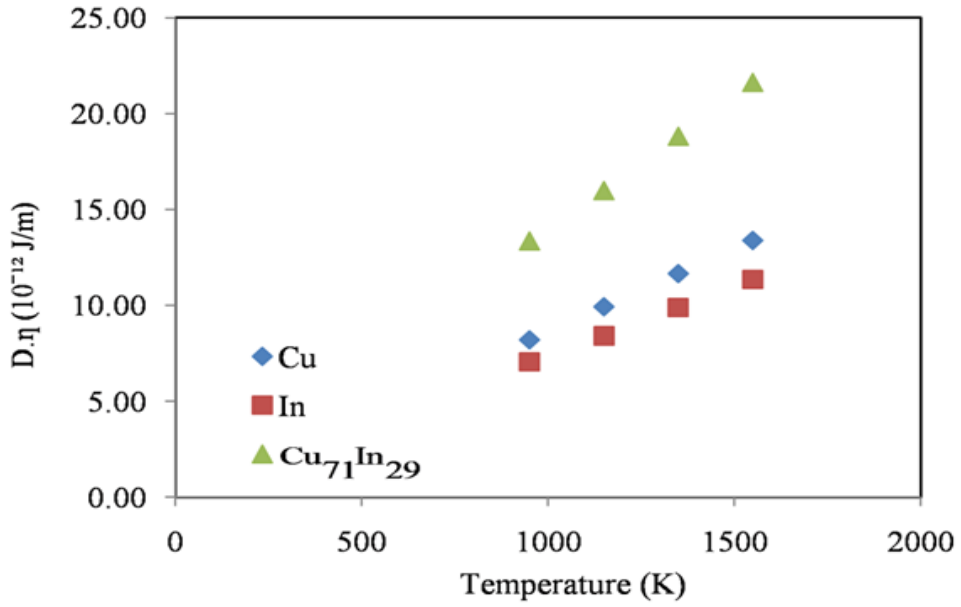
25.00
20.00
15.00
10.00
5.00
0.00
D.η (10⁻¹² J/m)
0
500
1000
1500
2000
Temperature (K)
Cu
In
Cu71In29

(c)

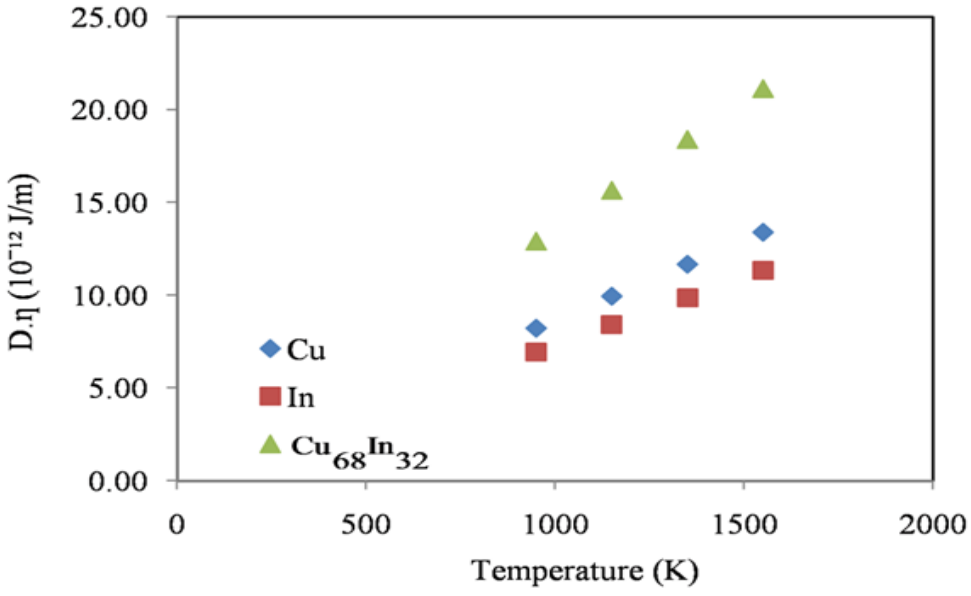
25.00
20.00
15.00
10.00
5.00
0.00
D.η (10⁻¹² J/m)
0
500
1000
1500
2000
Temperature (K)
Cu
In
Cu68In32

(d)

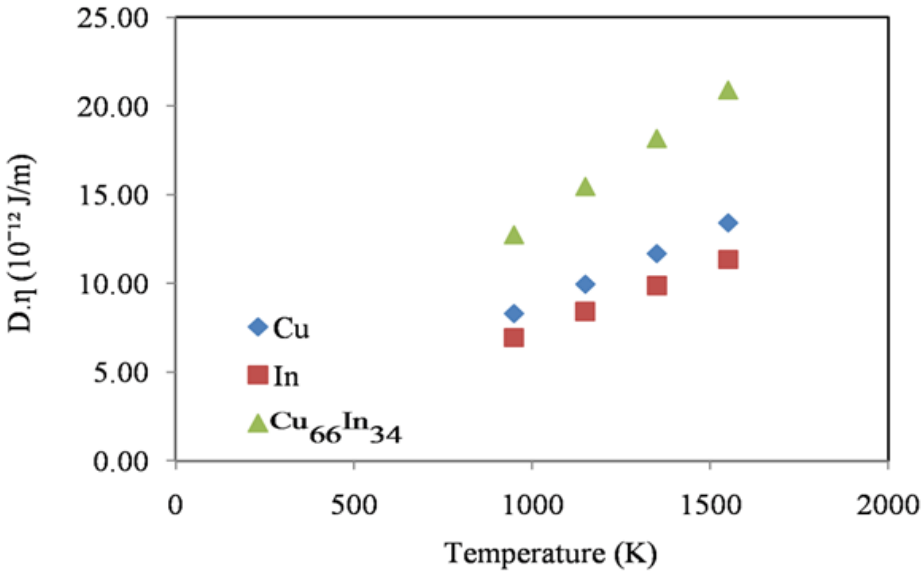

(e)

Figure 4.5: $D\eta$ versus temperature (a) 25% In (b) 27% In (c) 29% In (d) 32% In (e) 34% In.

Further, we demonstrate from Fig. 4.5 (a-e) that $D\eta$ linearly depends on temperature which indicates the SE relation holds in the considered liquid alloys.

Surface tension, surface energy, and surface entropy are important parameters to understand various metallurgical processes. Recently Bossa *et al*. investigated surface tension of a Yukawa fluid using mean field theory and finally concludes that the proposed model was not able to predict a correct value for the surface tension of phase boundary fluids (Bossa *et al*., 2017). Surface tension of ten liquid metals was thoroughly investigated by using SW potential under mean spherical model approximation (MSMA) (Mishra *et al*., 2015)

In this section, we determine the concentration-dependent surface tension of liquid Cu-In alloys (γ_{Cu-In}) from Eqn. (4.28) by extending the equation for binary system (Venkatesh *et al*., 2003).

Fig. 4.6 shows the comparison between the computed values of surface tension as a function of In composition with the data obtained by Akinlade and Singh using the QL model approach (Akinlade and Singh, 2002).

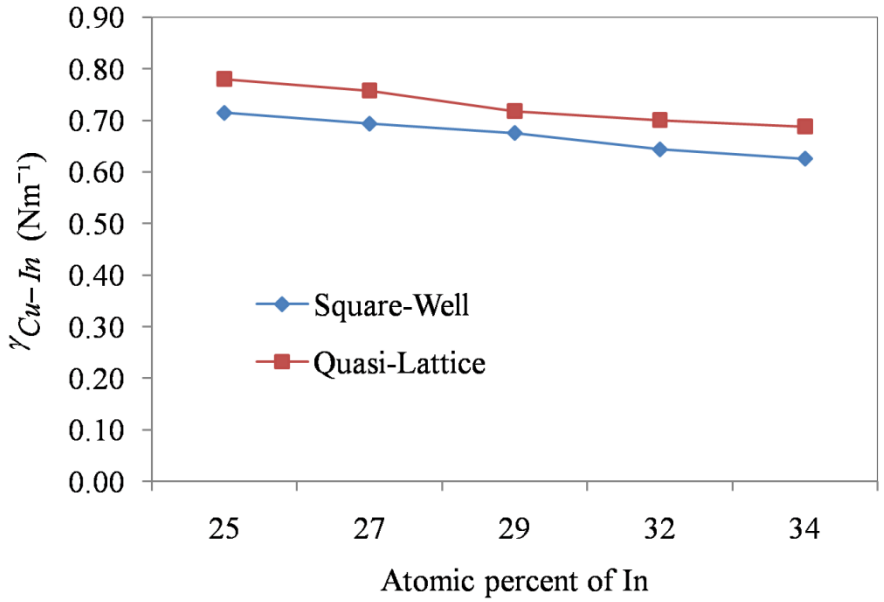

Figure 4.6: Surface tension versus atomic percent of In alloys at 1073 K.

We find that our computed values of surface tension by SW model are in close agreement with the results obtained from QL model (Akinlade and Singh, 2002) at all the investigated compositions. It can be seen from Fig. 4.6 that the surface tension of Cu-In melts decreases linearly with increase of In composition for the SW model. As we know that the applicability of materials is decided by their properties, hence the surface properties of liquid Cu-In alloys have been investigated. Due to the unavailability of any experimental data on the surface tension of this alloy, we compared our computed results with available QL model data (Akinlade and Singh, 2002).

Since the change in interatomic binding due to alloying of metallic melts in the considered liquid binary alloys is relatively small, which are also reflected in the thermodynamic properties of the melts.

4.3.2. Fe-Al alloys

4.3.2.1. Friction coefficients and diffusion coefficients of Fe-Al alloys

Given in Table 4.6, the friction coefficient from the equation of self diffusion calculation is approximately the combination of hard-core interaction, soft

interaction and the cross effect of hard-soft interactions. The friction contribution due to the hard-core interaction dominates over the soft and hard-soft interactions.

Table 4.6. Computed values of friction coefficients at different atomic % of Al in Fe-Al melts at 1873 K.

%Al in Fe-Al	ξ^Hx10^{-13}(Kg/s)		ξ^Sx10^{-13}(Kg/s)		ξ^{SH}x10^{-13}(Kg/s)	
	Fe	Al	Fe	Al	Fe	Al
70	11.09	10.34	2.44	1.66	2.65	1.39
78	10.85	10.19	2.35	1.60	2.47	1.29
82	10.74	10.12	2.31	1.56	2.38	1.25
86	10.62	10.05	2.26	1.53	2.29	1.20
90	10.50	9.97	2.21	1.49	2.20	1.16

In the intermediate step for the computation of self and mutual diffusion coefficient, have determined friction coefficients in the repulsive region (ξ^H), attractive region (ξ^S), and beyond the attractive region (ξ^{HS}) of the SW potential under the linear trajectory principle.

It can be inferred from Table 4.6 that the hard part, soft part, and hard-soft of the friction coefficients decrease with an increase in the concentration of Al in the Fe-Al melts. The reverse trend is seen for Fe composition. This is to be noted that metallic melts with smaller diameters have high values of friction coefficients in the entire range of potential function. Further, it is worth mentioning here that the contribution of the repulsive region of friction coefficients for both components plays an important role in the computation of diffusion parameters of the alloys. To the best of our knowledge, no literature data is available for the comparison of friction coefficients for the concerned alloys.

As can be seen from Table 4.7, the ratio D_{Fe} / D_{Al} is almost a constant irrespective of compositions with an average value of 0.837. Thus, Fe-Al binary liquid was predicted to form a regular solution and justify that the structure and its

associated properties together with the transport properties can be calculated with just the potential parameters of pure liquid metals (Gopala Rao and Bandyopadhyay, 1989; Mishra and Venkatesh, 2008).

Table 4.7. Diffusion coefficients of liquid Fe-Al binary alloys at 1873 K.

% Al in Fe-Al	D_{Fe} (10^{-9} m^2/s)	D_{Al} (10^{-9} m^2/s)	D_{Fe}/D_{Al}	D_{id}	D_m	D_m/D_{id}
70	15.96	19.30	0.82	16.96	18.86	1.09
78	16.48	19.74	0.83	17.19	19.51	1.13
82	16.75	19.97	0.84	17.32	20.21	1.16
86	17.03	20.21	0.84	17.45	21.32	1.22
90	17.31	20.45	0.85	17.26	21.76	1.26

In Fig. 4.7 we plot the self diffusivity of pure components as well as, intrinsic and mutual diffusion coefficients as a function of Al compositions in the considered liquid alloys at 1873 K. Unfortunately no experimental data for self and mutual diffusion coefficients are not available for the concerned liquid alloys. The high value of D_{Al} as compared to D_{Fe} is expected due to the lower atomic mass of Al. This trend suggests that atomic liquid with a smaller diameter is more responsible for generating friction in the liquid alloys which is also observed by Bhuiyan *et al*. in their study on liquid Ag-In alloys (Bhuiyan *et al*., 2003)

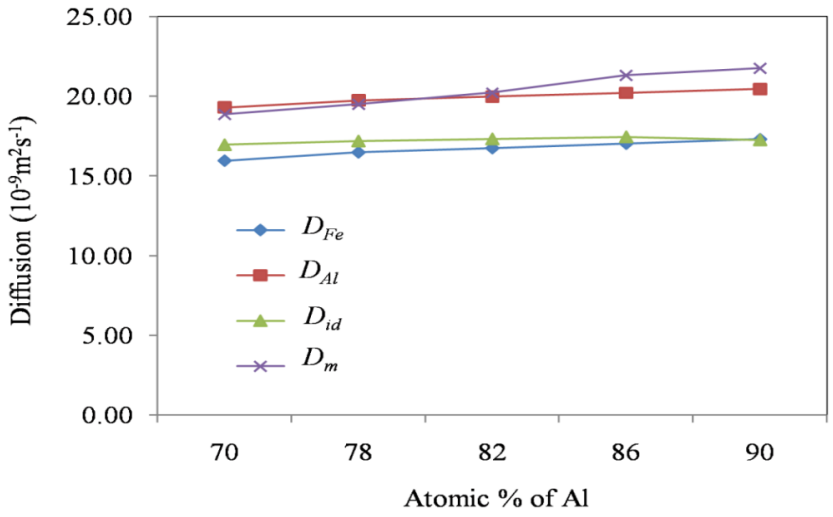

Figure 4.7: Self and mutual diffusion coefficient of Fe-Al melts as a function of Al compositions at 1873 K.

It was observed that both D_{Fe} and D_{Al} increase with an increase in the atomic percent of Al. It can be seen from Fig. 4.7 that D_m is greater than D_{id} ($D_m > D_{id}$) at all investigated compositions, which is an indication of hetero-coordination in Al-rich Fe-Al melts.

4.3.2.2. Viscosity coefficients and surface tension of Fe-Al alloys

The computed values of self and mutual diffusion coefficients have been employed to determine the viscosity coefficients of pure components and binary mixtures as a function of Al concentration in liquid Fe-Al alloys at 1173 K. In Fig. 4.8 we report the comparison between our computed values of shear viscosity at five different compositions of liquid Fe-Al alloys with available experimental data (Bel'tyukov *et al.*, 2015; Lihl *et al.*, 1964) with different approaches. It can be inferred from Fig. 4.8 that the computed values of shear viscosity using SW potential function are in excellent agreement with experimental results reported in reference (Bel'tyukov *et al.*, 2015; Lihl *et al.*, 1964).

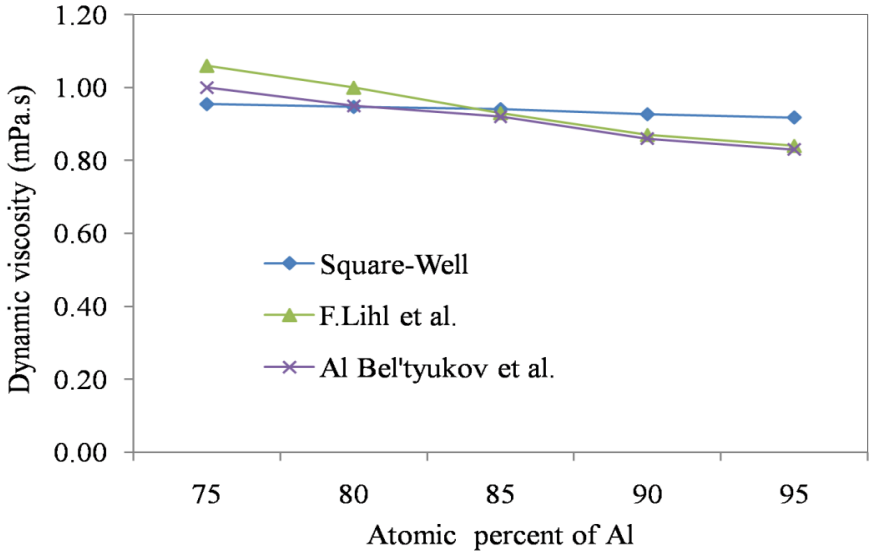

Figure 4.8: Square-well and experimental (Bel'tyukov *et al.*, 2015; Lihl *et al.*, 1964) values of concentration dependent coefficient in liquid Fe-Al alloy at 1173 K.

In Fig. 4.9 we plot $D\eta$ values against atomic % of Al. $D\eta$ under SE relation can be given as inverse of r^{max}. The constant value of $D\eta$ against temperature and

concentration indicates that the nearest neighbor distance of metal-metal pairs, which, is obtained by Fourier transform of computed partial and total structure factors are independent of compositions and validate the applicability of the SE relation in such melts.

Non linearity in case of liquid Al and liquid Fe-Al alloys can be addressed as dependency of separation between Al-Al and Fe-Al on Al concentration in melts. We observe a sharp change beyond 86% of Al in alloy which refers to that breakdown of SE relation around this composition.

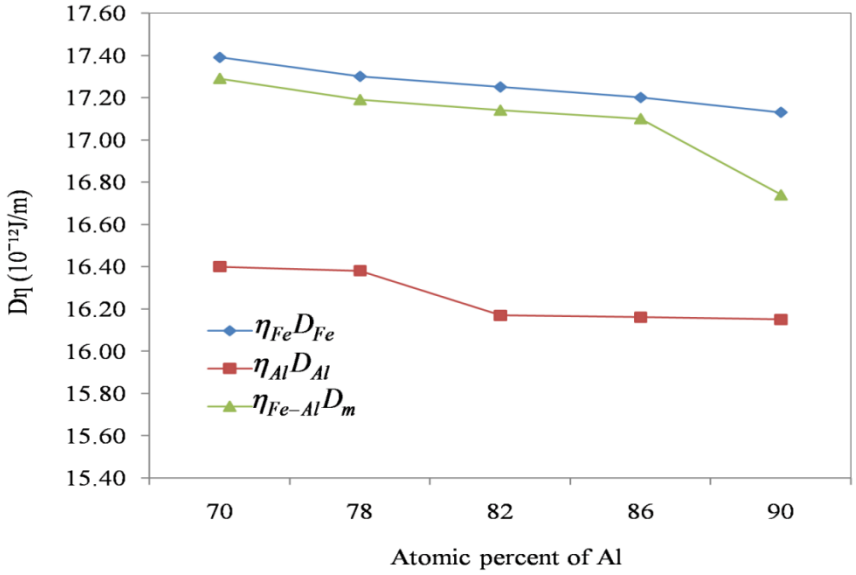

Figure 4.9: $D\eta$ as a function of Al compositions in Fe-Al melts at 1873 K.

Brillo and Pommrich (Brillo and Pommrich, 2011) also observed a breakdown of SE relation in the experimental study on Ni-Zr alloys. For pure component and four out of five investigated alloys, $D\eta$ is roughly independent of compositions, which means that nearest neighbor distance of homo and hetero metal pairs display a very weak composition dependency within the investigated range. As we know that the breakdown of the SE relation is associated with a temperature evolution or unusual values of the metal-metal pair separation in the binary melts (Pasturel and Jakse, 2015). $D\eta$ under SE relation can be given as inverse of $r^{\max}$. The constant value of $D\eta$ indicates that the nearest neighbor distance of metal-metal pairs ($r_{Fe-Fe}^{\max}$, $r_{Al-Al}^{\max}$ and $r_{Al-Fe}^{\max}$) which is obtained by Fourier transform of computed

partial and total structure factors are not changing in the considered alloys, which shows the applicability of the SE relation in considered melts.

The calculated values of concentration dependent surface tension for liquid Fe-Al alloys are shown in Fig. 4.10. It is observed that surface tension of mixture gradually decreases with the addition of Al component and exhibits linearity with concentration. A similar trend was observed for Hg-Na liquid alloys obtained by Sharma *et al.*(Sharma *et al*., 2014).

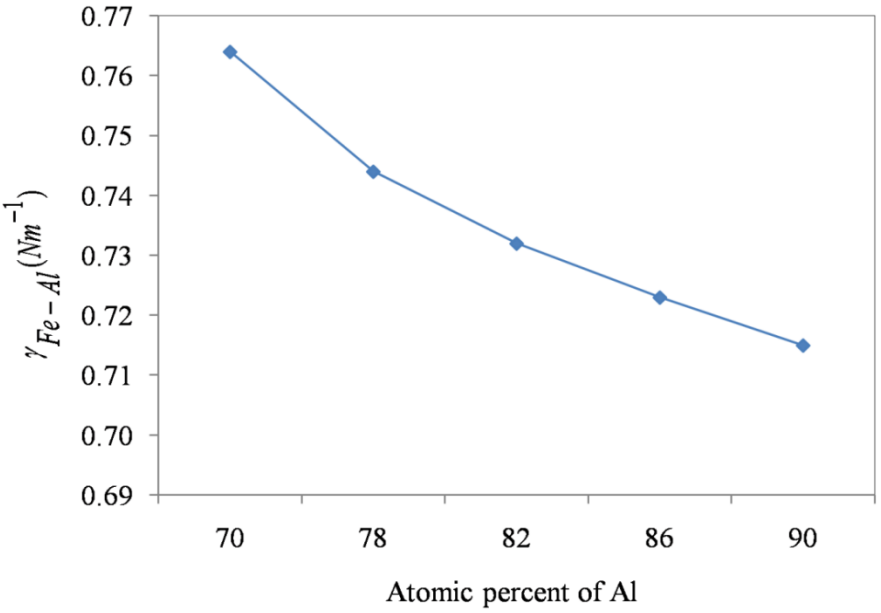

Figure 4.10: Surface tension versus atomic percent of Al alloys at 1873 K.

This decreasing nature of surface tension in Fe-Al melts is due to increase in chemical ordering with increase in Al concentration in considered alloys. We do not find any experimental data on surface tension of liquid Fe-Al alloys for comparing our theoretical results.

4.3.3. Scaling properties of binary liquids

To find a correlation between atomic structure and transport coefficient in terms of scaling law is reported by several researchers with different theoretical and simulation approaches (Wang *et al*., 2015; Mishra and Lalneihpuii, 2016; Mishra and Shrivastava, 2017; Dzugutov, 1996; Hoyt *et al*., 2000; Samanta *et al*., 2004; Pasturel and Jakse, 2015; Rosenfeld, 1999). Dzugutov (Dzugutov, 1996) correlated dynamic

behavior (diffusion) of liquid with static structural parameter s^{ex}, excess entropy under two body approximations. The computed values of S_E as a function of composition as well as S_E^{Cu} and S_E^{In} calculated at 1073 K are given in Table 4.8. The scaling factor (χ_{Cu} and χ_{In}), the dimensionless diffusion coefficient, D* of liquid Cu-In binary alloys at different compositions of In at 1073 K are also given in Table 4.8.

Table 4.8. Scaling factors, D*, partial and total excess entropy of liquid Cu-In binary alloys at different compositions of In at 1073 K.

% In in Cu-In	χ_{Cu} ($10^{-6}m^2/s$)	χ_{In} ($10^{-6}m^2/s$)	D*x10^{-3}	$-S_E^{Cu}/k_B$	$-S_E^{In}/k_B$	$-S_E/k_B$
25	2.74	1.99	2.331	3.061	2.996	3.045
27	2.79	1.97	2.352	3.060	2.970	3.036
29	2.77	1.94	2.422	3.035	2.935	3.006
32	2.81	1.91	2.478	3.024	2.898	2.984
34	2.77	1.90	2.551	2.994	2.878	2.954

Fig. 4.11 and Fig.4.12 illustrate the reduced values of diffusion coefficient D* and viscosity coefficient η* as a function of pair wise entropy s^{ex} at 1073 K temperature. It is interesting to note that the reduced values of D* and η* are scaled with exponential of s^{ex} for all the compositions with a slope of -0.056 and 0.244 respectively. Further, the regression coefficients R^2 values of two cases are 0.975 and 0.996 respectively. For the sake of comparison we compare our computed results with Dzugutov law and observe a close relation (Dzugutov, 1996).

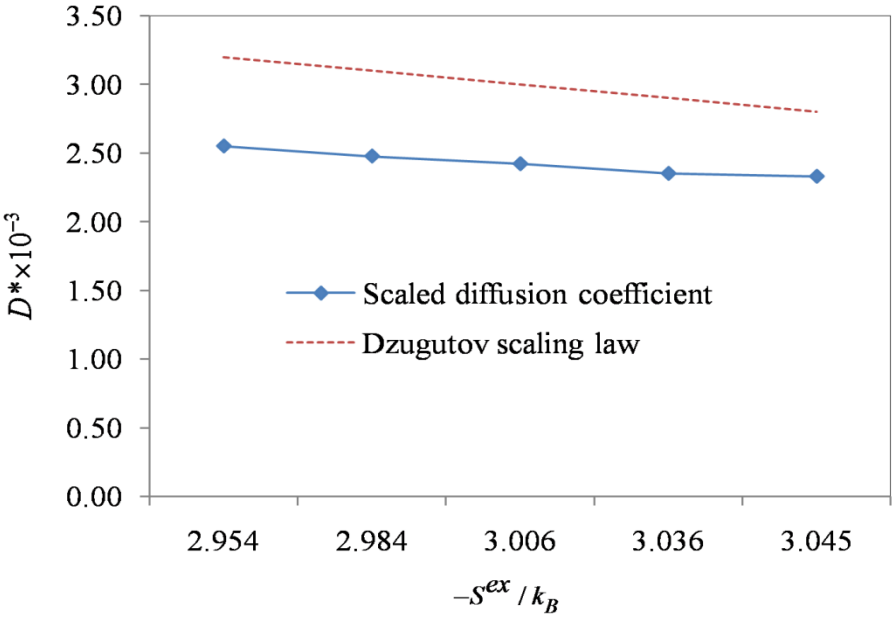

Figure 4.11: D* versus S^{ex} of Cu-In melts at different concentrations of In.

One can demonstrate from Figs. 4.11 and 4.12 the scaling laws diffusion and viscosity for the SW binary liquid and can be tested for binary liquid with different potential functions. We demonstrate in Fig. 4.12 a linear relationship between two body excess entropy with the shear viscosities of pure components and liquid Cu-In alloys.

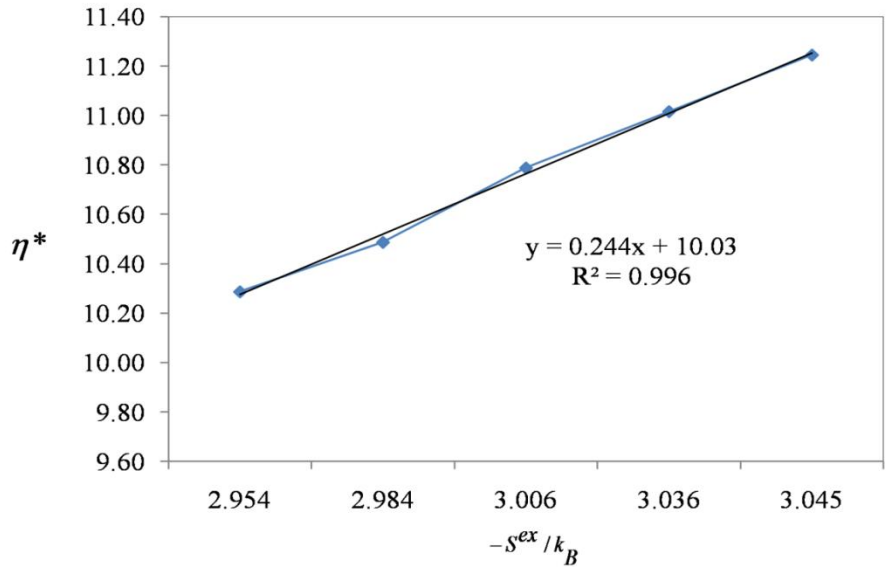

Figure 4.12: η* versus S^{ex} of Cu - In melts at different concentrations of In.

The computed values of S_E as a function of composition as well as S_E^{Fe} and S_E^{Al} calculated at 1873 K are given in Table 4.9. The scaling factor (χ_{Fe} and χ_{Al}), the dimensionless diffusion coefficient, D* of liquid Fe-Al binary alloys at different compositions of In at 1073 K are also given in Table 4.9.

Table 4.9. Scaling factors, D*, partial and total excess entropy of liquid Fe-Al binary alloys at different compositions of Al at 1873 K.

% Al in Fe-Al alloy	χ_{Fe} ($10^{-6}m^2/s$)	χ_{Al} ($10^{-6}m^2/s$)	D*x10^{-3}	$-S_E^{Fe}/k_B$	$-S_E^{Al}/k_B$	$-S_E/k_B$
70	3.46	3.32	5.42	2.363	2.131	2.201
78	3.68	3.32	5.59	2.392	2.104	2.167
82	3.84	3.42	5.54	2.418	2.123	2.176
86	3.92	3.41	5.67	2.422	2.111	2.154
90	3.88	3.34	5.93	2.395	2.080	2.112

In a condensed system, the constancy of the internal structural relaxation which defines the rate of diffusion is proportional to the number of its available arrangement (per atom). In an equilibrium system due to the force caused by the structural correlations, this number is reduced by a factor of e^S, where S is pairwise excess entropy (Dzugutov, 1996). So obviously, there is a relationship between the dimensionless diffusion coefficient, D*, and excess entropy S^{ex}.

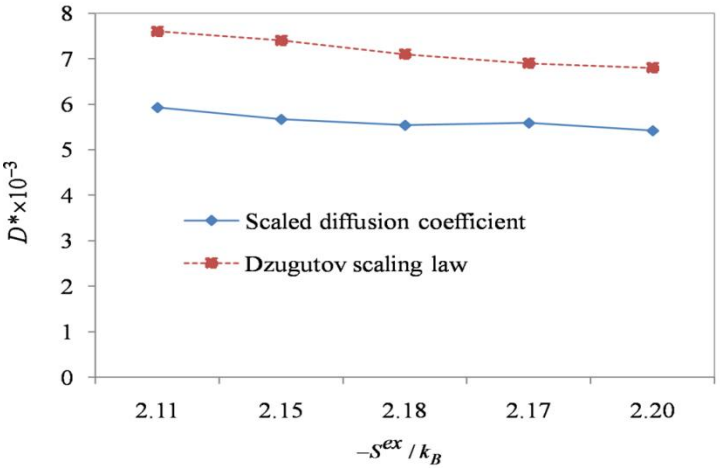

Figure 4.13: D* versus S^{ex} of Fe-Al melts at different concentrations of Al.

Figs. 4.13 and 4.14 illustrate the comparison of a plot for Dzugutov scaling law (Dzugutov, 1996) between the dimensionless diffusion coefficient, D* and viscosity coefficient η* as a function of excess entropy S^{ex}/k_B at 70, 78, 82, 86 and 90% Al concentration in liquid Fe-Al binary alloys.

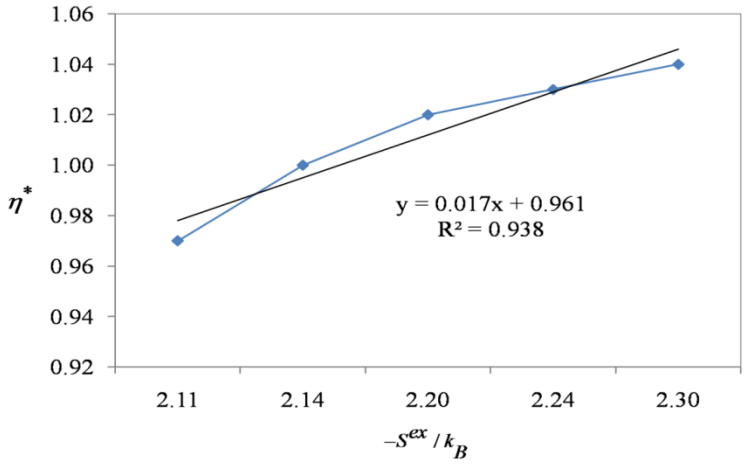

Figures 4.14: η* versus S^{ex} of Fe-Al melts at different concentrations of Al.

It was observed that the slope of the line for scaled D^* and η* are respectively -0.11 and 0.017. Further, the regression coefficients R^2 are found to be 0.832 and 0.938 respectively.

THERMODYNAMICS OF LIQUID BINARY ALLOYS

5.1. INTRODUCTION

The knowledge of structural functions, transport coefficients, chemical ordering, thermodynamic properties and surface phenomena of metallic melts is of great importance for various metallurgical processes like phase transition, glass formation and crystal growth (Dubinin, 2019; Mishra *et al*., 2015; Gopala Rao, U. Bandyopadhyay, 1989; Mc. Quarrie, 1976; Yakymovych *et al*., 2014; Sharma *et al*., 2014; Liu *et al*., 2010; Brillo *et al*., 2008; Wang *et al*., 2015; Venkatesh *et al*., 2003; Odusote, 2008). The computation of thermodynamic properties of alloy is a difficult task and the model calculations are not universally applicable. Hence, the investigation of transport and thermodynamic properties through microscopic structural functions in liquid alloys is always interesting and open new door to the applicability of alloys.

Thermodynamic mixing parameters like (enthalpy, free energy, entropy) are very important quantities, which decide the metallurgical processes and control over the alloying of metals. In recent years, various techniques have been studied to estimate such thermodynamic properties of alloys (Kanibolotsky *et al*., 2002; Yang *et al*., 2008). One of the purposes of this study is to estimate the thermodynamic mixing parameters through investigated SW model of structural functions and transport coefficients of liquid Cu-In and liquid Fe-Al binary alloys.

5.2. THEORY

5.2.1. Evaluation of enthalpy of mixing in liquid binary alloys

The Romanov-Kozlov-Petrov (RKP) model, which correlates the viscosity with enthalpy of mixing, has been used for estimating the enthalpy of mixing (Mudry *et al*., 2013). Mudry *et al*. also used this equation to estimate viscosity using experimental enthalpy data.

$$\ln\eta_{l\text{-}m} = \sum_{i=1}^{n} x_i \ln\eta_i - \frac{H_M}{3RT} \tag{5.1}$$

Here, x_i and η_i are the atomic fractions and viscosity of the i^{th} component respectively, H_M is the integral enthalpy of mixing, R and T are the ideal gas constant, and the working temperature respectively.

5.2.2. Evaluation of entropy of mixing in liquid binary alloys

All entropies are expressed in terms of per atom unit i.e. $\frac{S^{ex}}{Nk_B}$. Here S^{ex} is the total excess entropy (Dubinin *et al*., 2014) which can be obtained via scaling properties defined as:

$$S^{ex}=S^{bin}-\sum_{i=1}^{2} x_i S_i^{Pure}-S^{id} \tag{5.2}$$

where S^{bin} is the total entropy of the system per atom and S^{id} is the entropy per atom of an ideal gas system, which can be given as

$$S^{id}=-k_B(x_l \ln C_l + x_m \ln C_m) \tag{5.3}$$

The excess entropy of the liquid Cu-In system has been calculated using a SW model of pair correlation function under two body approximations (Dzugutov, 1996)

$$S^{ex}=-2\pi\rho_{l\text{-}m}\sum_{1}^{2} x_l x_m \int_0^{\infty}\left\{g_{l\text{-}m}(r)\ln\left[g_{l\text{-}m}(r)\right]-\left[g_{l\text{-}m}(r)-1\right]\right\} r^2 dr \tag{5.4}$$

5.2.3. Evaluation of free energy of mixing in liquid binary alloys

The molar Gibbs free energy of mixing in the binary melt is obtained as a function of composition as follows

$$G_M^{ex}=H_M-TS_M^{ex} \tag{5.5}$$

where the enthalpy of mixing, H^{mix} is obtained through the RKP equation, Eq. (5.1).

5.3. RESULTS AND DISCUSSION

5.3.1. Cu-In

5.3.1.1. Enthalpy of mixing

The thermodynamic approach namely the RKP equation has been applied for the investigation of the correlation between the enthalpy of mixing and the viscosity of the melts.

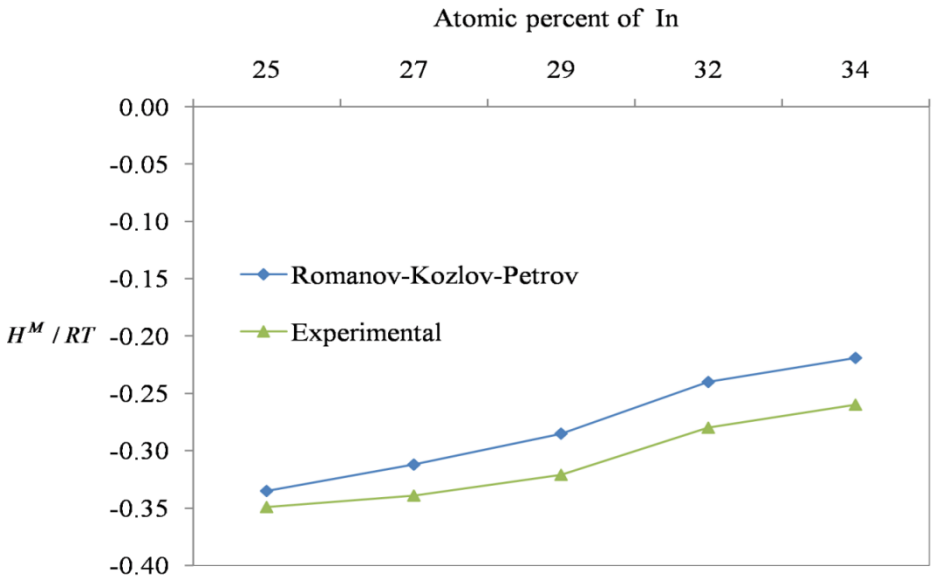

Figure 5.1: Theoretical and experimental (Hultgren, 1973) values of the concentration dependence of enthalpy of mixing in liquid Cu-In alloy at 1073 K.

As shown in Fig. 10, the enthalpy of mixing calculated from the RKP equation is in good agreement with the experimental value (Hultgren, 1973) and so we used the computed results for the calculating free energy of mixing.

5.3.1.2. Entropy of mixing

The pair wise excess entropy of liquid Cu-In alloy and partial excess entropies S_{Cu}^{ex} and S_{In}^{ex} of pure components were computed using Eqns. (4.32) to (4.34) in chapter 4 and illustrated in Fig. 12 as a function of In composition. Fig. 12 shows an excellent agreement between the computed and experimentally measured (Hultgren, 1973) values for the pair wise excess entropy S_M^{ex} / R of Cu-In melts. We

observe a high value of partial and total S^{ex} in In rich region which also reflects chemical ordering in this region.

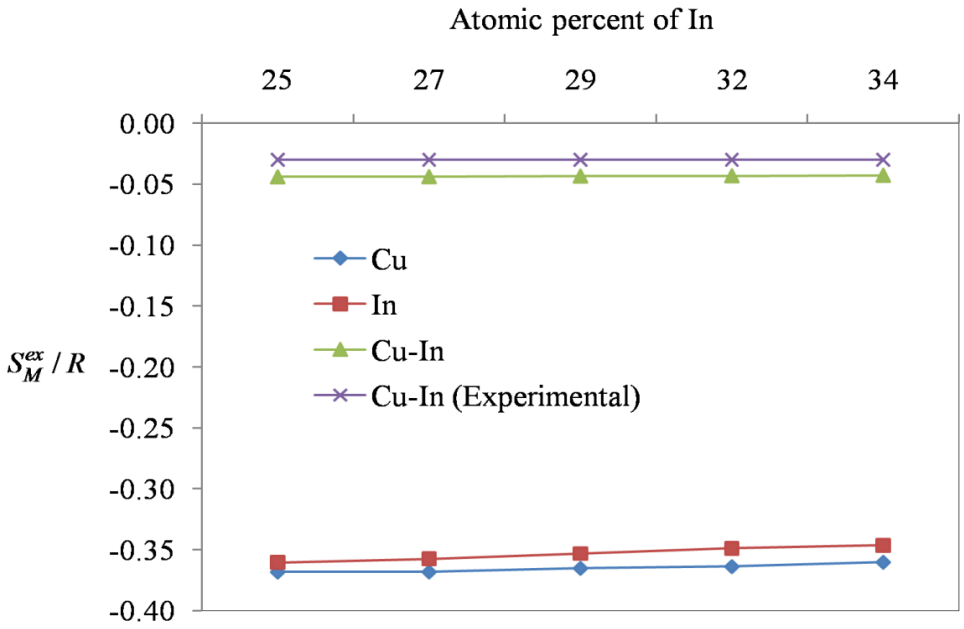

Figure 5.2: Theoretical and experimental (Hultgren, 1973) values of the concentration dependence of excess entropy of mixing in liquid Cu-In alloy at 1073 K.

The partial excess entropies were linearly related with the self-diffusion coefficient and therefore the self-diffusion coefficient values were used to calculate the partial excess entropies of Cu and In in the investigated alloys through Eqns. (4.32) and (4.33) in Chapter-4. The total excess entropy of mixing was obtained from the partial excess entropies through Eqn. (4.34) and was shown in Fig. 5.2. It can be seen from Fig. 5.2 that the computed partial as well as the total entropy of mixing were having negative values and were found to increase slightly with an increase in the atomic percent of In. The negative values of entropies show that the mixing of Cu and In were found to be thermodynamically exothermic at the working temperature i.e.1073 K.

5.3.1.3. Free energy of mixing

The computed and observed values from activity data (Hultgren, 1973) for the Gibbs free energy of mixing, G_M^{ex} as a function of In concentration, are shown Fig. 5.3. It must be noted that a negative value for G_M^{ex} was observed for investigated compositions of Cu-In melts at 1073 K.

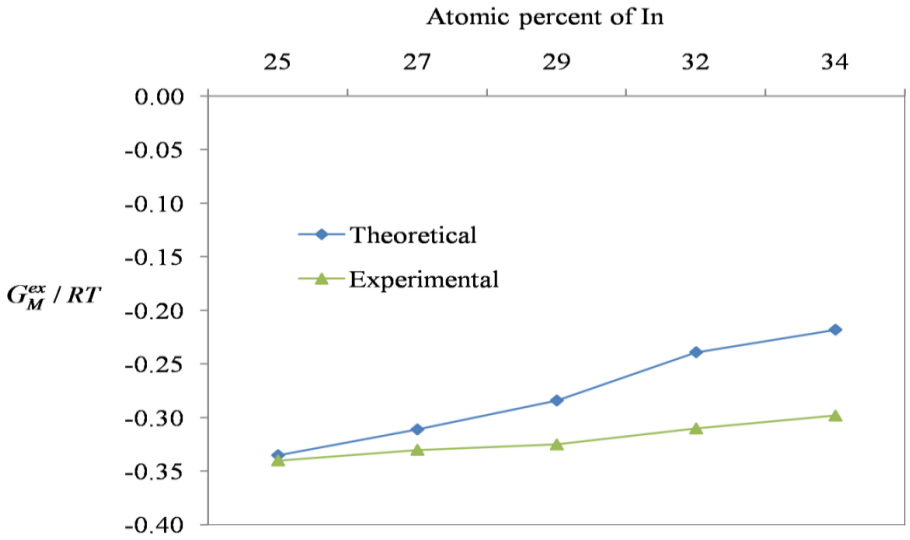

Figure 5.3: Theoretical and experimental (Hultgren, 1973) values of concentration dependence of the free excess energy of mixing in liquid Cu-In alloy at 1073 K.

We observe a positive deviation of the computed data from experimental values (Hultgren, 1973) and it increases with In concentration. The computed thermodynamic parameters are in good agreement in Cu-rich regions of the alloys.

5.3.2. Fe-Al

5.3.2.1. Enthalpy of mixing

RKP equation, Eqn. (5.1) for the correlation between viscosity and enthalpy of mixing (H_M) was used for the investigation of H_M as a function of Al concentration. The computed values of viscosity coefficients from the modified SE relation were used in this investigation.

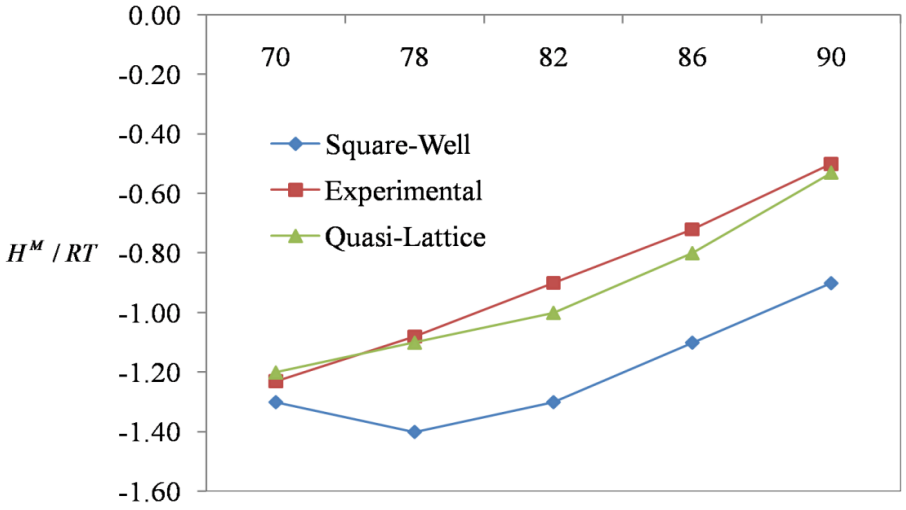

Figure 5.4: Square-Well, Quasi-Lattice (Akinlade *et al*., 2000) and experimental (Batalin *et al*., 1973) values of concentration dependence of enthalpy of mixing in liquid Fe-Al alloys at 1873 K.

As observed from Fig. 5.4, the enthalpy of mixing obtained from square-well, quasi-lattice (Akinlade *et al*., 2000) and experimental results (Batalin *et al*., 1973) at all concentrations of Al are showing negative values. This is a clear indication that Fe-Al is a chemically ordered system. Although our computed results is showing more difference from the experimental H_M values as compared to the QL model, it follows the same trend as experimental results (Batalin *et al*., 1973) with an average difference of 0.34 J mol^{-1}.

5.3.2.2. Entropy of mixing

The pair wise excess entropy of liquid Fe-Al and partial excess entropies S_{Fe}^{ex} and S_{Al}^{ex} were computed using Eqns. (4.32) and (4.33) in chapter 4 and presented in Fig. 5.5 as a function of Al compositions. It can be seen that the computed and experimental values of total excess entropy of mixing were having negative values at all investigated compositions of Al.

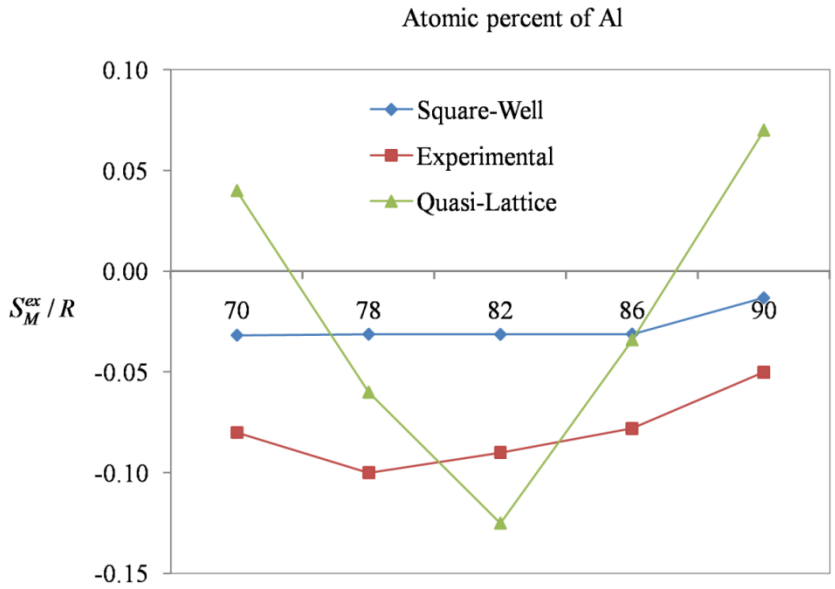

Figure 5.5: Square-Well, Quasi-Lattice (Akinlade *et al*., 2000) and experimental (experimental points obtained from the difference between H^M and G^M) values of concentration dependence of excess entropy of mixing in liquid Fe-Al alloys at 1873 K.

Theoretical and experimental (experimental points obtained from the difference between H^M and G^M) values of the concentration dependence of excess entropy of mixing in liquid Cu-In alloy at 1073 K.

The negative values of entropies show that the mixing of Fe and Al were found to be thermodynamically exothermic at the working temperature i.e.1873 K. We find that the values of S_{ex}^M / R computed from SW model and experimental results are in better agreement then the QL model.

5.3.2.3. Free energy of mixing

The values of Gibbs free energy of mixing, G_M^{ex} as a function of Al composition observed from SW model computation, QL model (Akinlade *et al*., 2000) and experimental results (Belton and Fruehan, 1969) were plotted in Fig. 5.6.

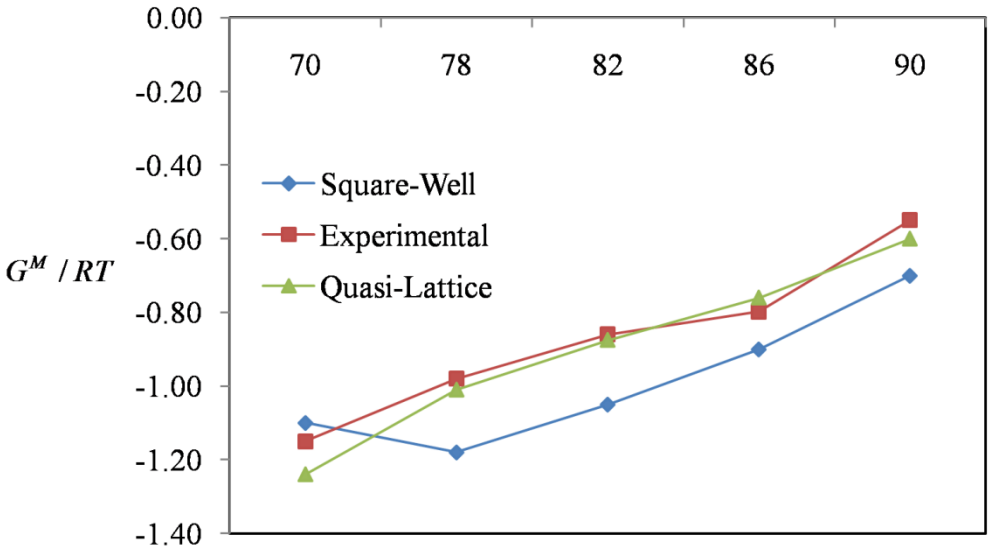

Figure 5.6: Square-Well, Quasi-Lattice (Akinlade *et al*., 2000) and experimental (Belton and Fruehan, 1969) values of concentration dependence of free energy of mixing in liquid Fe-Al alloys at 1873 K.

It can be seen that all the observed G_M^{ex} values are showing positive deviations with increase in atomic percent of Al. The computed values of G_M^{ex} are showing fair agreement with experimental values (Belton and Fruehan, 1969) except for 78 to 82 % of Al. This may due to existence of eutectic composition in this range.

TEMPERATURE EFFECT ON STRUCTURAL AND TRANSPORT COEFFICIENT OF LIQUID COPPER

6.1. INTRODUCTION

Due to lacking of long range order in liquids, the best way to characterize the structure of a liquid is through correlation functions. The pair correlation function or radial distribution function is one of the important parameter to explain the structural features of a liquid. This is also formed as density-density correlation which is defined as the probability of finding an atom at a distance 'r' at time 't' from an atom at origin at time t=0. The average number of nearest neighbor to first coordination cells which is called coordination numbers are reported in recent years due to its importance in explaining the local structure of liquid metals and alloys. These local structural functions are correlated with important macroscopic properties of liquid metals and alloys like diffusion.

Super heating of crystals has been one of the highly interest work out in the advancement of material sciences (Xiufang and Weimin, 2000). For the complete understanding of various liquid state properties like molecular structure, dynamic behavior at the atomic level, it is highly essential to study the local atomic structure and observing how it changes as a function temperature (Wang *et al*., 2009).

The structure factor for pure liquid metals closely resemble to those for the hard sphere atomic structure (Khaleque *et al*., 2002). In the effort to understand liquid metal structure factors, S(k), we take into consideration an attractive part with the hard sphere reference system. The square well fluid is the simplest one possessing the basic characteristics of a real fluid (Wu *et al*., 2004).The square-well (SW) system thereby serves as a very efficient reference system, where liquid state theoreticians gives an effort from different approaches like DFT, Gaussian, integration by the perturbation of hard sphere model by the SW potential system (Lang *et al*., 2009).

The study of transport coefficients such as diffusion and viscosity coefficients of liquid metals is of crucial importance for understanding of liquid dynamics, nucleation, nitrification and crystal growth and serves as one of the main thermo

physical parameter for the production of new materials. For the microstructure development, diffusion coefficient plays a key role and serves as a crucial parameter for the results of molecular dynamics (MD) simulation (Meyer and Kargl, 2013). The critical cooling rates for glass transition for a liquid depend on their viscosity parameter. However it is not well understood how the structure and thermodynamic properties of liquid metals has an effect on the viscosity (Sonvane *et al*., 2012).

The self diffusion coefficients of liquid Cu at different temperatures has been obtained by using Einstein equation for diffusion coefficients (Venkatesh *et al*., 2003). A model calculation provides a way to compute three friction coefficients arising from the forces of hard core and soft part of the potential function.

The viscosity coefficient of liquid Cu has been obtained by replacing the hydrodynamic radius in the Stokes-Einstein relation by the first peak position of g(r) and computed values of diffusion coefficients, D.

The study of coordination number, diffusion coefficients and viscosity of liquid metals is of fundamental importance and the better understanding of these properties is helpful in material processing technology. Co-ordination of liquid metals is determined by integrating g(r) functions between first two minima. The understanding of liquid state theories depends on the information available for the structure, transport and thermodynamic properties of the liquid (Fima and Sobezak, 2010).

6.2. THEORETICAL MODEL

6.2.1. Evaluation of Structure Factor and Radial Distribution Function

The square well potential can be given as

$$U(SW) = \begin{cases} \infty & ; \quad r < \sigma \\ -\varepsilon & ; \quad \sigma < r < \lambda\sigma \\ 0 & ; \quad r > \lambda\sigma \end{cases} \tag{6.1}$$

where λ and ε are the breadth and depth of the potential well respectively and σ is the hard sphere diameter.

The Direct Correlation Function (DCF) of square well fluid is given as

$$C(k) = C_{SW}(k) + C_{HS}(k) \tag{6.2}$$

Where,

$$\rho C_{SW}(k) = [24\eta\varepsilon / k_B T]\ (x)^3\ [\sin(\lambda x) - \lambda x \cos(\lambda x) + x\ \cos(x)\ -\ \sin(x)] \tag{6.3}$$

$$\begin{aligned}\rho C_{HS}(k) = &-[24\eta/(x)^6][\alpha(x)^3\{\sin(x\sigma x - x\cos(x)\} + \beta(x)^2 \\ &\{2x\sin(x) - (x^2-2)\cos x - 2\} + \gamma\{(4x^3 - 24x) \\ &\sin(x) - (x^4 - 12x^2 + 24)\cos x - 24\}].\end{aligned} \tag{6.4}$$

and x = kσ, ρ is the number density, ε and λ represent depth and breadth respectively of the SW.

Wertheim's (Wertheim, 1963) solution of Percus-Yevick's equation for hard spheres reference system perturbed with a square well attractive tail to evaluate the structure factors as (Mishra and Venkatesh, 2008)

$$S(k) = 1/1 - \rho C(k) \tag{6.5}$$

Here ρ is the number density and C(k) is the total correlation function of liquid metals. The Fourier inversion of S(k) gives, the radial distribution function, g(r)

$$g(r) = 1 + \frac{1}{2\pi^2\rho}\int_0^\infty k^2[S(k) - 1]\frac{\sin kr_{nm}}{kr_{nm}}dk \tag{6.6}$$

6.2.2. Evaluation of Transport Coefficients

6.2.2.1. Self Diffusion Coefficient

The self diffusion coefficient of pure metal can be given by Einstein' equation as

$$D = k_B T / \xi \tag{6.7}$$

Here k_B is the Boltzmann constant, ξ is the friction coefficient, which is a sum of the friction coefficients arising from the forces of hard-core, soft-part and hard-soft part as (Mishra and Venkatesh, 2005).

$$\xi = \xi^{HP} + [\xi^{SP} + \xi^{SHP}] \tag{6.8}$$

The contribution from ξ^{HP}, ξ^{SP} and ξ^{SHP} which incorporate the radial and structural aspects, are given as follows

$$\xi^{HP} = \frac{8}{3}\rho g(\sigma)\sigma^2(\pi m k_B T)^{1/2} \tag{6.9}$$

$$\xi^{SP} = -\frac{1}{3}\frac{\rho}{4\pi^2}\left(\frac{\pi m}{k_B T}\right)^{1/2}\int_0^\infty k^3 u^s(k)G(k)dk \tag{6.10}$$

$$\xi^{SHP} = -\frac{1}{3}\rho g(\sigma)\left(\frac{m}{\pi k_B T}\right)^{1/2} \times \int_0^\infty [k\sigma\cos(k\sigma) - \sin(k\sigma)]\, u^s(k) \tag{6.11}$$

$$u^{sw}(k) = \frac{4\pi\xi}{k^3}[Ak\sigma\cos(Ak\sigma) - \sin(Ak\sigma) - k\sigma\cos(k\sigma) + \sin(k\sigma)] \tag{6.12}$$

$$G(k) = \frac{1}{\rho}[S(k)1] \tag{6.13}$$

The logarithmic variation of the diffusion coefficient with temperature is evaluated from Einstein's equation and it is given by

$$\frac{dlnD}{dT} = \frac{1}{T} - \frac{dln\xi}{dT} \tag{6.14}$$

Hence to evaluate $\frac{dlnD}{dT}$ we have to evaluate $\frac{dln\xi}{dT}$.Thus the gradient of the hard sphere part with respect to temperature is given by

$$\frac{d\xi^{HP}}{dT} = \frac{\xi^{HP}}{2T} - k\xi^{HP} + \frac{8}{3}\rho\sigma^2(\pi m k_B T)^{1/2} \times \left\{\frac{2k}{3}[g(\sigma) - 1] + \frac{k}{6\pi^2\rho}\int_0^\infty k^2\,[S(k) - 1]\cos(k\sigma)\,dk + \frac{1}{2\pi^2\rho\sigma}\int_0^\infty k\sin(k\sigma)S(k)dk\right\} \tag{6.15}$$

The temperature derivative of the soft-part and hard-soft part of the friction coefficients are given by the following equations

$$\frac{d\xi^{SP}}{dT} = -\frac{\xi^{SP}}{2T} - \left(\frac{\pi m}{k_B T}\right)^{1/2}\int_0^\infty k^3\, u^s(k)S(k) \tag{6.16}$$

$$\frac{d\xi^{SHP}}{dT} = -\frac{\xi^{SHP}}{2T} - k\xi^{SHP} - \frac{1}{3}\rho\left(\frac{m}{\pi k_B T}\right)^{1/2} \times \int_0^\infty [k\sigma\cos(k\sigma) - \sin(k\sigma)]u^S(k)dk \quad \left\{\frac{2k}{3}[g(\sigma) - 1] + \frac{k}{6\pi^2\rho}\int_0^\infty k^2[S(k) - 1]\cos(k\sigma)\,dk + \frac{1}{2\pi^2\rho\sigma}\int_0^\infty k\sin(k\sigma)S(k)dk\right\} \tag{6.17}$$

Here,

$$S(k) = \frac{dS(k)}{dT}$$

$$= k[S(k)]\left\{[1 - S(k)] + \frac{24\eta S(k)}{(k\sigma)^6}\left[\frac{4X1\alpha\eta(2+\eta)}{(1+2\eta)(1-\eta)}\right] + \frac{X2\beta(\eta^2+9\eta+2)}{(2+\eta)(1-\eta)} + \frac{X3\gamma(2\eta^2+9\eta+1)}{(2+\eta)(1-\eta)} - \frac{\varepsilon X4}{\kappa k_B T^2}\right\} \tag{6.18}$$

The other coefficients that enter in Eq. (5.16) are given by the following equation

$$\alpha = \frac{(1+2\eta)^2}{(1-\eta)^4} \tag{6.19}$$

$$\beta = -\frac{6\eta(1+\frac{\eta}{2})^2}{(1-\eta)^4} \tag{6.20}$$

$$\gamma = \frac{\eta(1+2\eta)^2}{2(1-\eta)^4} \tag{6.21}$$

$$X1 = (k\sigma)^3[\sin(k\sigma) - k\,\sigma\cos(k\sigma)] \tag{6.22}$$

$$X2 = (k\sigma)^2[2k\sigma\sin(k\sigma) - (k^2\sigma^2 - 2)\cos(k\sigma) - 2] \tag{6.23}$$

$$X3 = (4k^3\sigma^3 - 24k\sigma)\sin(k\sigma) - (k^4\sigma^4 - 12k^2\sigma^2 + 24)\cos(k\sigma) + 24 \tag{6.24}$$

$$X4 = (k\sigma)^3[\sin(Ak\sigma) - Ak\sigma\cos(Ak\sigma) + k\sigma\cos(k\sigma) - \sin(k\sigma)] \tag{6.25}$$

6.2.2.2. *Viscosity Coefficient*

The shear viscosity coefficient, η_v is obtained under the SW model with the Stokes-Einstein relation

$$\eta_v = \frac{k_B T}{2\pi r_{max} D} \tag{6.26}$$

Where k_B is the Boltzmann's constant, r_{max} is the first peak position of g(r) and D is the diffusion coefficient.

6.2.3. Evaluation of coordination number

The nearest-neighbor coordination number, ψ, can be obtained by integrating the g(r) function between the first two minimum i.e. the left edge of the first peak to the first minimum on the right hand side of the first peak, r_{min}. ψ characterizes several types of short-range order present in the liquids. The microstructure of liquids can also be characterized by ψ.

$$\psi = 4\pi\rho \int_0^{r_{min}} g(r) r^2 dr \tag{6.27}$$

6.2.4. Evaluation of Coefficient of Thermal Expansion

Equation of states for square-well fluids

$\boldsymbol{\alpha_1} = \frac{\mathbf{1}}{\mathbf{V}}\frac{\mathbf{dV}}{\mathbf{dT}}$ = coefficient of thermal expansion (6.28)

$$\frac{d\eta}{dT} = -\eta\alpha_1 \tag{6.29}$$

$$\frac{PV}{RT} = \frac{1+\eta+\eta^2}{(1-\eta)^3} - \frac{4\epsilon\eta(\lambda^3-1)}{k_B T} \tag{6.30}$$

$$\frac{\mathbf{PV}}{\mathbf{R}} = \frac{\mathbf{(1+\eta+\eta^2)T}}{\mathbf{(1-\eta)^3}} - \frac{\mathbf{4\epsilon\eta(\lambda^3-1)}}{\mathbf{k_B}} \tag{6.31}$$

$$\frac{P}{R}\left(\frac{dV}{dT}\right)_P = \frac{1+\eta+\eta^2}{(1-\eta)^3}\frac{dT}{dT} + \frac{T}{(1-\eta)^3}\left(0 + \frac{d\eta}{dT} + 2\eta\frac{d\eta}{dT}\right) + T(1+\eta+\eta^2)\frac{(-3)}{(1-\eta)^4}(-1)\frac{d\eta}{dT} - \frac{4\epsilon\eta(\lambda^3-1)}{k_B}\frac{d\eta}{dT} \tag{6.32}$$

$$\frac{1+\eta+\eta^2}{(1-\eta)^3} + \frac{T}{(1-\eta)^3}(-\eta\alpha_1 + 2\eta \times -\eta\alpha_1) + T(1+\eta+\eta^2)\frac{(-3)}{(1-\eta)^4} \times -\eta\alpha_1 - \frac{4\epsilon\eta(\lambda^3-1)}{k_B} \times -\eta\alpha_1 \tag{6.33}$$

$$\frac{P}{R}\frac{dV}{VdT} = \frac{(1+\eta+\eta^2)}{(1-\eta)^3} - \frac{-\eta\alpha_1 T(2\eta+1)}{(1-\eta)^3} - \frac{3T(1+\eta+\eta^2)\alpha_1\eta}{(1-\eta)^4} + \frac{4\epsilon(\lambda^3-1)}{k_B}\eta\alpha_1 \tag{6.34}$$

$$\frac{PV}{R} \times \alpha_1 = \frac{(1+\eta+\eta^2)}{(1-\eta)^3} - \frac{-(2\eta+1)\eta\alpha_1 T}{(1-\eta)^3} - \frac{3T\eta\alpha_1(1+\eta+\eta^2)}{(1-\eta)^4} + \frac{4\epsilon(\lambda^3-1)\eta\alpha_1}{k_B} \tag{6.35}$$

$$= \frac{(1+\eta+\eta^2)}{(1-\eta)^3} - \frac{(2\eta+1)(1-\eta)\,\eta\,\alpha_1 T + 3T\eta\alpha_1(1+\eta+\eta^2)}{(1-\eta)^4} + \frac{4\epsilon(\lambda^3-1)\eta\alpha_1}{k_B} \tag{6.36}$$

$$= \frac{(1+\eta+\eta^2)}{(1-\eta)^3} - \frac{(2\eta^2-2\eta^3+\eta-\eta^2)\,\alpha_1 T + \alpha_1 T(3\eta+3\eta^2+3\eta^3)}{(1-\eta)^4} + \frac{4\epsilon(\lambda^3-1)\eta\alpha_1}{k_B} \tag{6.37}$$

$$= \frac{(1+\eta+\eta^2)}{(1-\eta)^3} - \frac{\alpha_1 T(2\eta^2-2\eta^3+\eta-\eta^2+3\eta+3\eta^2+3\eta^3)}{(1-\eta)^4} + \frac{4\epsilon(\lambda^3-1)\eta\alpha_1}{k_B} \tag{6.38}$$

$$= \frac{(1+\eta+\eta^2)}{(1-\eta)^3} - \frac{(\eta^3+4\eta^2+4\eta)\alpha_1 T}{(1-\eta)^4} + \frac{4\epsilon(\lambda^3-1)\eta\alpha_1}{k_B} \tag{6.39}$$

$$\alpha_1 T\left[\frac{(1+\eta+\eta^2)}{(1-\eta)^3} - \frac{4\epsilon\eta(\lambda^3-1)}{k_B T}\right] + \frac{\alpha_1 T\eta(\eta+2)^2}{(1-\eta)^4} - \frac{\alpha_1\eta 4\epsilon(\lambda^3-1)}{k_B} = \frac{(1+\eta+\eta^2)}{(1-\eta)^3} \tag{6.40}$$

$$\alpha_1 T\left[\frac{(1+\eta+\eta^2)}{(1-\eta)^3} - \frac{4\epsilon\eta(\lambda^3-1)}{k_B T} + \frac{\eta(\eta+2)^2}{(1-\eta)^4}\right] - \frac{\alpha_1\eta 4\epsilon(\lambda^3-1)}{(1-\eta)^4} = \frac{(1+\eta+\eta^2)}{(1-\eta)^3} \tag{6.41}$$

$$\alpha_1 T\left[\frac{(1+\eta+\eta^2)}{(1-\eta)^3} - \frac{4\epsilon\eta(\lambda^3-1)}{k_B T} + \frac{\eta(\eta+2)^2}{(1-\eta)^4} - \frac{4\epsilon\eta(\lambda^3-1)}{k_B T}\right] = \frac{(1+\eta+\eta^2)}{(1-\eta)^3} \tag{6.42}$$

$$\alpha_1 T\left[\frac{(1+\eta+\eta^2)(1-\eta)+\eta(\eta+2)^2}{(1-\eta)^4} - \frac{8\epsilon\eta(\lambda^3-1)}{k_B T}\right] = \frac{(1+\eta+\eta^2)}{(1-\eta)^3} \tag{6.43}$$

$$\alpha_1 T\left[\frac{1-\eta+\eta-\eta^2+\eta^2-\eta^3+\eta^3+4\eta^2+4\eta}{(1-\eta)^4} - \frac{8\epsilon\eta(\lambda^3-1)}{k_B T}\right] = \frac{(1+\eta+\eta^2)}{(1-\eta)^3} \tag{6.45}$$

$$\alpha_1 T\left[\frac{(2\eta+1)^2}{(1-\eta)^4} - \frac{8\epsilon\eta(\lambda^3-1)}{k_B T}\right] = \frac{(1+\eta+\eta^2)}{(1-\eta)^3} \tag{6.46}$$

$$\alpha_1 T = \frac{(1+\eta+\eta^2)/(1-\eta)^3}{\frac{(2\eta+1)^2}{(1-\eta)^4} - \frac{8\epsilon\eta(\lambda^3-1)}{k_B T}} \quad (6.47)$$

6.3. RESULTS AND DISCUSSION

The input parameters for liquid Cu are taken for this computation from Mishra and Venkatesh (Mishra and Venkatesh, 2008) as ($\sigma = 2.253$; $\lambda = 1.68$; $\varepsilon/k_B = 300$). Figure 6.1 shows the total structure factor S(k) of liquid Cu in the temperature range from 1097 to 1600 °C, here k is diffraction vector, equal to $4\pi \sin\theta/\lambda_1$, where θ is the scattering angle and λ_1 is the wave length. With increasing temperature up to 1247 °C, the peak height of the first maximum of S(k) progressively decreases, and then becomes constant in the range between 1192 to 1247 °C, after which it decreases gradually with increasing temperature. The change in height of the first peak of S(k) versus temperature is shown in Figure 6.2.

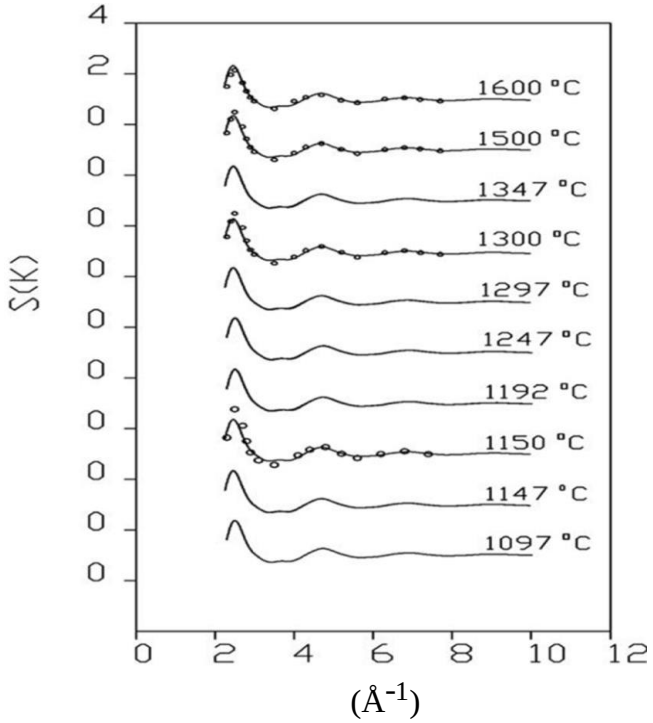

Figure 6.1: The total structure factor S(k) of liquid Cu at different temperatures, (—) theoretical values; (o o o) experimental values.

The experimental values available for the structure factors S(k) and pair correlation function g(r) at temperature 1150, 1300, 1500, 1600 °C (Waseda, 1980)

agree well with the computed results and are shown in Figures 6.1 and 6.3 respectively.

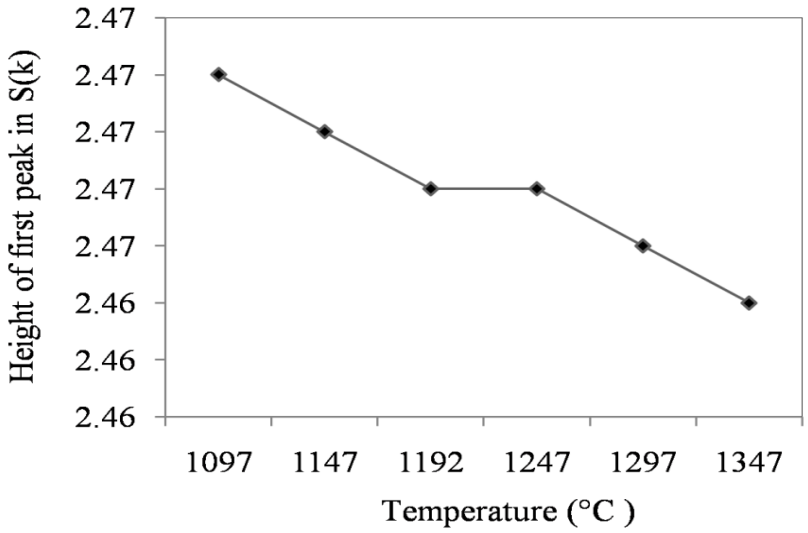

Figure 6.2: Height of first peak in S(k) of liquid Cu against temperature.

The height of the S(k) and g(r) peaks have a nonlinearity decrease and their positions does not change with increasing temperature. Similar trends were observed by Xiufang and Weimin (Xiufang and Weimin, 2000) for liquid Al-13 wt% Si alloy.

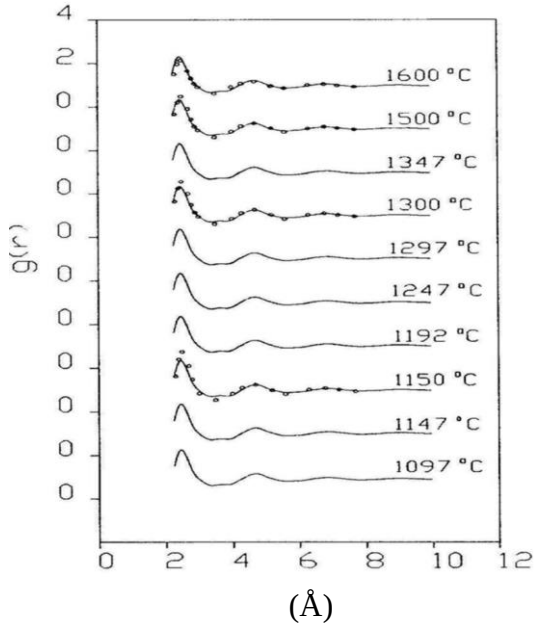

Figure 6.3: The pair correlation function g(r) of liquid Cu at different temperatures, (——) theoretical results; (o o o) experimental results.

Figures 6.2 and 6.4 show that the peak height of both S(k) and g(r) decreases gradually at first with increasing temperature up to 1192 °C. These suggest that the break of bonds happens in the melt and that Cu atoms diffuse from Cu-Cu cluster. The peak height does not change within the temperature range 1192 to 1247 °C suggests that the rate of diffusion of Cu atoms from Cu-Cu clusters is the same to the rate of that Cu atoms to form a new Cu-Cu clusters, meaning that the amount of destroyed bond is exactly the same to that of produced bonds.

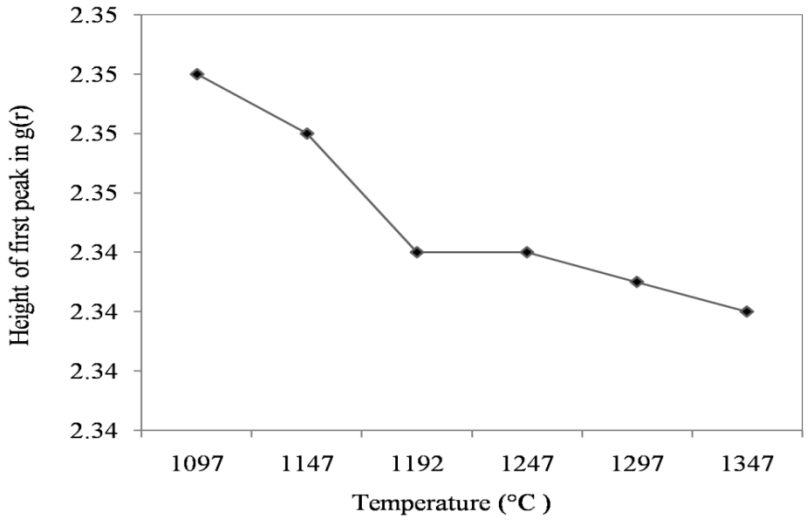

Figure 6.4: Height of first peak in g(r) of liquid Cu against temperature.

Similar trends were observed by Xiufang and Weimin (Xiufang and Weimin, 2000) for liquid Al-13 wt% Si alloy. Then onward as the temperature increases further high beyond 1297 °C the peak height of both S(k) and g(r) keeps on decreasing gradually with increasing temperature. This is due to the fact that, the diffusion process of Cu-Cu clusters reached a limit, and the structure change of the melt is such that a new fewer bonds will be formed from the destroyed original bonds.

ξ^{HP}, ξ^{SP} and ξ^{SHP} were computed through Eqns. (6.9) to (6.11) which incorporate temperature derivative of S(k) and g(r). These computed values are presented in Table 6.1. It is revealed from Table 6.1 that the contribution of ξ^{HP} in the calculation of ξ is dominating at all temperatures. Further hard part ξ^{HP} is increasing with increasing temperature, however, ξ^{SP} soft part decreases by a small amount with increasing temperature.

Table 6.1. Friction coefficients $\boldsymbol{\xi^{HP}}$, $\boldsymbol{\xi^{SP}}$ and $\boldsymbol{\xi^{SHP}}$($\boldsymbol{10^{-13}}$Kg/s) and D ($\boldsymbol{10^{-9}m^2/s}$)

Temperature (K)	ξ^{HP}	ξ^{SP}	ξ^{SHP}	D(theoretical)	D(experimental)
1370	31.36	5.29	3.87	4.66	3.35
1420	31.92	5.20	3.80	4.78	3.70
1465	32.42	5.12	3.74	4.89	4.18
1520	33.03	5.02	3.67	5.02	4.59
1570	33.57	4.94	3.61	5.14	4.85
1620	34.10	4.87	3.56	5.25	5.20

Figure 6.5 shows a satisfactory agreement of self-diffusion, D at different temperatures between computed and experimental values (Meyer and Kargl, 2013). It is worth to mention here that at higher temperature 1620 K, we find a very good agreement between theory and experiment (Meyer and Kargl, 2013). However, in the lower temperature range especially between 1370 and 1570 K, there may be existence of few Cu-clusters which is not predicted by proposed model.

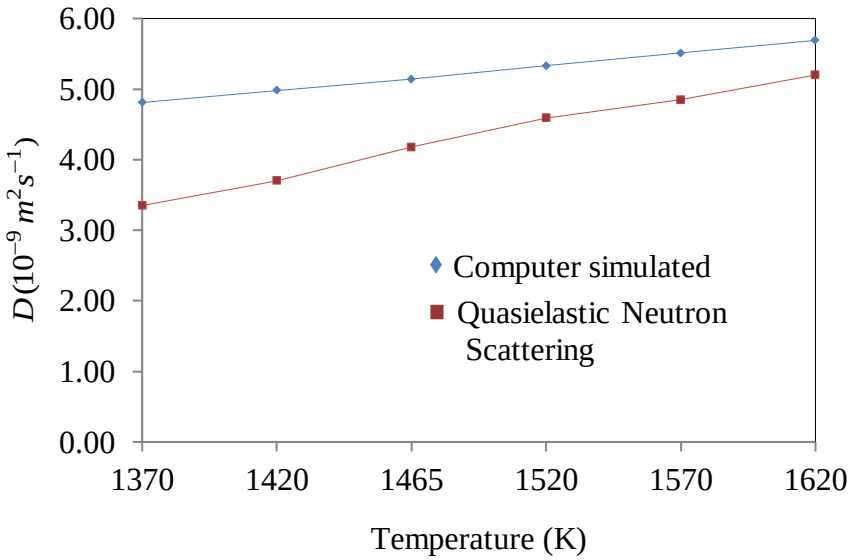

Figure 6.5: Self-diffusion coefficients in liquid Cu from Quasielastic Neutron Scattering (QNS) and computer simulated results

The mechanism of the thermal expansion is determined by an increase in free volumes of holes and not on the change in the interatomic distances due to the anharmonicity in the potential energy of the interatomic interaction as the temperature rises (Bar'yakhtar et al., 1989).

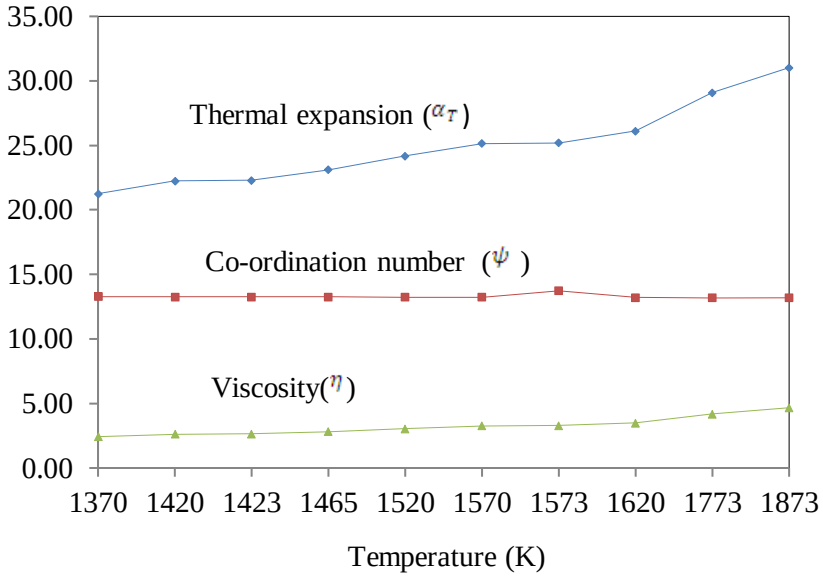

Figure 6.6: Thermal expansion coefficients (α_T) (K^{-1}), co-ordination number (ψ) and viscosity(η) (m Pas).

Figure 6.6 demonstrate an increase in the thermal expansion coefficients of liquid Cu with increase in temperature when the position of the first maxima on the radial distance, r^{max} = 0.246 (Å) remains constant with change in temperature. While the shear viscosity shows an increase with increase in temperature, Waseda (Waseda, 1980) tells us that the overall coordination number decreases with increase in temperature for liquid Tn which we find the same for liquid Cu as shown in Figure 6.6.

CONCLUSIONS

The thermodynamic and transport coefficients of Cu-In binary melts have been determined by using SW inter-atomic potential of pure metals under random phase approximation. Theoretical formalisms and computations establish the correlation between kinetics, thermodynamics of the SW liquid with microscopic structural parameters without using any adjustable and experimental parameters. The RKP model is suitable for the description of concentration dependent enthalpy of mixing of SW mixtures. It is worth to mention here that the chemical ordering between unlike atoms decreases in the mixture with In concentration and shows a good agreement with experimental data for all the investigated compositions of Cu-In melts. The Cu-Cu coordination number is decreasing with increasing atomic percent of In and hence increase in self diffusion of Cu with increasing atomic percent of In was observed.

Current viscosity data are in fair agreement with experimental data [1] and an excellent agreement of these two data were observed beyond 31 atomic percent of In in liquid Cu-In alloys validate the Stokes-Einstein relation for this alloy.

First time detailed diffusivity parameters of Cu-In melts were computed and presented in this letter. The constant ratio of D_{In} / D_{Cu} is an indication of the formation of regular solution in the considered melt. A new correlation is observed between the ratios of self diffusivities and two body excess entropies of pure components as $\frac{D_{In}}{D_{Cu}} \approx \frac{S_{Cu}^{ex}}{S_{In}^{ex}}$. This study established a very good correlation between atomic scale structure with dynamics and thermodynamics of liquid Cu-In alloys. The model calculations can be extended to study the high entropy alloys of desirable properties.

Theoretically formulated and computed results of Cu-In binary melts show good coherence with available experimental data which supports the model calculations and its physical basis. Furthermore, most of the computed atomic structures, transport coefficients and thermodynamic properties via different approaches confirm the compound forming tendency in the investigated alloys.

The theoretically formulated and computed BT correlation functions have been employed to investigate the mass (diffusion) and momentum transfer (viscosity) in the binary melts as a function of In composition. We find an excellent agreement between the computed and experimental data of $S_{CC}(0)$ which infers about the compound forming tendency in the liquid Cu-In alloys. It is worth mentioning here that $S_{CC}(0)$ is computed without using any adjustable data. The constant first peak position of the partial radial distribution functions throughout the whole concentration range of In and the linearity dependence of $D\eta$ as a function of temperature proves that SE relation holds for the considered liquid binary alloys. Further, transport coefficients, surface tension, and all other results presented in this manuscript provide an understanding of the effect of microscopic structural functions on these properties.

The structure and derived associated properties like diffusion coefficients (mass transport), viscosity (momentum transport), chemical ordering parameters and pair wise excess entropy of liquid Fe-Al alloys as a function Al concentration have been theoretically investigated using square-well model potential function under Mean Spherical Model Approximation. Moreover, we have evidenced that the investigated alloys are compound forming melts. It is worth to mention here that the computed values of concentration dependent *S(k)* are in fair agreement with results reported by using X-ray diffraction data. Stokes-Einsten (SE) relation is verified by computing shear viscosity values using diffusion data. Two sets of experimental data suggest that the SE relation is suitable for considered melts.

Finally, we conclude that thermodynamic perturbation model calculations quickly covered a wide concentration range compared to molecular dynamic simulation under *ab* initio calculations.

Temperature effect on structure and transport properties of liquid Cu has been investigated by using a square well model under random phase approximation. These model calculations show a fair agreement with experimental results. Analytical expressions of temperature derivative of diffusion coefficient and friction

coefficients in repulsive and attractive region were determined and computed using Fortran 77 codes.

Einstein's form of diffusion of liquid Cu has been computed under a thermal gradient. We find satisfactory result in high temperature regions.

Future perspective:

Part A: Work will be taken immediate after submission of my thesis

1. Establish a new correlation between microscopic structural functions obtained through square-well (SW) model potential with various thermodynamic properties.
2. Extend the theory to three component system.

Part B: Work plan for after Ph.D.

1. Try to establish a link between SW model calculations with molecular volume interaction model (MVIM).
2. Learn *ab initio* molecular dynamic simulation for metallic melts.
3. Work on high entropy alloys (high demand in defense industry) using *ab initio* molecular dynamic simulation.

REFERENCES

Adersen, H. C., Chandler, D., Weeks, J. D., (1972). Roles of Repulsive and Attractive Forces in Liquids: The Optimized Random Phase Approximation. *J. Chem. Phys.*, **56**: 3812-3822.

Akinlade, O., Singh, R.N., Somer, F., (2000). Thermodynamics of liquid Al – Fe alloys. *J. Alloys Compd*., **299**: 163-168.

Akinlade, O., Singh, R.N., (2002). Bulk and surface properties of liquid In–Cu alloys. *J. Alloys Compd*., **333**: 84-90.

Arzpeyma, G., Aïmen, E. G., Mamoun, M., (2013). On the prediction of Gibbs free energy of mixing of binary liquid alloys. *J. Chem. Thermodynamics*, **57**: 82-89.

Ashcroft, N.W., Langreth, D.C., **(**1967). Structure of Binary liquid mixtures. II. Resistivity of Alloys and the Ion-Ion interaction. *Phys. Rev.*, **159:** 500-510.

Barker, J.A., Henderson, D., (1967). Perturbation theory and equation of state for fluids. II. A successful theory of liquids. *The Journal of Chemical Physics*, **47 (11)**: 4714-4721.

Barker, J.A., Henderson, D., (1967). Perturbation theory and equation of state for fluids: the square-well potential. *The Journal of Chemical Physics*, 47 (8): 2856-2861.

Barker, J.A., Henderson, D., (1968). The equation of state of simple liquids. *J. Chem. Educ.*, **45**: 2-6.

Barker, J.A., Henderson, D., (1971). Some Aspects of the Theory of Liquids. *Accounts of Chem. Res*., **4**: 303-307.

Barker, J.A., Henderson, D., (1972). Theories of Liquids. *Ann. Rev. Phys. Chem*., **23**: 439-484.

Bar'yakhtar, V.G., Mikhailova, L.E., Il'inskii, A.G., Romanova, A.V., Khristenko, T. M., (1989). Thermal expansion mechanism of liquid metals. *J. of Experimental and Theoretical Physics*, **95**: 1404-1411.

Batalin, G.I., Beloborodova, E.A., Kazimirov, V.P., (1983). *Thermodynamics and Structure of Liquid Aluminium Alloys*, Metallurgiya, Moscow.

Baxter, R.J., (1967). Method of Solution of the Percus-Yevick, Hypernetted-Chain, or Similar Equations. *Phys. Rev*., **154**: 170-174.

Belton, G.R., Fruehan, R.J., (1969). Mass spectrometric determination of activities in iron-aluminum and silver-aluminum liquid alloys. *Trans Met Soc AIME*, **245(1)**: 113-117.

Bel'tyukov, A.L., Menshikova, S.G., Lad'yanov, V.I., (2015). The viscosity of binary Al-Fe melts in Al-rich area. *J. Non-cryst. Solids*, **410**: 1-6.

Bhuiyan, G.M., Ali, I., Rahman, S.M.M., (2003). Atomic transport properties of AgIn liquid binary alloys. *Physica B*, **33**4: 147-159.

Blairs, S., (2006). Correlation between surface tension, density, and sound velocity of liquid metals. *Journal of colloid and interface science*, **302 (1)**: 312-314.

Bogolyubov, N.N., (1960). *The Problems of Dynamic Theory in Statistical Physics*, Gostechizdat, Moscow-Leningrad.

Born, M., Green, H.S., (1949). *A general kinetic theory of Liquids,* University Press, Cambridge.

Bossa, G.V., Norris, J., May, S., (2017). Surface tension of a Yukawa fluid according to mean-field theory. *J. Chem. Phys.*, **146**: 134701(1-10).

Brillo, J., Chathoth, S.M., Koza, M.M, Meyer, A., (2008). Liquid Al80Cu20: Atomic diffusion and viscosity. *Appl. Phys. Lett*., **93**: 121905(1-3).

Brillo, J., Pommrich, A.I., Meyer, A., (2011). Relation between Self-Diffusion and Viscosity in Dense Liquids: New Experimental Results from Electrostatic Levitation. *Phys. Rev. Lett.*, **107**: 165902(1-4).

Chandler, D., Weeks, J.D., (1970). Equilibrium structure of simple liquids. *Physical review letters,* **25(3)**: 149-152.

Cheng, H., Lu, Y.J., Chen, M., (2009). Interdiffusion in liquid Al–Cu and Ni–Cu alloys. *J. Chem. Phys.*, **13**:1044502(1-6).

Clark, D.B., (1989). The ideal gas law at the center of the sun. *J. Chem. Educ*., 66: 826.

Cromer, D.T., Waber, J.T., (1965). Scattering factors computed from relativistic Dirac-Slater wave functions, *Acta. Cryst*., **18**: 104-109.

Das, S.K., Horbach, J., Koza, M.M., Mavila Chatoth, S., Meyer, A., (2005). Influence of chemical short-range order on atomic diffusion in Al–Ni melts, *Appl. Phys. Lett.* **86**: 011918 (1-3).

Davis, H.T., Palyvos, J.A., (1967). Contribution to the friction coefficient from time correlations between hard and soft molecular interactions. *The Journal of Chemical Physics*, **46(10)**: 4043-4047.

Debye, P., (1915). Scattering of X-rays. *Ann. Physik*. **46**: 809-823.

Debye, P., Menke, H., (1930). Bestimmung der inneren Struktur von Flüssigkeiten mit Röntgenstrahlen. *Z. Physik.*, **31**: 797-798.

Dubinin, N.E., Filippov, V.V., Malkhanova, O.G., Vatolin, N.A., (2009). Structure factors of binary liquid metal alloys within the square-well model. *Eur. J. phys.*, **7(3)**: 584-590.

Dubinin, N.E., Filippov, V.V., Yueryev, A.A., Vatolin, N.A., (2014). Excess entropy of mixing for binary square-well fluid in the mean spherical approximation: Application to liquid alkali-metal alloys, *J. Non-Cryst. Sol*., **401**: 101-104.

Dubinin, N.E., (2019). Square-well self-diffusion coefficients in liquid binary alloys of alkali metals within the mean spherical approximation. *J. Alloys Compd.*, **803**: 1100-1104.

Dzugutov, M., (1996). A universal scaling law for atomic diffusion in condensed matter, *Nature London*, **381**: 137-139.

Ehrenfest, P., (1915). On interference phenomena to be expected when Roentgen rays pass through a diatomic gas. *Proceedings KNAW* , **17**: 1914-1915.

Enderby, J.E., North, D.M., (1968). Percus-Yevick structure factors for liquid alloys. *Physics and Chemistry of Liquids*, **1(1)**: 1-11.

Fima, P., Sobezak, N., (2010). Thermophysical Properties of Ag and Ag–Cu Liquid Alloys at 1098K to 1573K. *Int. J. Thermophys*., **31**: 1165-1174.

Gopala Rao, R.V., Murthy, A.K., (1975). Self Diffusion in Liquid Metals. *Zeitschrift für Naturforschung A, **30*****(5)**:619-622.

Gopala Rao, R.V., Satpathy, A., (1982). On the structure of liquid metals in the improved random phase approximation. *Physics Letters A,* **89 (6)**: 291-293

Gopala Rao, R.V., Das Gupta, B., (1985). Partial structure factors and diffusion coefficients of liquid potassium-cesium alloys, *Phy. Rev. B,* **32**: 6429-6436.

Gopala Rao, R.V., Bandyopadhyay, U., (1989). Theoretical evaluation of structural and transport properties of liquid magnesium-zinc alloy. *Phys.: Condens. Matter*, **1**: 8621-8628.

Gopala Rao, R.V., Venkatesh, R., (1989). Computation of total and partial structure factors, coordination number, and compressibility with self- and mutual-diffusion coefficients of Hg-In alloy. *Phys. Rev. B,* **39**: 3563-3569.

Gopala Rao, R.V., Venkatesh, R., (1989). Theoretical evaluation of structure factors and computation of coordination number, compressibility, and self- and mutual-diffusion coefficients of the Hg-Tl alloy. *Phys. Rev B*, **39 (12)**: 8142-8149.

.

Gopala Rao, R.V., Satpathy, A., (1990). Statistical-mechanical model in the evaluation of partial and total structure factors, atomic distribution functions, and diffusion coefficients of silver-tin liquids at various concentrations. *Phys. Rev B* **4**: 11938-11945.

Gringrich, N.S., (1943). The Diffraction of X-Rays by Liquid Elements. *Rev. Mod. Phys.*, **15**: 90-110.

Gingrich, N.S., Henderson, R.E., (1952). The diffraction of x-rays by liquid alloys of sodium and potassium. *J. Chem. Phys.*, **20**: 1117-1120.

Gruner, S., Hoyer, W., (2008). The dynamic viscosity of liquid Cu–Si alloys. *Journal of alloys and Compounds*, **460(1-2)**: 496-499.

Hansen, J.P., Mc Donald, I.R., (2013). *Theory of Simple Liquids*, Academic Press, London.

Helfand, E., (1961). Theory of the Molecular Friction Constant. *Phys. of fluids*, **4(6)**: 681-691.

Henderson, D., (1967). Structure of the triplet distribution function. *The Journal of Chemical Physics*, **46(11)**: 4306-4310.

Henderson, D., (1971). "*An Advanced Treatise in Physical Chemistry*" *Vol – VIII A*, Academic Press, London.

Hiroike, K., (1972). Long-range correlations of the distribution functions in the canonical ensemble. *Journal of the Physical Society of Japan*, **32(4)**: 904-911.

Hoyt, J.J., Asta, M., Sadigh, B., (2000). Test of the Universal Scaling Law for the Diffusion Coefficient in Liquid Metals. *Phys. Rev. Lett.*, **85**: 594-597.

Hultgren, R., Desai, P.D., Hawkins, D.T., Gleiser, M., Kelley, K., (1973). *Selected Values on the Thermodynamic Properties of Binary Alloys*, American Society for Metals, Metal Park, OH.

Il'inskii, A., Slyusarenko, S., Slukhovskii, O., Kaban, I., Hoyer, W., (2002). Structure of liquid Fe–Al alloys. *Materials Science and Engineering: A*, **325**: 98-102.

Itabashi, S., Kameda, K., Yamaguchi K., Kon, T., (1999). Activity of indium in liquid In-Bi-Cu and In-Sb-Cu alloys measured by an EMF method using a zirconia electrolyte. *J. of Japan Institute of Metals*, **63**: 817-821.

Jakse, N., Pasturel, A., (2008).Glass forming ability and short-range order in a binary bulk metallic glass by *ab initio* molecular dynamics, *Appl. Phys. Lett*., **93**: 113104(1-3).

Jakse, N., Pasturel, A., (2015). Correlation between dynamic slowing down and local icosahedral ordering in undercooled liquid $Al_{80}Ni_{20}$ alloy. *J. Chem. Phys.*, **143**: 084508(1-10).

Jakse, N., Pasturel, A., (2016). A Relationship between structural and dynamic properties of Al-rich Al-Cu melts: Beyond the Stokes-Einstein relation. *Phys. Rev. B*, **94**: 224201(1-13).

Jakse, N., Pasturel, A., (2016). Transport properties and Stokes-Einstein relation in Al-rich liquid alloys. *J. Chem Phys*, **144**: 244502(1-12).

Jonas, J., Akaii, J.A., (1977). Transport processes in compressed liquid methanol. *J. Chem. Phys.*, **66**: 4946-4950.

Kanibolotsky, D.S., Bieloborodova, O.A., Kotova, N.V., Lisnyak, V.V., (2002). Thermodynamic properties of liquid Al-Si and Al-Cu alloys. *J. Ther. Ana. Cal.*, **70**: 975-983.

Karmkar, R.C., Gosh, R.C., (2021). Validity of Stoke-Einstein relation in liquid 3d transition metals for a wide range of temperatures. *J. Mol. Liq*., **328**: 115434(1-10).

Khaleque, M.A., Bhuiyan, G.M., Sharmin, S., Rashid, R.I.M.A., Rahman, S.M.M., (2002). Calculation of partial structure factors of a less-simple binary alloy. *Eur. Phys. J. B*, **26**: 319-322.

Kirkwood, J.G., (1935). Statistical mechanics of fluid mixtures. *The Journal of chemical physics*, **3(5)**: 300-313.

Kirkwood, J.G., (1946). The statistical mechanical theory of transport processes I. General theory. *The Journal of Chemical Physics*, **14 (3)**: 180-201.

Knott, S., Mikula, A., (2006). Calorimetric investigation of the binary Cu–In system. *Inter. J. Mat. Res*., **97**: 1098-1101.

Lalneihpuii, R., Shrivastava, R., Lalnuntluanga, C., Mishra, R.K., (2019). Bhatia–Thornton fluctuations, transport and ordering in partially ordered Al–Cu alloys. *J. Stat. Mech.*, 053202: 1-12.

Lalnuntluanga, C., Shrivastava, R., Lalneihpuii, R., Mishra, R.K., (2021). Influence of atomic-scale structure on the transport, ordering, and thermodynamics of partially ordered Cu-In alloys. *J Mol. Liq.*, **347**: 117958.

Lalnuntluanga, C., Mishra, R.K., (2016). Concentration dependent structural parameters of liquid Al-Fe alloys. *Journal of Physics: Conference Series*, **765**: 012009-012014.

Lang A., Khal, G., Likos, C.N., Lowen, H., Watzlawek, M., (1999). Structure and thermodynamics of square-well and square-shoulder fluids. *J. Phys. Condens. Matter*, **11**: 10143-10161.

Lebowitz, J.L., Percus, J.K., (1966). Mean spherical model for lattice gases with extended hard cores and continuum fluids. *Physical Review*, **144(1)**: 251-258.

Li, G.X., Liu, C.S., Zhu, Z.G., (2005). Excess entropy scaling for transport coefficients: diffusion and viscosity in liquid metals, *J. Non-Cryst. Sol*., **351**: 946-950.

Lihl, F., Nachtigall, E., Pointner, G., (1964). Messung der Viskositat von Aluminium schmelzen. *Metallurgy*, **18 (10)**: 1054-1064.

Liu, D., Quin, J.Y., Gu, T.K., (2010). The structure of liquid Mg-Cu binary alloys, *J. Non-Cryst. Sol*., **356**: 1587-1592.

Mansoori, G.A., Canfield, F.B., (1969). Variational approach to the equilibrium thermodynamic properties of simple liquids. I. *The Journal of Chemical Physics*, **51(11)**: 4958-4967.

Mansoori, G. A., Canfield, F.B., (1970). Perturbation and variational approaches to equilibrium thermodynamics of gases, liquids, and phase transitions. *Industrial & Engineering Chemistry*, **62(8)**: 12-29.

Massobrio, C., Celino, M., Pasquarello, A., (2004). Charge fluctuations and concentration fluctuations at intermediate-range distances in the disordered network-forming materials SiO2, SiSe2, and GeSe2. *Phys. Rev. B*, **70**: 174202 (1-6).

McQuarrie, D. A., (2011). *Statistical Mechanics*, Harper & Row, New York.

Mikolaj, P. G., Pings, C. J., (1967). Structure of Liquids. III. An X-Ray Diffraction Study of Fluid Argon. *The Journal of Chemical Physics*, **46(4)**: 1401-1411.

Meyer, A., Kargl, F., (2013). Diffusion of Mass in Liquid Metals and Alloys - Recent Experimental Developments and New Perspectives. *Int. J. Microgravity Sci. Appl.*, **30**: 30-35.

Meyer, N., Xu, H., Wax, J.F., (2019). The role of chemical order in the temperature and composition dependence of the viscosity of liquid alloys. *J. Chem. Phys.*, **150**: 174502(1-8).

Mikolaj, P. G., Pings, C. J., (1967). Structure of liquids. IV. Direct correlation functions of liquid argon. *The Journal of Chemical Physics*, **46(4)**: 1412-1420.

Mishra R.K., Venkatesh, R., (2005). Evaluation of activation energies and other properties from structural studies of liquid metals and their extension to liquid Ag–In alloy. *J. of Non-Crystalline Solids*, **35**: 705-710.

Mishra, R.K., Venkatesh, R., (2008). Theoretical evaluation of structural and various associated properties of Al-Si melts. *Chem. Phys*., **354**: 112-117.

Mishra, R.K., Lalneihpuii, R., (2016). Test of the universal scaling law for square well liquid metals. *J Non-Cryst Sol*., **444**: 11-15.

Mishra R.K., Shrivastava, R., (2017). Transport coefficients and validity of the Stokes-Einstein relation in metallic melts: From excess entropy scaling law. *Chem. Phys.*, **493**: 115-119.

Mishra, R.K., Lalneihpuii, R., Venkatesh, R., (2020). Statistical mechanical studies of Al rich Al–Cu melts. *Physica A*, **550**: 123901-123916.

Morris, D.G., Gunther, S., (1996). Strength and ductility of Fe-40Al alloy prepared by mechanical alloying. *Materials Science and Engineering: A*, **208(1)**: 7-19.

Mudry, S., Korolyshyn, A., Vus, V., Yakymovych, A., (2013). Viscosity and structure of liquid Cu–In alloys. *J. Mol. Liq.*, **179**: 94-97.

Ning, S., Xiufang, B., Zhenfeng, R., (2010). Correlation between viscous-flow activation energy and phase diagram in four systems of Cu-based alloys. *Physica B: Condensed Matter*, **405(17)**: 3633-3637.

Odusote, Y.A., (2008). Investigation of ordering phenomenon in Me–Pt (Me=Fe,Ni) liquid alloys. *Sci. Technol. Adv. Mater*, **9**: 015001(1-7).

Okamoto, H., (2005). Cu-In (copper-indium). *J Phs Eqil and Diff* , **26**: 645.

Ornstein, L.S., Zernike, F., (1914). Integral equation in liquid state theory. In. *Proc. Acad. Sci. Amsterdam*, **17**:793.

Orton, B.R., Shaw, B.A., Williams, G.I., (1960). An X-ray structure investigation of the liquids of sodium, potassium and sodium-potassium alloys. *Acta metallurgica*, **8(3)**: 177-186.

O'Toole, J.T., Dahler, J.S. (1960). Molecular friction in dilute gases. *The Journal of Chemical Physics*, **33(5)**: 1496-1504.

Palyvos, J.A., Davis, H.T., (1967). Self-diffusion in simple fluids. *The Journal of Physical Chemistry*. **71(2)**: 439-444.

Pasturel, A., Jakse, N., (2015). On the role of entropy in determining transport properties in metallic melts. *J. Phys. Cond. Matt.*, **27**: 325104(1-6).

Peng, H.L., Voigtmann, Th., Kolland, G., Kobatake, H., Brillo, J., (2015). Structural and dynamical properties of liquid Al-Au alloys. *Phys. Rev. B*, **92** 184201(1-13).

Percus, J.K., Yevick, G.J., (1958). Analysis of classical statistical mechanics by means of collective coordinates. *Physical Review*, **110(1)**: 1-13.

Percus, J.K. (1962). Approximation methods in classical statistical mechanics. *Physical Review Letters*, **8(11)**: 462-463.

Prasad, L.C., Singh, R.N., (1991). Surface segregation and concentration fluctuations at the liquid-vapor interface of molten Cu-Ni alloys. *Physical Review B*, **44(24)**: 13768-13771.

Prasad, L.C., Singh, R.N., Singh, V.N., Singh, G.P., (1998). Correlation between bulk and surface properties of Ag-Sn liquid alloys. *J. Phys. Chem. B*, **1029**: 921-926.

Reed, T.M., Gubbins, K.E., (1973). *Applied Statistical Mechanic*, pages 262 – 269, Mc. Graw Hill, New York.

Rice, S.A., Gray, P., (1963). *Statistical Mechanics of Simple Liquids*, page 196, Wiley Inter Science, New York.

Rice, S.A., Gray, P., (1965). *The Statistical Mechanicals of Simple Liquids*, page 84, Interscience, New York.

Rice, S.A., Boon, J.P., Davis, H.T., (1968). *Simple Dense Fluids*, page 252,

Academic Press, New York.

Roik, O.S., Muratov, O.S., Yakovenko, O.M., Kazimirov, V.P., Golovataya, N.V., Sokoskii, V.E., (2014). X - ray diffraction studies and Reverse Monte Carlo simulations of the liquid binary Fe-Si and Fe-Al alloys. *J. Mol. Liquids*, **197**: 215-222.

Rosenfeld, Y., (1999). A quasi-universal scaling law for atomic transport in simple fluids. *J. Phys. Cond. Matt.*, **11**: 5415-5427.

Rowlinson, J.S. (1965). Self-consistent approximations for molecular distribution functions. *Molecular Physics,* **9(3)**: 217-227.

.

Rushbrooke, G. S., Scoins, H.I., (1953). On the theory of fluids. *Proceedings of the Royal Society of London. Series A. Mathematical and Physical Sciences*, **216(1125)**: 203-218.

Salmon, P.S., Zeidler, A., (2013). Identifying and characterising the different structural length scales in liquids and glasses: an experimental approach. *Physical Chemistry Chemical Physics,* **15(37)**: 15286-15308.

Samanta, A., Ali, S.M., Gosh, S.K., (2004). New Universal Scaling Laws of Diffusion and Kolmogorov-Sinai Entropy in Simple Liquids. *Phys. Rev. Lett.*, **92**: 145901(1-4).

Shimoji, M., Itami, T., (1986). *Atomic transport in liquid metals*., Trans Tech Publications, Aedermannsdorf, Switzerland.

Sharma, N., Thakur, A., Ahluwalia, P.K., (2014). Thermodynamic, surface and, structural properties of HgNa and HgZn liquid alloys. *J. Mol. Liq.*, **195**: 73- 79.

Singh, R.N., (1987). Short-range order and concentration fluctuations in binary molten alloys. *Canadian journal of physics*, **65(3)**: 309-325.

Singh, R.N., (1993). Higher order conditional probabilities and short range order in molten alloys. *Physics and Chemistry of Liquids*, **25(4)**: 251-267.

Smith, W.R., Henderson, D., Barker, J.A., (1970). Approximate Evaluation of the Second-Order Term in the Perturbation Theory of Fluids. *The Journal of Chemical Physics*, **53 (2)**: 508-515.

Smith, W.R., Henderson, D., Barker, J.A., (1971). Perturbation Theory and the Radial Distribution Function of the Square-Well Fluid. *J. Chem. Phys.*, **55**: 4027-4033.

Sonvane, Y.A., Thakor, P.B., Jani, A.R., (2012). Atomic transport and surface properties of some simple liquid metal using one component plasma system. *J. of Theo. Appl. Phys.*, **6(43)**: 1-6.

Souto, J., Alemany, M.M.G., Gallego, L.J., Gonzalez, L.E., (2013). Static structure, microscopic dynamics and electronic properties of the liquid Bi–Li alloy. An *ab initio* molecular dynamics study. *Mod. Simul. Mater. Sci. Eng.*, **21**: 075006(1-16).

Speedy, R.J., Prielmeier, F.X., Vardag, T., Lang, E.W., Lüdemann, H.D., (1989). Diffusion in simple fluids. *Molecular Physics*, **66(3)**: 577-590.

Thiele, E., (1963). Equation of state for hard spheres. *The Journal of Chemical Physics*, **39(2)**: 474-479.

Trybula, M., Jakse, N., Gasior, W., Pasturel, A., (2014). Structural and physico-chemical properties of liquid Al–Zn alloys: A combined study based on

molecular dynamics simulations and the quasi-lattice theory. *J. Chem. Phys*., **141**: 224504 (1-8).

Trybula, M.E., (2016). Structure and transport properties of the liquid $Al_{80}Cu_{20}$ alloy – A molecular dynamics study. *Comput. Mater. Sci.*, **122**: 341-352.

Trybula, M.E., Szafranski, P.W., Korzhavyi, P.A., (2018). Structure and chemistry of liquid Al–Cu alloys: molecular dynamics study versus thermodynamics-based modeling. *J. Mater. Sc*i., **53**: 8285-8301.

Van der Ven, A., Ceder, G., (2005). First Principles Calculation of the Interdiffusion Coefficient in Binary Alloys. *Phys. Rev. Lett*., **94**: 045901 (1-4).

Venkatesh, R., Mishra, R.K., Gopalao Rao, R.V., (2003). Structural, thermodynamic and other associated properties of partially ordered Ag-In alloy. *Phys. Stat. Solidi b*, **240**: 549-560.

Venkatesh, R., Mishra, R.K., (2005). Evaluation of activation energies and other properties from structural studies of liquid metals and their extension to liquid Ag–In alloy. *J. Non-Cryst. Sol.*, **351**: 705-710.

Verlet, L., (1964). On the theory of classical fluids-III. *Physica*, **30(1)**: 95-104.

Wang, S.Y., Kramer, M.J., Xu, M., Wu, S., Hao, S.G., Sordelet, D.J., Ho, K.M., Wang, C.Z., (2009). Experimental and *ab initio* molecular dynamics simulation studies of liquid Al60Cu40 alloy. *Phys. Rev. B* , **79**: 144205-144209.

Wang, T., Zhang, F., Yang, L., Fang, X.W., Zhou, S.H., Kramer, M.J., Wang, C.Z., Ho, K.M., Napolitano, R.E., (2015). A computational study of diffusion in a glass-forming metallic liquid. *Scientific Reports*, **5**: 10956 (1-9).

Waseda Y., (1980). *The Structure of Non-crystalline Materials*, McGraw-Hill, New York,

War, N., (2014). *Selected Papers on Noise and Stochastic Processes*, Dover Publications, New York.

Weeks, J.D., Chandler, D., Andersen, H.C. (1971). Role of repulsive forces in determining the equilibrium structure of simple liquids. *The Journal of chemical physics*, **54(12)**: 5237-5247.

Wertheim, M.S., (1963). Exact Solution of the Percus-Yevick Integral Equation for Hard Spheres. *Phys. Rev. Lett.*, 10: 321-323.

Wertheim, M.S., (1964). Analytic solution of the Percus-Yevick equation. *Journal of Mathematical Physics*, **5(5)**: 643-651.

Xiufang, B., Weimin, W., (2000). Thermal-rate treatment and structure t ransformation of Al–13 wt.% Si alloy mel. *Mat. Lett*. **44**: 54-58.

Yang, H.W., Tao, D.P., Zhou, Z.H., (2008). Prediction Of The Mixing Enthalpies Of Binary Liquid Alloys By Molecular Interaction Volume, *Model Acta. Metall. Sin*. **21**: 336-340.

Yan, J., Lu, Y., Chen. G., Yang, M., Gu, Z., (2018). Advances in liquid metals for biomedical applications. *Chem. Soc.*, **47**: 2518-2533.

Yakymovych, A., Furtauer, S., Elmahfoudi, A., Ipser, H., Flandorfer, H., (2014). Enthalpy of mixing of liquid Co-Sn alloys. *J. Chem. Ther.*, **74**: 269-285.

Yuan, Y.Q., Zeng, X.G., Chen, H.Y., Yao, A.L., Hu, Y.F., (2013). Molecular dynamics simulation on microstructure evolution during solidification of copper nanoparticles, *J. Kor. Phys. Soc.*, **62**: 1645-1651.

Yu, Y.X., Han, M.H., Gao, G.H., (2001). Self-diffusion in a fluid of square-well spheres, *Phys. Chem. Chem. Phys*., **3**: 437-443.

Yvon, J., (1935). *La Theorie Statistique des Fluides et Equation d' Etat. Actualites Scientifiques et Industrielles, Vol 203*, Hermann & Cie, Paris.

Zhang, B., Gresche, A., Meyer, A., (2010). Diffusion in Al-Cu Melts Studied by Time Resolved X-Ray Radiography. *Phys. Rev. Lett.*, **104**: 035902 (1-4).

Zwanzig, R.W., (1954). High-temperature equation of state by a perturbation method. I. Nonpolar gases. *The Journal of Chemical Physics*, **22(8)**: 1420-1426.

BIO-DATA OF THE CANDIDATE

Personal information

Name	:	C. Lalnuntluanga
Father's name	:	C. L. K. Thanga
Mother's name	:	Sangzuali
Date of Birth	:	06. 07. 1986
Nationality	:	Indian
Gender	:	Male
Marital Status	:	Single
Present Address	:	Ramhlun Venglai, B-162, Aizawl, Mizoram
Email	:	lnt_2013@rediffmail.com
Academic Records	:	

EXAMINATION	BOARD/UNIVERSITY	YEAR	DIVISION	PERCENTAGE
H.S.L.C.	M.B.S.E., Mizoram	2002	FIRST	70.30
H.S.S.L.C.	C.B.S.E.	2004	FIRST	63.16
B.Sc. Chemistry	Mizoram University	2007	FIRST	63.25
M.Sc. Chemistry	Mizoram University	2012	FIRST	75.22

LIST OF PUBLICATIONS IN JOURNALS

1. C. Lalnuntluanga, R. K.Mishra, Concentration dependent structural parameters of liquid Al-Fe alloys, Journal of Physics: Conference Series 765 (2016) 012009 (1-6).
   http://dx.doi.org/10.1088/1742-6596/765/1/012009
2. R. Lalneihpuii, R. Shrivastava, C. Lalnuntluanga, R.K. Mishra, Bhatia–Thornton fluctuations, transport and ordering in partially ordered Al–Cu alloys, J. Stat. Mech., (2019) 053202 (1-12). https://doi.org/10.1088/1742-5468/ab11bd
3. C. Lalnuntluanga, Raj Kumar Mishra, Temperature effect on structural and transport coefficient of liquid copper under square-well interaction. AIP Conference Proceedings, 2327 (2021), 020043(1-8).
   https://doi.org/10.1063/5.0039716
4. C. Lalnuntluanga, R. Shrivastava, R. Lalneihpuii, R. K. Mishra, Influence of atomic-scale structure on the transport, ordering, and thermodynamics of partially ordered Cu-In alloys, J. Mol. Liq. (2021) 117958.
   https://doi.org/10.1016/j.molliq.2021.117958
5. C Lalnuntluanga, R Lalneihpuii, Zodinpuia Pachuau, and Raj Kumar Mishra, Correlation between structures and atomic transport properties of compound forming liquid Cu-In alloys, Phys. Scr., 98 (2022) 015708.
   https://doi.org/10.1088/1402-4896/aca5ca
6. Raj Kumar Mishra, C. Lalnuntluanga, Sanjeev Kumar Mishra, Theoretical Investigation of Structure, Dynamics and Entropy Correlation in Liquid Fe–Al Alloys, Met. Mat. Trans. B, 54 (2023) 331–341.
   https://doi.org/10.1007/s11663-022-02693-1

LIST OF PAPER PRESENTED IN CONFERENCE/SYMPOSIUM

1. R. Lalneihpuii, C. Lalnuntluaga, Raj Kumar Mishra. Theoretical and Computational studies on liquid Al-Cu alloys. 8th Mid-Year CRSI National Symposium in Chemistry, 10^{th}-12^{th} July 2014. Organized jointly by CSIR-North East Institute of Science and Technology, Jorhat and Tezpur University, Tezpur.
2. C. Lalnuntluanga, Raj Kumar Mishra. A comparative study of Quasielastic Neutron Scattering (QNS) data of self-diffusion in liquid Cu with computer data. Orientation Workshop on Radiation-Its Applications in Chemical, and Life Sciences, 29^{th}-31^{st} October 2014. Organized jointly by UGC-DAE Consortium for Scientific Research, Kolkata Centre and Department of Chemistry, Mizoram University, Aizawl.
3. C. Lalnuntluanga, Raj Kumar Mishra. Temperature effect on Structure of Liquid Cu. 18^{th} CRSI National Symposium in Chemistry, 5^{th}-7^{th} February, 2016. Organized by Institute of Nano Science and Technology and Panjab University, Chandigarh, India.
4. C. Lalnuntluanga, Raj Kumar Mishra. Mathematical Model for calculation of structure factor in metallic liquids. National Conference on Application of Mathematics, 25^{th}-26^{th} February 2016. Organized by Department of Mathematics and Computer Science, Mizoram University.
5. C. Lalnuntluanga, Raj Kumar Mishra . Concentration-dependent structural parameters of liquid Al-Fe alloy. Condensed Matter Days-2016, National Conference, 29^{th}-31^{st} August 2016. Organized by Department of Physics, Mizoram University.
6. C. Lalnuntluanga, Raj Kumar Mishra. A New approach for the pressure derivative of diffusion coefficient and the determination of Gruneisen constant in liquid metals. 20^{th} CRSI National Symposium in Chemistry, 3^{rd}-5^{th} February 2017. Organized by Department of Chemistry, Gauhati university.

7. C. Lalnuntluanga, Raj Kumar Mishra. Theoretical studies on liquid Cu-In alloys. National Symposium on Contemporary Trends and Future Prospects of Functional Materials (CTFM-2019), 29th-30th November 2019. Organised by Department of Chemstry, Institute of Science, Banaras Hindu University, Varanasi-221005.
8. C. Lalnuntluanga, Raj Kumar Mishra. Temperature Effect on Structural and Trnsport Coefficient of Liquid Copper Under Square-well Interaction. 3rd International Conference on Material Science, Smart Structures and Applications (ICMSS 2020), 15th-16th October 2020. AIP Conference Proceedings held in association with Inventive Research Organization and Surya Engineering College, India.

PARTICULARS OF THE CANDIDATE

NAME OF CANDIDATE	**:**	**C. LALNUNTLUANGA**
DEGREE	**:**	**DOCTOR OF PHILOSOPHY**
DEPARTMENT	**:**	**CHEMISTRY**
TITLE OF THESIS	**:**	**STATISTICAL MECHANICAL STUDIES OF ELEMENTAL LIQUIDS AND BINARY MELTS**
DATE OF ADMISSION	**:**	**7th Aug 2013**
APPROVAL OF RESEARCH PROPOSAL:		
1. BOS	**:**	**24th Apr 2014**
2. SCHOOL BOARD	**:**	**16th May 2014**
MZU REGISTRATION NO.	**:**	**3752 of 2008-09**
Ph.D. REGISTRATION NO. AND DATE	**:**	**MZU/Ph.D/675 of 16.05.2014**
EXTENSION (IF ANY)	**:**	**17.5.2019 to 16.5.2021**

Head

Department of Chemistry

Mizoram University

ABSTRACT

STATISTICAL MECHANICAL STUDIES OF ELEMENTAL LIQUIDS AND BINARY MELTS

AN ABSTRACT SUBMITTED IN PARTIAL FULFILLMENT OF THE REQUIREMENTS FOR THE DEGREE OF DOCTOR OF PHILOSOPHY

C. LALNUNTLUANGA

MZU REGISTRATION NO. : 3752 of 2008-09

Ph. D REGISTRATION NO. : MZU/ Ph.D/ 675 of 16.05.2014

DEPARTMENT OF CHEMISTRY

SCHOOL OF PHYSICAL SCIENCES

DECEMBER, 2021

STATISTICAL MECHANICAL STUDIES OF ELEMENTAL LIQUIDS AND BINARY MELTS

BY

C. LALNUNTLUANGA

Department of Chemistry

Supervisor: Dr. ZODINPUIA PACHUAU

Co-Supervisor: Prof. RAJ KUMAR MISHRA

Submitted

In partial fulfillment of the requirement of the degree of Doctor of Philosophy in Chemistry of Mizoram University, Aizawl.

Abstract

The present study used a thermodynamic perturbation theory in which square-well (SW) potential is perturb over hard-sphere reference system to compute structure, transport and thermodynamic properties of liquid binary alloys and metals. Knowledge of the structure, transport and thermodynamic properties of liquid state is crucial for understanding their applications in nucleation of crystals, glass formation, metallurgy, medical and other industrial technologies. The SW potential is an extension of hard sphere potential and has been successfully applied for metallic liquids, colloidal particles, hetero-chain molecules and complex systems. The SW potential is completely solvable and applicable for real liquids. The SW potential gives analytical expressions in which numerical computations dominate relatively. Analytical expressions are more appropriate and hence the applicability of SW potential is superior then other potentials for different theoretical techniques, such as integral equations or perturbation theories.

In binary alloys, the structure factor and its Fourier transform, the radial distribution function and other related structural properties like coordination number, transport properties like diffusion coefficients and shear viscosity coefficients were determined and compared with available experimental data. The concentration-concentration fluctuation in long wavelength limit is an important parameter to explain the complexity in binary liquid mixtures. In present investigation, the theoretical and computational values of $S_{CC}(0)$ are in excellent agreement with experimental values at all the investigated compositions. The surface tension and chemical short range order parameter were also computed and compared with Quasi-Lattice (QL) model results. Further, we performed the test on Dzugutov's universal scaling law by establishing a link between reduced diffusion and viscosity with respect to the computed excess entropy. Other then the structural properties, the diffusion coefficient, viscosity coefficient, co-ordination number and the coefficient of thermal expansion were computed from the equation of states for square-well fluids within the temperature range for investigation of structure factor. The following objectives are taken up in the thesis:

- To determine the structure of square-well fluids and the study of concentration and temperature effect on it.
- To derive and evaluate a wide variety of thermo-physical and thermodynamic properties of liquid metals and alloys using structure factor, radial distribution function and potential function.
- To derive and evaluate atomic transport properties like self, mutual, inter-diffusion coefficients and shear viscosity and their variation with composition and temperature in binary liquid alloys.

The comparison between simulation results and those of analytical models essentially allow us to test the models, whereas the comparison of simulation results with experimental results is the ultimate test to judge the efficiency of proposed model.

The first chapter is the general introduction of the thesis which include background, theory of distribution functions, integral equations, perturbation theories, structure factor in liquids, transport, surface and scaling properties in liquid binary alloys, thermodynamic properties of liquid binary alloys, temperature effect on structural and transport coefficient of liquid copper, outlines of present work.

In chapter-2 a detailed understanding of the structural features of binary alloys is described. Using the Lebowitz solution of hard sphere mixtures as a reference system, and perturbed the hard sphere direct correlation function with square well attractive tail the partial and total structure factors, radial distribution functions and associated derived properties of Cu-In and Fe-Al alloys at different compositions have been calculated and compared with the available experimental values. There is an excellent agreement between theoretical and experimental results. We also obtained partial and total coordination numbers from partial and total pair correlation functions respectively. Finally we emphasize that square-well potential is an appealing model in understanding the structural aspects of binary alloys.

In the third chapter, thermodynamically important Bhatia-Thornton correlation functions and in specific the concentration-concentration correlation functions at various compositions of the Cu-In and Fe-Al alloys in the entire momentum space with special emphasis on the values at long wave limit of the same alloys are calculated. The chemical short-range order parameter has been computed as a function of composition for the same systems through structural studies in the long wave limit, which gives valuable information regarding the nature of the liquid alloys at various compositions.

The fourth chapter describes the calculation of diffusion coefficients of binary alloys through their structural studies. A detailed investigation on transport properties of binary alloys is considered. The diffusion coefficient of the alloys is calculated through the use of Helfand's linear trajectory principle. Equations have been derived for the temperature variation of diffusion coefficients, which were applied successfully to the investigated binary alloys. The viscosity coefficients of pure components in liquid binary alloys are determined by assuming Stokes-Einstein (SE) form of equations. The concentration-dependent surface tension of liquid binary alloys is derived by extending the equation for binary system. Further, Dzugutov and Rosenfeld universal scaling law has been tested for the investigation of correlation between atomic dynamics and thermodynamics with square-well model potential.

In fifth chapter, we deduce information on thermodynamic mixing parameters of binary alloys such as, Gibbs free energy of mixing, enthalpy of mixing and entropy of mixing through investigated square-well model structural functions and transport coefficients of liquid binary alloys. The Romanov-Kozlov-Petrov (RKP) model, which correlates the viscosity with enthalpy of mixing, has been used for estimating the enthalpy of mixing. The entropy of mixing has been calculated using a SW model of pair correlation function under two body approximations. The Gibbs free energy of mixing was the computed from the difference between the computed enthalpy of mixing and entropy of mixing.

In sixth chapter, we investigated a detailed effect of temperature on structure and transport properties of liquid Cu using a square-well model potential under random phase approximation. Computed structure factor and square-well potential

were applied to determine the self diffusion of liquid Cu within the available experimental temperature range by using well known Einstein's equation. Then the computed results were compared with available experimental results obtained by Quasielastic Neutron Scattering (QNS). Also, the viscosity coefficient, co-ordination number and the coefficient of thermal expansion were computed from the equation of states for square-well fluids within the temperature range for investigation of structure factor.

Chapter-7 is conclusion. Finally, list of references is given at the end.